



CHALMERS
UNIVERSITY OF TECHNOLOGY



Techno-economic analysis of green H₂ production and Power-to-X pathways

Future energy solutions for the HSY
Ämmässuo eco-industrial centre

Master's thesis in Innovative Sustainable Energy Engineering

Paolo Cardarelli

Author Paolo Cardarelli

Title of thesis Techno-economic analysis of green H₂ production and Power-to-X pathways: future energy solutions for the HSY Ämmässuo eco-industrial centre

Programme SEEX30 - Nordic Master Programme in Innovative Sustainable Energy Engineering

Thesis supervisor Prof. Mika Järvinen

Thesis advisor Prof. Tobias Mattisson

Collaborative partner Helsingin Seudun Ympäristöpalvelut (HSY)

Date 31.12.2021 **Number of pages** 116 **Language** English

Abstract

From a sustainability perspective, a synergy between hydrogen production and renewable energy sources is particularly attractive. Considering the many potential end uses of hydrogen, the implementation of Power-to-X has become one of the most relevant technologies for reaching a carbon-free future.

This master's thesis sets off with a detailed description of the core concepts necessary for the assessment, such as the hydrogen colour code, the H₂ production methods (with a focus on electrolysis) and the Power-to-X concept. After this, a general description of the HSY Ämmässuo eco-industrial centre is provided, to offer a perspective of the energy self-sufficiency issues that need to be solved, for both heat and electricity production.

The possible future energy scenarios of the eco-centre are then analysed, for which the implementation of renewable energy sources would simultaneously ensure its self-sufficiency and open the possibility of green hydrogen generation via electrolysis. Since various investments are considered to achieve said objectives, the economic perspective is of upmost importance: the potential assets' feasibility is studied, considering both their payback period and the effective benefits that can be brought to the eco-centre.

The results of the work show that, while it is possible to simultaneously achieve energy self-sufficiency by implementing additional renewable sources and to invest in an electrolyser for hydrogen production, the generation of compounds such as methanol or methane is not feasible in the near future. Four energy scenarios of increasing complexity are analysed, which indicate that the installation of a wind turbine and solar panels would be a useful asset, while the acquisition of a hydrogenation system for the production of methanol or methane would not be feasible with the amount of surplus energy at disposal of the eco-centre.

Keywords Green Hydrogen, H₂, Power-to-X, P2X, Renewable Energy, Sustainability

List of contents

1. Background theory
 - 1.1. Introduction: the sustainability objective
 - 1.2. Green hydrogen and Power-to-X
 - 1.2.1. The hydrogen colour code
 - 1.2.2. Green hydrogen production methods
 - 1.2.3. Hydrogen density enhancements for storage systems
 - 1.2.4. The Power-to-X concept
 - 1.2.5. Hydrogen based economy: H₂ end-uses
 - 1.3. Economic indicators
 - 1.3.1. Levelized Cost Of Energy/Hydrogen
 - 1.3.2. PayBack Period and Discounted PayBack Period
 - 1.3.3. Net Present Value and Internal Rate of Return
2. The HSY Ämmässuo eco-industrial centre
 - 2.1. Overview
 - 2.2. Current resources
 - 2.2.1. Landfill gas and biogas production
 - 2.2.2. Electricity production
 - 2.2.3. Heat production
 - 2.3. Energy consumption and self-sufficiency
 - 2.3.1. Electricity consumption
 - 2.3.2. Heat consumption
 - 2.3.3. Methanol demand
 - 2.4. Production vs consumption energy summary
 - 2.5. Ämmässuo weather data
3. Potential investments
 - 3.1. Overview and technical characteristics
 - 3.1.1. Wind turbine
 - 3.1.2. Solar panels

- 3.1.3. Additional renewable energy production summary
 - 3.1.4. Heat pump
 - 3.1.5. Alkaline water electrolyser
 - 3.1.6. Methanol production
 - 3.1.7. Methane production
 - 3.1.8. Electric powered buses and hydrogen powered buses
 - 3.2. Economic point of view
- 4. Future energy scenarios
 - 4.1. Methodology
 - 4.2. Power-to-X perspectives
 - 4.3. Scenario 1: Heat pump acquisition, biogas engine utilization factor doubling
 - 4.4. Scenario 2: Addition of the wind turbine and the electrolyser
 - 4.5. Scenario 3: Addition of solar panels
 - 4.6. Scenario 4: Addition of a methanation system
 - 4.7. End products, revenues and costs comparison
 - 4.7.1. Scenario 1 cost analysis
 - 4.7.2. Scenario 2 cost analysis
 - 4.7.3. Scenario 3 cost analysis
- 5. Summary
- 6. References

1. Background theory

1.1. Introduction: the sustainability objective

The achievement of carbon neutrality is one of the most critical matters in the energy field today. This issue became more and more relevant considering the rapid and continuous growth of the industry sector, as well as the world's population, which resulted in a colossal increase of the energy demand. In order to satisfy said demand, fossil fuels have been utilised as the principal source of energy since the industrial revolution (1760-1840); this generated a massive increase of CO₂ levels and other greenhouse gases (GHG) in the atmosphere, which in turn heavily contributed to global warming.

A two-pronged plan is necessary to overcome the current energy scenario's problems: on one hand, sustainable energy sources must be deployed and utilised to reduce the GHG impact on the climate; on the other hand, the energy demand must be kept satisfied, hence the reliability of the energy sources must be ensured. Different tools have been developed to face these issues.

The European Green Deal is an agreement developed by the European Commission to reduce emissions by at least 55% by 2030, as compared to 1990 levels. This plan incorporates other relevant initiatives as well, including to enshrine the 2050 climate-neutrality objective and to engage citizens and all parts of society towards climate action [1].

The EU will:



Become
climate-neutral
by 2050



Protect human life,
animals and plants,
by cutting pollution



Help companies
become world leaders
in clean products and
technologies



Help ensure a
just and inclusive
transition

Figure 1: the key points of the European Green Deal [2]

The Sustainable Development Goals (SDGs) [3] are assortments of global targets designed to achieve a more sustainable future worldwide. The SDGs were set up in 2015 by the United Nations; specific targets were implemented for each one of the seventeen goals, as well as indicators that are used to measure progress toward each target.

To facilitate said monitoring, a variety of tools was deployed to track the progress towards each goal, e.g. the SDG-tracker [4], a website launched in 2018 which presents the data across each indicator.



Figure 2: The 17 Sustainable Development Goals (SDGs) [3]

Of the various measures to be taken to accomplish the previously described sustainability objectives, the utilization of hydrogen (H₂) stood out to be one of the tools with the highest potential. According to the 2019 Hydrogen Roadmap Europe report's Executive Summary, using renewable hydrogen is fundamental to accomplish carbon neutrality, mainly for three reasons:

- Hydrogen is essentially the best choice for at-scale decarbonization of specific sectors. An example of this can be seen for transport: compared to batteries, hydrogen generates higher energy density, lower initial costs, and the issues of recharging and disposal of the batteries are not present. Also, regarding aviation, H₂-based synthetic fuels are the only option for direct decarbonization [5].
- Hydrogen can make the transition to renewable energy sources feasible, especially considering its affinity for sector coupling. It's a technology which allows to convert generated power directly into usable energy, as well as to store it and to channel it towards end-use, in order to meet demand [5].
- Hydrogen can generate a transition which can be convenient to both energy companies and customers. Alternative low carbon energy sources might face adoption difficulties if they can't satisfy the customers' preferences; hydrogen, however, can be introduced into the gas grid via Power-to-X (Power-to-gas) plants using the previously installed piping, making the switch between fuels trifling to consumers [5].

In the following chapter some of the more relevant characteristics of hydrogen will be discussed, as well as the notion of Power-to-X, another key concept for this work.

1.2: Green hydrogen and Power-to-X

1.2.1: The hydrogen colour code

As mentioned before, the potential of a hydrogen-based energy market is astonishing. However, to contribute to reducing the GHG impact and moving towards carbon neutrality, it's necessary to utilize renewable sources to produce H₂, otherwise it's back to the drawing board. To understand the impact that hydrogen production methods can have, a classification based on colours has been developed.

The hydrogen produced from methods which generate CO₂ is defined as grey hydrogen. According to Kothari R. et al [6], the main methods used to produce grey H₂ are hydrocarbon reforming and pyrolysis, and the main sources used are natural gas (48%), heavy oils (30%) and coal (18%). The hydrogen produced from methods which generate CO₂, which is then later removed and stored using Carbon Capture and Storage (CCS) or Carbon Capture and Utilization (CCU) methods is defined as blue hydrogen. The H₂ produced from methods which do not generate CO₂ (renewable sources) is defined as green hydrogen; an overview of the various production methods will be shown in the following chapter. Below, a picture that summarizes the hydrogen colour classification:

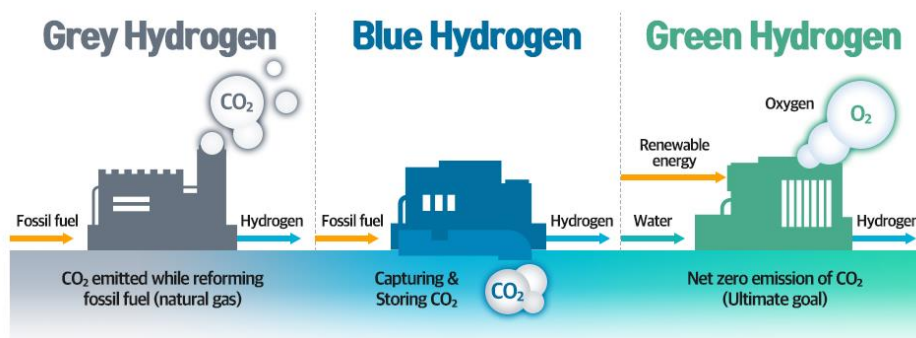


Figure 3: Hydrogen colour code [7]

The problem about this colour code is that it fails to determine precisely how clean can the hydrogen generated be; even though the threshold emission for green H₂ could be fixated as 4.4 kg CO_{2eq}/kg H₂ [8], the three-colour code itself does not accurately identify the amount of GHG emitted from the production process, the sub-systems and the lifecycle of the utilized equipment.

To solve this issue, Dawood F. et al [9] developed a more precise model using the concept of spectrum. As it can be seen on Figure 4 (next page), the cleanliness percentage of H₂ production ranges from the cleanest possible, in green, to the least clean possible, in grey. This cleanliness parameter has been named Hydrogen Cleanliness Index (HCI). Together with the spectrum, the model includes the Depth Of Assessment level, represented by the column on the right, for which the contribution of each part of the H₂ production process was given its own level, or "Scope".

Scope 1 considers the production process H₂ by itself, which depends on the energy source; Scope 2 considers indirect emissions, for example due to H₂ leaks; Scope 3 considers the life cycle of any third party equipment used in the process; Scope 4 considers the CO₂ emissions generated by the hydrogen purification process. Below, a picture of the described model.

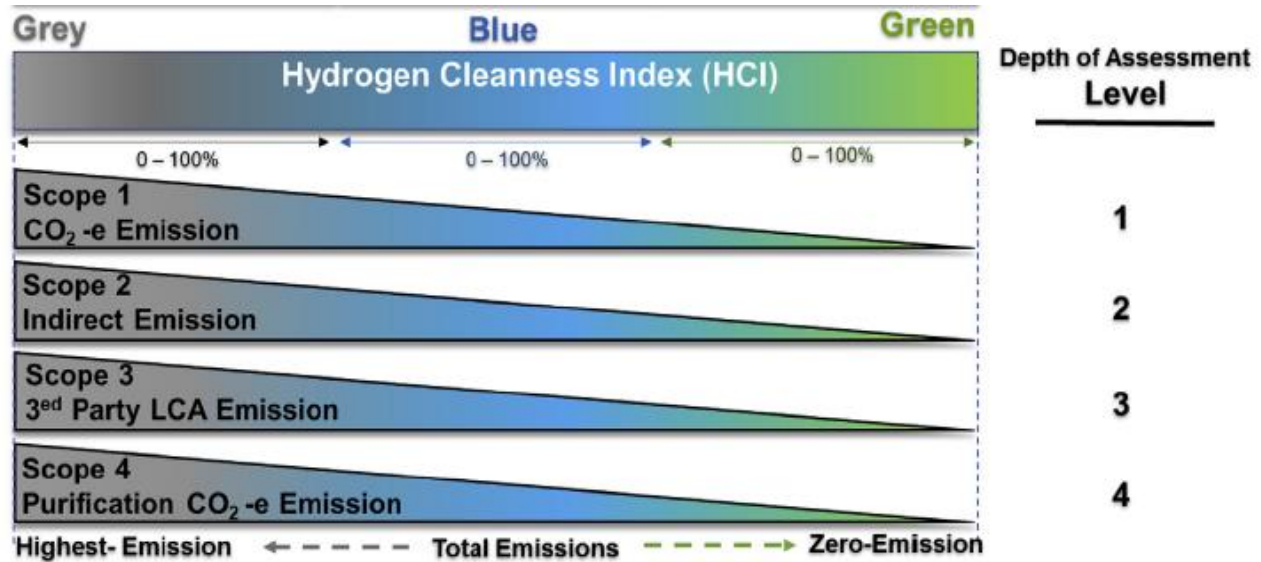


Figure 4: The hydrogen spectrum model: Hydrogen Cleanliness Index (HCI) [9]

1.2.2 Green hydrogen production methods

There are numerous methods to produce hydrogen; a comparative list of H₂ generation technologies is shown next page (Table 1).

CHALMERS UNIVERSITY OF TECHNOLOGY
Gothenburg, Sweden, December 2021
www.chalmers.se

Table 1: Summary of hydrogen production process category, feedstock and technology possibility

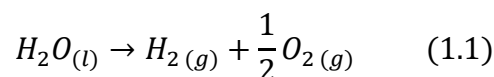
*Cleaness: Clean with no emissions (C), Non-clean with emissions (N), Quasi-clean by using Carbon Capture and Storage (CCS); **Technology maturity level (TML) [9]

Process Category	Energy I/P	Feedstock Hydrocarbons (H) Non-Hydrocarbons (N)	Technology	Eff. (%)	*Clean (C/N/CCS)	**TML (1–10)
Electrolysis	Electric	Water (N)	AE	62–82	C	9–10
		Brine (N)	PEM	67–84	C	7–9
			SOC	75–90	C	3–5
Electro-photolysis	Electric-Photonic	Water (N)	chlor-alkali	NA	C	2–42–4
		Water (N)/Algae (H)	Photoelectrochemical	0.5–12	C	1–2
		Microalgae	Photosynthesis	1.6–5	C/N	1–3
Biophotolysis	Bioenergy Photonic	Cyanobacteria	Photo-fermentation	<1	N	1–3
		Photosynthetic-Bacteria	Algal Hydrogen	1–3	N	1–3
		Fat (H)		2–7	N	1–3
Bioelectrolysis	Bioenergy Electric	Nutrients (H)		12–14	N	1–3
		Waste (H)/Biomass (H)			C/N	1–3
		Biomass (H)	Microbial electrolysis	70–80	N	1–3
Biolysis	Bioenergy	Hydrogenases	Nitrogen fixation	10		
		Microorganism	Dark fermentation	60–80	N	3–5
		Fermentative bacterias	Hydrolysis	NA	N	2–4
Bio-thermolysis	Bioenergy-Heat	Biomass (H)+Water (N)	Aqueous phase reforming	35–55	N	5–7
		CO (N) + Water (N)	Biological Shift Reaction	NA	N	2–4
		Biomass (H) (microwave) acid pretreated	Co-fermentation hydrothermal	NA	N	2–4
Thermolysis	Heat	Water (N)		35–45	N	1–3
		Biomass (H) (absence of O ₂)	Waterthermolysis	20–55	C	1–3
		Biomass (H)	Pyrolysis	35–50	N	8–10
		Coal (H)	Gasification	35–50	N	10
		Fuels (H)	Coal gasification	74–85	N/CCS	10
		Fuels (H)	Steam Reforming (SR)	60–85	N/CCS	10
		Biomass (H)	Membrane Reactors	64–90	N/CCS	7–9
		Methane (H)+CO ₂	Partial oxidation	60–75	N	7–9
			Autothermal	60–75	N	6–8
Thermo-electrolysis	Heat-Electric		CO ₂ Dry Reforming	NA	C/N	
		Fuels (H)	Plasma Reforming	9–85	N	1–3
		Water (N)	Redox	3–5 wt	C	4–6
Chemical	Chemical reaction	Metals (N)		NA	C	4–6
		Metal Hydrides (N)		NA	C/N	
		Gas-based hydrides (N)		NA	C	
Radiolysis	Radiation	Metal Hydroxides (N)				
		Hydrogen peroxide (H ₂ O ₂)	Radiolysis	NA	C	1–3
		γ-radiolysis				

It's possible to classify the green (renewable) H₂ production methods into two categories: water splitting methods and biomass processing methods.

The most known water splitting method existing, as well as the one of the most established, is electrolysis; its fundamentals will be described below.

The overall chemical reaction governing the process is the following:



The components required to achieve electrolysis are two electrodes, an electrolyte, and an external power source. Knowing this, the simplest electrolysis cell is an electrochemical chain created by the connection in series of three different parts: one electron conductor (anode), one ionic conductor (electrolyte), and a second electron conductor (cathode).

One of the most conventional configurations is composed of the two electrodes placed face-to-face in a liquid electrolyte, with a membrane placed in the interpolar gap; said membrane (also called diaphragm) prevents prevent the spontaneous recombination of the chemical products. The described configuration is shown below [10].

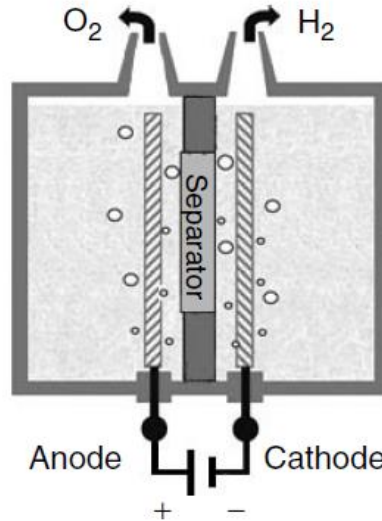
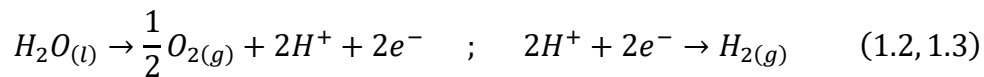


Figure 5: Alkaline water electrolyser schematics [10]

The overall reaction is known as a redox transformation: the anode is the electrode where an oxidation takes place, while the cathode is the electrode where a reduction takes place. The charge transfer process is driven by a power source, which applies a current through the electrolyte, supplying the electricity necessary to drive the water decomposition.

The hydrogen production via electrolysis described by Equation 1.1 is a process that occurs according to the two following half reactions:



Equation 1.2 and 1.3, which happen respectively at the anode and the cathode of the electrolysis cell, are called Oxygen Evolution Reaction, or OER (Equation 1.2) and Hydrogen Evolution Reaction, or HER (Equation 1.3).

From a thermodynamics standpoint, the chemical reaction which regulates the water splitting is a non-spontaneous one; the energy which needs to be supplied for said reaction to occur is equivalent to the enthalpy of formation of H_2O . The enthalpy variation of the overall reaction can be expressed by the following formula:

$$\Delta H(T, p) = \Delta G(T, p) + T \cdot \Delta S(T, p) \quad (1.4)$$

$T [K]$ represents the temperature, $\Delta S [J/K]$ the variation of entropy, while $\Delta G [J]$ the variation of Gibbs free energy associated with the reaction. All three variations, as indicated by the parenthesis, are function of the operating temperature and pressure.

ΔG can be expressed like so as well [11]:

$$\Delta G = -nFU_{rev} \quad (1.5)$$

The term n represents the electrons transferred in the reaction, F is the Faraday constant (96,485.34 [C/mol]) while U_{rev} [V], called reversible voltage or equilibrium voltage, is the lowest required voltage necessary for the chemical reaction to occur. Conventionally, U_{rev} is a positive value when the reaction is spontaneous [11]. Since, as mentioned before, the reaction is non-spontaneous, U_{rev} is negative, which in turn makes ΔG positive; this is coherent, since ΔG is positive for non-spontaneous reactions. It's possible to express the ΔG term in Equation 1.4 with the relation showed in Equation 1.5, obtaining the following formula:

$$\Delta H = (-nFU_{rev}) + T \cdot \Delta S \Rightarrow U_{rev} = \frac{\Delta H - T \cdot \Delta S}{-nF} = \frac{\Delta G}{-nF} \quad (1.6)$$

It's possible to define a second voltage, called thermoneutral voltage (U_{tn}), which represent the voltage related to the total energy demand ΔH for the considered chemical reaction (Equation 1.4):

$$U_{tn} = \frac{\Delta H}{-nF} \quad (1.7)$$

It's possible to calculate both U_{rev} and U_{tn} by choosing the operating temperature and pressure, and using the standard Gibbs free energy (ΔG°) and standard enthalpy (ΔH°). In STP (standard conditions: $T = 298$ K, $p = 1$ bar):

$$\Delta G_{H_2O}^\circ = 273.22 \left[\frac{kJ}{mol} \right] \Rightarrow |U_{rev,H_2O}| = \left| \frac{\Delta G_{H_2O}^\circ}{-nF} \right| = \frac{273.22 \left[\frac{kJ}{mol} \right]}{2 [mol] \cdot 96485.34 \left[\frac{C}{mol} \right]} = 1.23 [V] \quad (1.8)$$

$$\Delta H_{H_2O}^\circ = 285.84 \left[\frac{kJ}{mol} \right] \Rightarrow |U_{tn,H_2O}| = \left| \frac{\Delta H_{H_2O}^\circ}{-nF} \right| = \frac{285.84 \left[\frac{kJ}{mol} \right]}{2 [mol] \cdot 96485.34 \left[\frac{C}{mol} \right]} = 1.48 [V] \quad (1.9)$$

The difference between the two voltages, related to the minimum requirement for the reaction to happen, can be seen in the graph next page (Figure 6).

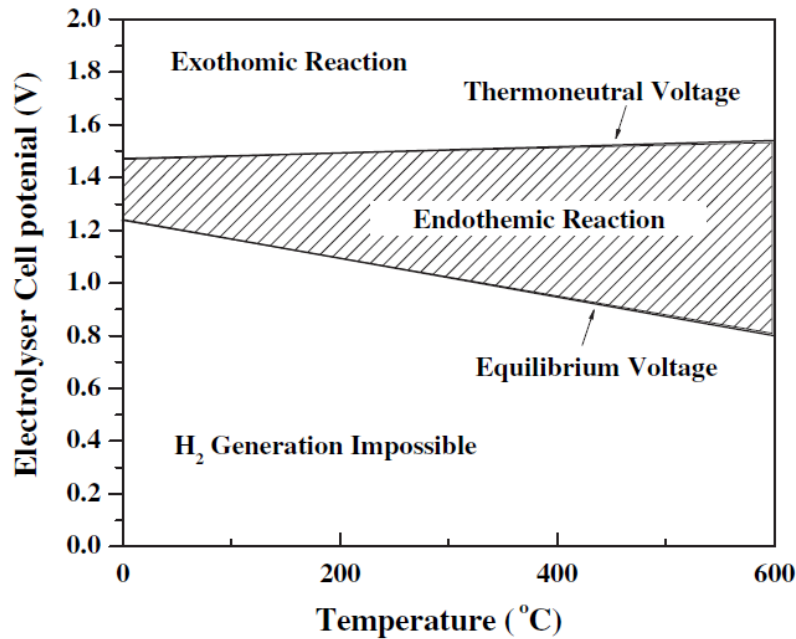


Figure 6: Equilibrium voltage and thermoneutral voltage against electrolysis cell temperature [12]

It's important to understand that, as mentioned before, the energy needed is equivalent to the enthalpy of formation of H_2O ; this means that, for the conditions chosen, the reaction requires $\Delta H_{H_2O}^\circ = 285.84 \left[\frac{kJ}{mol} \right]$ of energy. A part of it, represented by $\Delta G_{H_2O}^\circ = 272.22 \left[\frac{kJ}{mol} \right]$, will be electricity, while the rest, represented as $T \cdot \Delta S$, will be heat. This also explains why the electricity required, as well as the U_{rev} voltage, is reduced when the temperature grows, while the heat required increases. The U_{tn} required instead remains constant with the temperature, since the energy needed for the reaction to occur remains the same, even though it's partitioned differently between electricity and heat.

The voltage gap shown in Figure 6 represents the interval for which the electrolysis can occur, but as an endothermic reaction. For $U > U_{tn}$ the electrolysis can occur, but as an exothermic reaction, and so waste heat is produced; for $U < U_{rev}$ the electrolysis cannot occur at all. Knowing this, U_{rev} sets the minimum energy necessary to transform 1 mol of reactant (once the temperature is fixed), which is given by $\Delta G_{H_2O}^\circ$.

A satisfying value of operating current density needs to be reached for the chemical reaction to occur. For commercial water alkaline electrolyzers the range is $0.2 - 0.4 \text{ A/cm}^2$ [13]; in order to reach those values, and thus simultaneously reduce investment costs, it's not possible to perform the electrolysis so close to equilibrium: it is necessary to overcome different kinds of current inefficiencies, and in turn to have operating voltages higher than U_{rev} and U_{th} . The concept of reaching said higher voltages is called overvoltage, or overpotential; its characteristics won't be discussed for this work, since a deeper analysis of this (and related) phenomena prescinds the scope of this thesis.

The technology maturity level (TML) of electrolysis, shown in Table 1 (page 9), is fairly high, depending on its specific type. Alkaline water electrolysis (ALK) is the most mature technology of the electrolysis types, as indicated by its TML level (9-10), since it has been used by industry since the 1920s, particularly for chemistry processes such as chlorine manufacturing [14]. PEM electrolysis, whose TML level is slightly lower (7-9) is rapidly emerging, and even though its capital expenditure (CAPEX) is higher than the ALK's one, this cost is expected to be lowered in the future. The table below shows a comparison between the two technologies.

Table 2: Techno-economic characteristics of ALK and PEM electrolyzers (2017, 2025) [14]

Technology		ALK		PEM	
	Unit	2017	2025	2017	2025
Efficiency	kWh of electricity/ kg of H ₂	51	49	58	52
Efficiency (LHV)	%	65	68	57	64
Lifetime stack	Operating hours	80 000 h	90 000 h	40 000 h	50 000 h
CAPEX – total system cost (incl. power supply and installation costs)	EUR/kW	750	480	1 200	700
OPEX	% of initial CAPEX/year	2 %	2 %	2 %	2 %
CAPEX – stack replacement	EUR/kW	340	215	420	210
Typical output pressure*	Bar	Atmospheric	15	30	60
System lifetime	Years	20		20	

* Higher output pressure leads to lower downstream cost to pressurise the hydrogen for end use.

Solid oxide (SOC) electrolysis has the lowest TML (3-5) of the three electrolysis technologies. This is mainly due to its higher CAPEX and its need to operate at high temperature, which not only can cause difficulties, but also the only renewable sources that can be utilized for it are concentrated solar power and high temperature geothermal [14].

There are various other water splitting methods other than electrolysis.

Thermolysis is a water splitting H₂ generation method for which H₂O is heated to the point of which hydrogen and oxygen spontaneously decompose. In order to make this process possible, the Gibbs function variation ΔG must be equal to zero, and this happens only for very high temperatures, namely $T > 2500$ °C [15].

The TML of water-thermolysis shown in Table 1 indicates a very low level of maturity (1-3), since it has been proven difficult to reach a temperature that high using renewable energy sources only. Thermochemical water-splitting cycles have been proposed to overcome this issue, in order to lower the required temperature and improve the overall efficiency [15].

Photo-electrolysis is another water splitting H₂ generation method; it's a process in which the energy of light is absorbed and utilised to decompose water into H₂ and O₂ [16]. The TML of this process is even worse than water-thermolysis' (1-2); although the energy necessary to separate the H₂O molecule into hydrogen and oxygen is only 1.23 eV, the electron separation requires a high bandgap energy, which in turn makes the overall efficiency incredibly low [17].

As mentioned before, hydrogen can be generated not only via water splitting methods, but also via biomass processing methods, which can be further categorized into biological and thermochemical methods.

The most used biomass processing biological methods are bio-photolysis and fermentation. The former, which can be direct or indirect, is a technology that utilizes algae to produce H₂, since they possess hydrogenase, an enzyme which can catalyse the production of hydrogen (the process is similar to photosynthesis) [18]. The latter, which can be dark fermentation or photo fermentation, is a technology for which the carbohydrates present in the biomass are converted into organic acids and then into H₂. Dark and photo-fermentation can be deployed in sequence, in order to increase the efficiency of the overall process [18].

By looking again at Table 1 (page 9), it can be seen that both the TML and the efficiency of these processes is very low; the only exception seems to be dark fermentation, which has an efficiency of 60-80% and a TML of 3-5 (which is still low, but relatively higher compared with the other biological biomass processing methods).

The most used biomass processing thermochemical methods for H₂ production are pyrolysis and gasification. In the former process, the biomass is heated at a temperature range of 650-800 K, at 1-5 bar, in order to obtain charcoal, liquid oils and gaseous compounds [19]. In the latter process, the biomass is thermochemically converted into a gaseous fuel called syngas, using a medium such as O₂, air, and/or steam. The operating temperatures range from 800 to 1700 K, while the operating pressures can vary from 1 to 35 bar, depending on parameters such as the plant dimensions and the syngas end-uses [20]. In addition to these two methods, combustion and liquefaction can be alternatives, but they are usually frowned upon, considering the shortcoming of emitting polluting by-products (combustion) and having difficulty in achieving anaerobic operating pressures of 50-200 bar (liquefaction) [21].

The picture next page (Figure 7) summarizes the different methods to produce hydrogen from renewable sources:

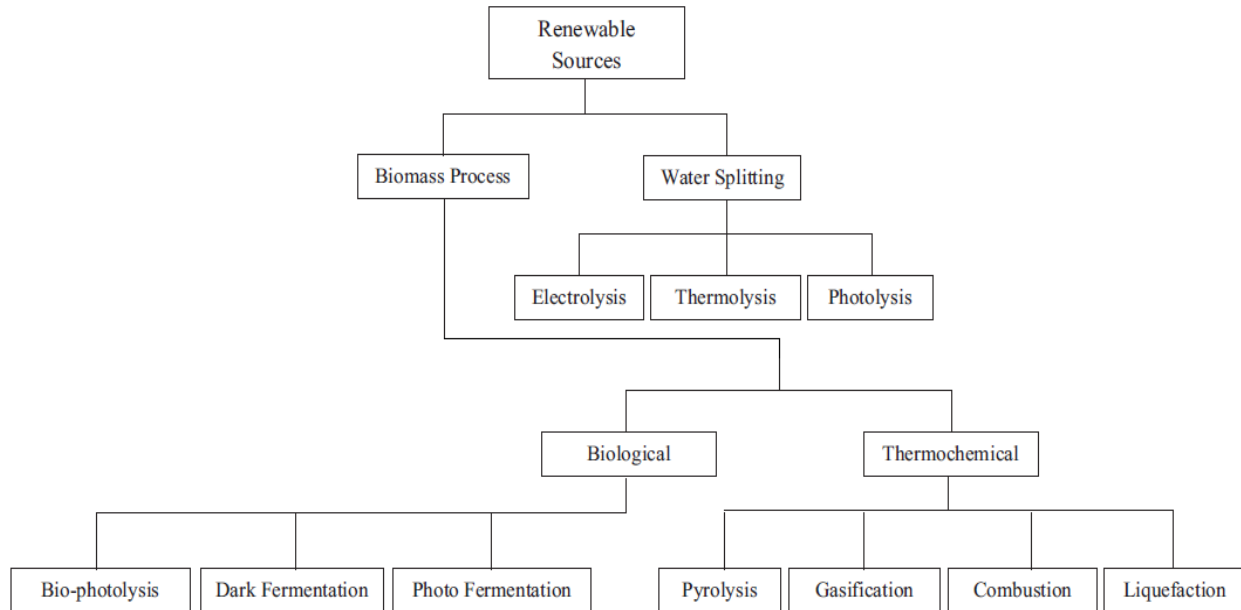


Figure 7: H_2 production methods from renewable sources [22]

1.2.3: H_2 density enhancement for storage systems

The biggest drawbacks of using hydrogen as a fuel are related to its storage. At NTP (Normal Temperature and Pressure, $T = 293.15 \text{ K}$, $p = 1.013 \text{ bar}$), the density of H_2 is 0.08375 kg/m^3 , which means that, in these conditions, a tank of almost 12 m^3 would be needed to store 1 kg of hydrogen only.

There are two ways to measure the density in regards as materials such as hydrogen: volumetric density and gravimetric density. The former refers to how many kg of hydrogen are contained per each m^3 ; it's often indicated as ρ_V . The latter refers to the weight percent of hydrogen, which can be also defined as the ratio of the between the stored gas and the mass of the containing vessel; it's often indicated as ρ_m , or wt%.

One of the most known H_2 storage method is to compress the hydrogen at high pressures in its gaseous phase [23]. The higher the pressure, the higher the density that can be reached; the function for which the density grows with the pressure can be seen next page (Figure 8).

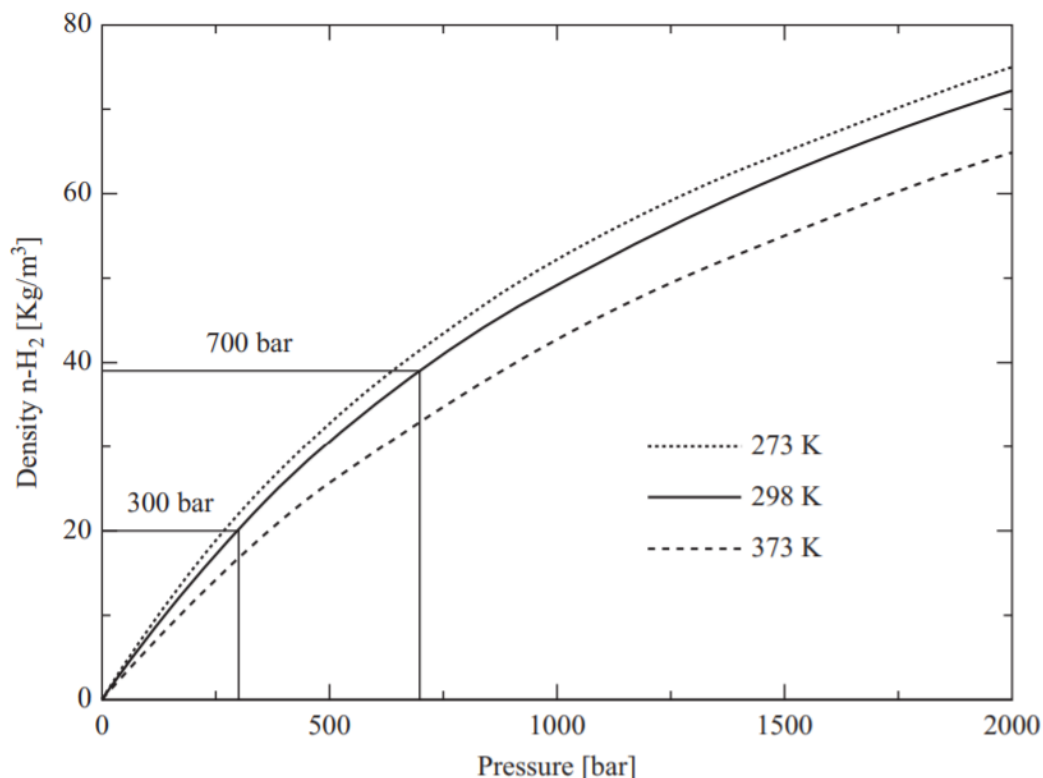


Figure 8: Evolution of H₂ volumetric density as a function of pressure, for three different temperatures [24]

At NTP, increasing the H₂ pressure to 300 bar brings the volumetric density to 20 kg/m³, which can be almost doubled bringing the pressure up to 700 bar. The gravimetric density obtained from this operation is 13 wt%. The tanks' material has to be able to withstand the high pressure levels; steel cylinders can withstand pressures up to 200 bar, while lightweight composite cylinders can withstand up to 800 bar [23]. The drawbacks of this method are the still relatively low hydrogen density, and the high gas pressures to maintain.

Another method to increase the H₂ density is to bring it to its liquid phase, at constant (ambient) pressure. The boiling point temperature of hydrogen is very low, -252.87 °C (20.28 K); in fact, liquid H₂ can only be stored in open systems: since there is no H₂ liquid phase that exists over its critical temperature, its pressure in a closed storage system could reach levels of 100,000 bar at room temperature.

The volumetric density obtained with the liquefaction process is 70.8 kg/m³, while the gravimetric density depends on the tank size. The most known liquefaction cycle is the Linde-Hampson cycle [25], shown next page (Figure 9). During this process, the gas is first compressed and then cooled in a heat exchanger, then it passes through a throttle valve, where it undergoes an isenthalpic Joule-Thomson expansion, after which liquid is produced.

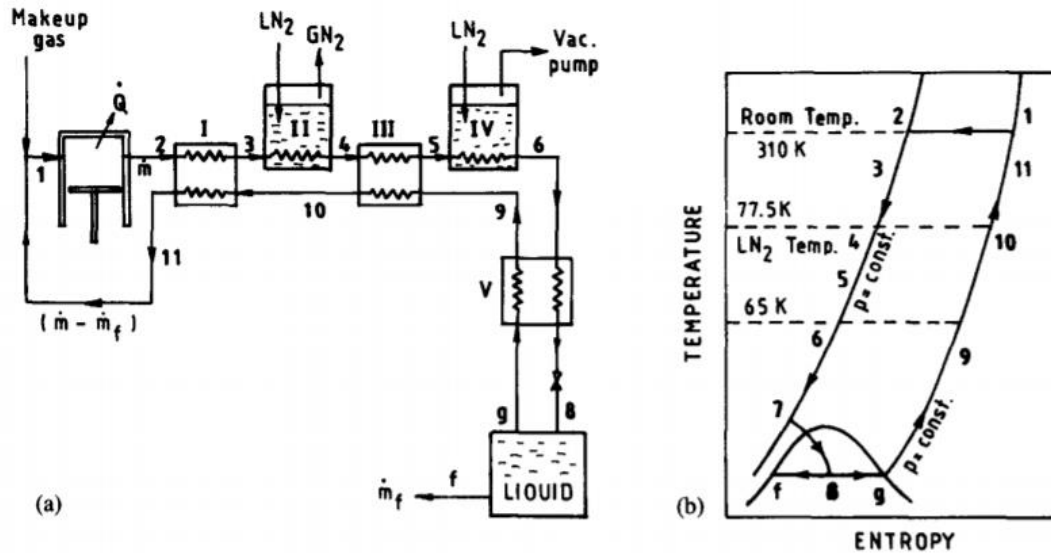


Figure 9: Linde-Hampson cycle [25]

Regarding the amount of work needed to increase the H₂ density, according to DOE Hydrogen and Fuel Cells Program Record [26], the theoretical energy to compress hydrogen isothermally to 700 bar is only 1.36 kWh/kg. However, greater compression energies are usually required, due to factors such as compressor inefficiencies, which bring the energy needed to the range of 1.7-6.4 kWh/kgH₂. Regarding the energy needed to liquefy H₂, the theoretical value needed (starting from NTP conditions) is 3.3 kWh/kg, but the actual range, depending on the size of the operation, was found to be 10-13 kWh/kg. For comparison, the LHV (lower heating value) of hydrogen is 33.3 kWh/kg, which means that the storage processes consume respectively 5-20% and 30-40% of H₂'s LHV.

The table below summarizes the characteristics of the two H₂ storage methods:

Table 3: H₂ storage methods characteristics [26]

Storage method	$\rho_V [kg_{H_2}/m^3]$	$\rho_m [mass\ %]$	$T [^\circ C]$	$p [bar]$	$W [kWh/kg_{H_2}]$
High pressure gas cylinders	20 – 40	13	25 (room temperature)	300 – 800	1.7 – 6.4
Liquid H ₂ in cryogenic tanks	70.8	tank size dependent	-252.87	1 (ambient pressure)	10 – 13

Another category of methods to increase the density of hydrogen, which could be characterized as “material storage methods”, include physisorption of hydrogen, reaction with metal and complex hydrides, and absorption on interstitial sites in a host metal. Their characteristics won't be covered, as they are not relevant to the scope of this thesis.

1.2.4: The Power-to-X concept

The term “Power-to-X” (P2X) refers to a multistage process for which electricity is transformed into a generic end use, product or application, indicated with the letter ‘X’. It is possible to utilise a more precise nomenclature if there is a known manufacturing aim for specific products, such as Power-To-Hydrogen (P2H) or Power-to-Methane; similarly, this denomination can be applied for a specific group of products, e.g. Power-to-Gas, Power-to-Heat, or for a specific sector, e.g. Power-to-Transport [27].

The term “Power” can refer to any kind of electricity production, but considering the scenario described in Chapter 1.1, the most relevant P2X systems completely (or at least extensively) utilize renewable energy sources to produce electricity.

Two very important parameters for P2X chains are H₂O and CO₂. For the former, water treatment is especially significant for electrolysis, since the impurities found in tap water make it an unacceptable resource for the process. Also, since large quantities of H₂O are required to produce a significant amount of hydrogen via electrolysis (to produce 1 kg of H₂, AEL and SOC electrolyzers require around 10 litres of de-ionized water, while PEM electrolyzers require around 18 litres [28]), it’s necessary to consider a location for which water scarcity would not become an issue once the electrolyser is installed. For the latter, the integration of captured CO₂ into P2X processes offers the possibility to avoid its direct emission into the atmosphere by converting into useful products, a process which contributes to a circular economy [29].

A picture representing Power-to-X towards carbon neutral fuels can be seen below, while the most common Power-to-X pathways are shown next page (Figure 11).

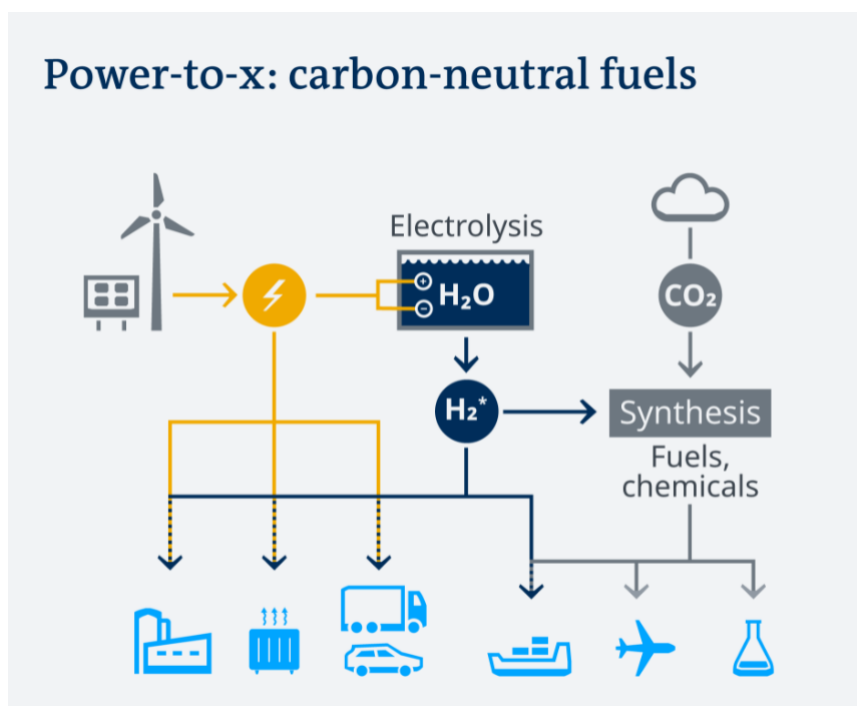


Figure 10: Power to x towards carbon-neutral fuels [30]

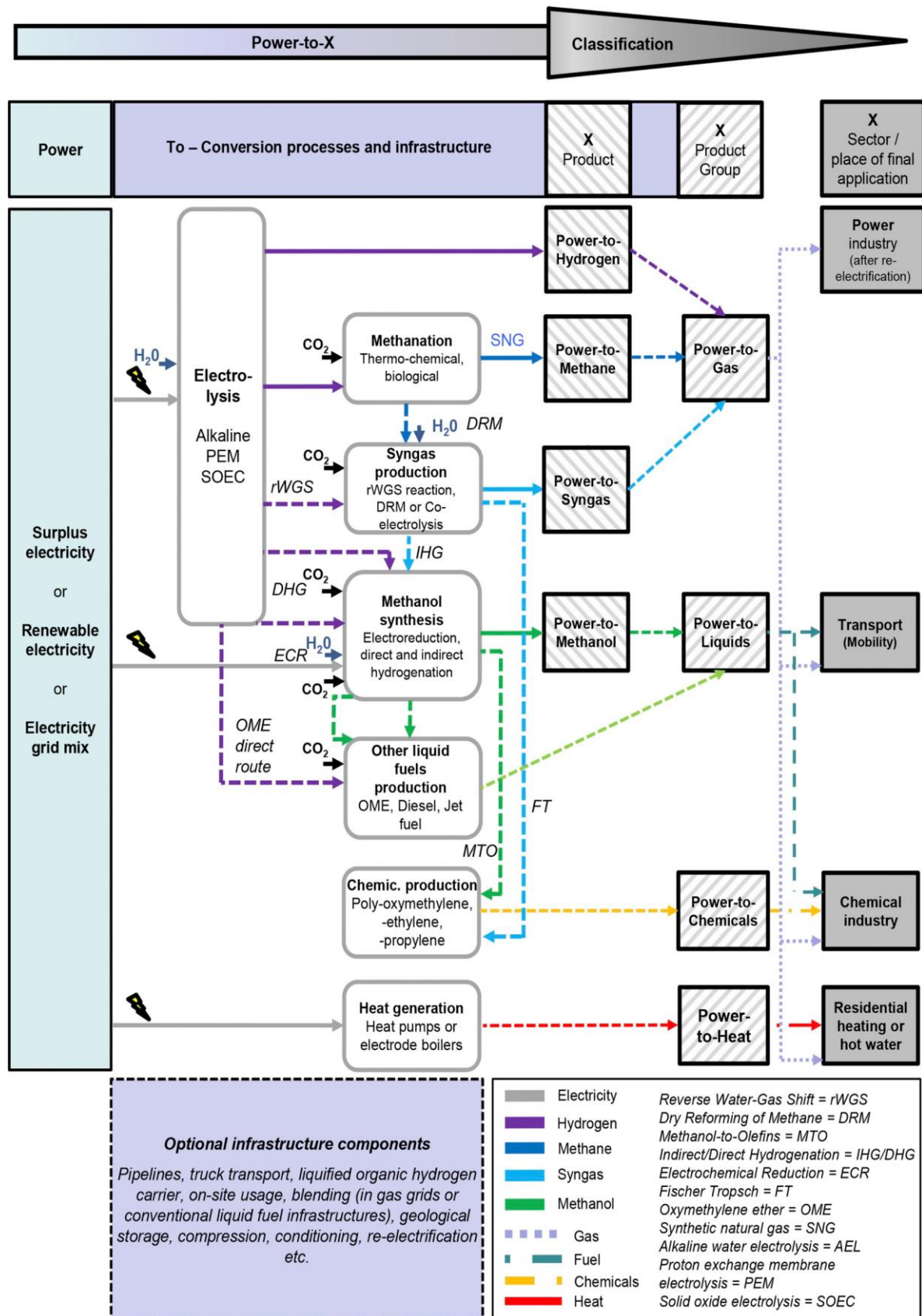


Figure 11: Power-to-X pathways [31]

By looking at Figure 11 (previous page), it is possible to see the importance of hydrogen for the Power-to-X pathways, since its presence, indicated by purple arrows, is required to manufacture many of the product/product groups of P2X chains.

Even though for the scope of this work it's assumed that only renewable sources will be utilised, and so the aim would be to not produce any CO₂ (at least directly), it's possible to understand why the concept of P2X gained so much attention in the latest years. By integrating the hydrogenation process into P2X chains, which is a chemical reaction between H₂ and another compound (namely CO₂), it's possible to convert carbon dioxide into useful fuels/chemicals, as shown below.

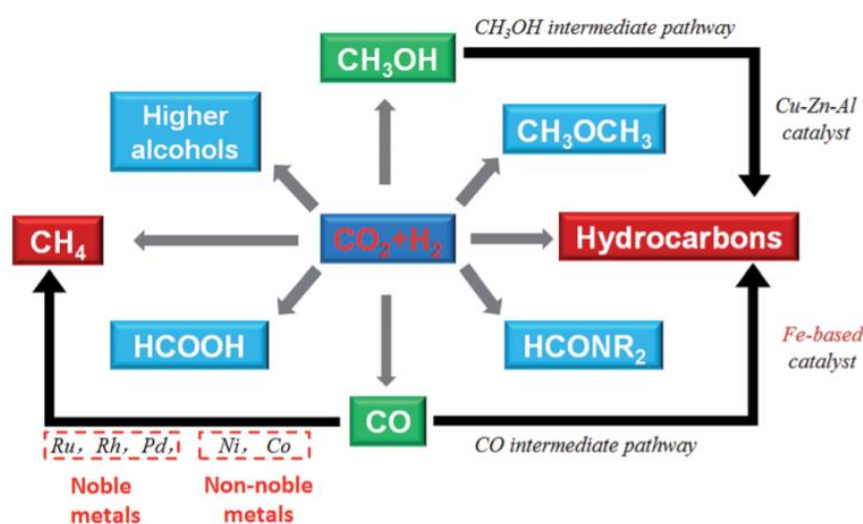


Figure 12: CO₂ conversion into useful products through hydrogenation [32]

1.2.5 Hydrogen based economy: H₂ end-uses

Even though green H₂ utilisation is the most suitable path for a fully sustainable energy transition, the quantity of hydrogen produced via electrolysis is only 5% globally, and only a small part of it is generated using renewable sources. This is mainly due to its high production costs, the energy losses from the various conversion processes necessary to generate it, and a general lack of dedicated infrastructure.

However there are also many advantages to switching towards a hydrogen-based economy [100]:

- The price of electricity procured from solar PV and wind power plants has been substantially declining, which makes the production of green H₂ increasingly attractive from an economic standpoint.
- With the declining costs of the H₂ production process chain, the technologies have proven to be ready to be scaled up. The capital costs of electrolyzers have fallen by 60% since 2010 (which in turn reduced the price of H₂/kg), while the cost of fuel cell vehicles has decreased by at least 70% since 200.

- With the increase of variable renewable energy utilised in the energy sector, power systems are going to need for flexibility, which can be provided by the electrolyzers, which can quickly ramp up or down to compensate for fluctuations in the demand.
- Various countries chose to adopt net-zero emission goals, such as the SDGs discussed in chapter 1.1 of this work: green H₂ can play an important role in the achievement of said objectives.
- The use of hydrogen was mainly focused on the transportation sector in the past, while this more recent wave of green H₂ interest includes the usage of hydrogen throughout the whole energy sector, including the conversion of H₂ into other useful products (as mentioned in the end of chapter 1.2.4 of this work).

To summarize the last point of the previous list, hydrogen is a very versatile product. A representative picture of the many different applications for which the energy carrier can be used is shown below.

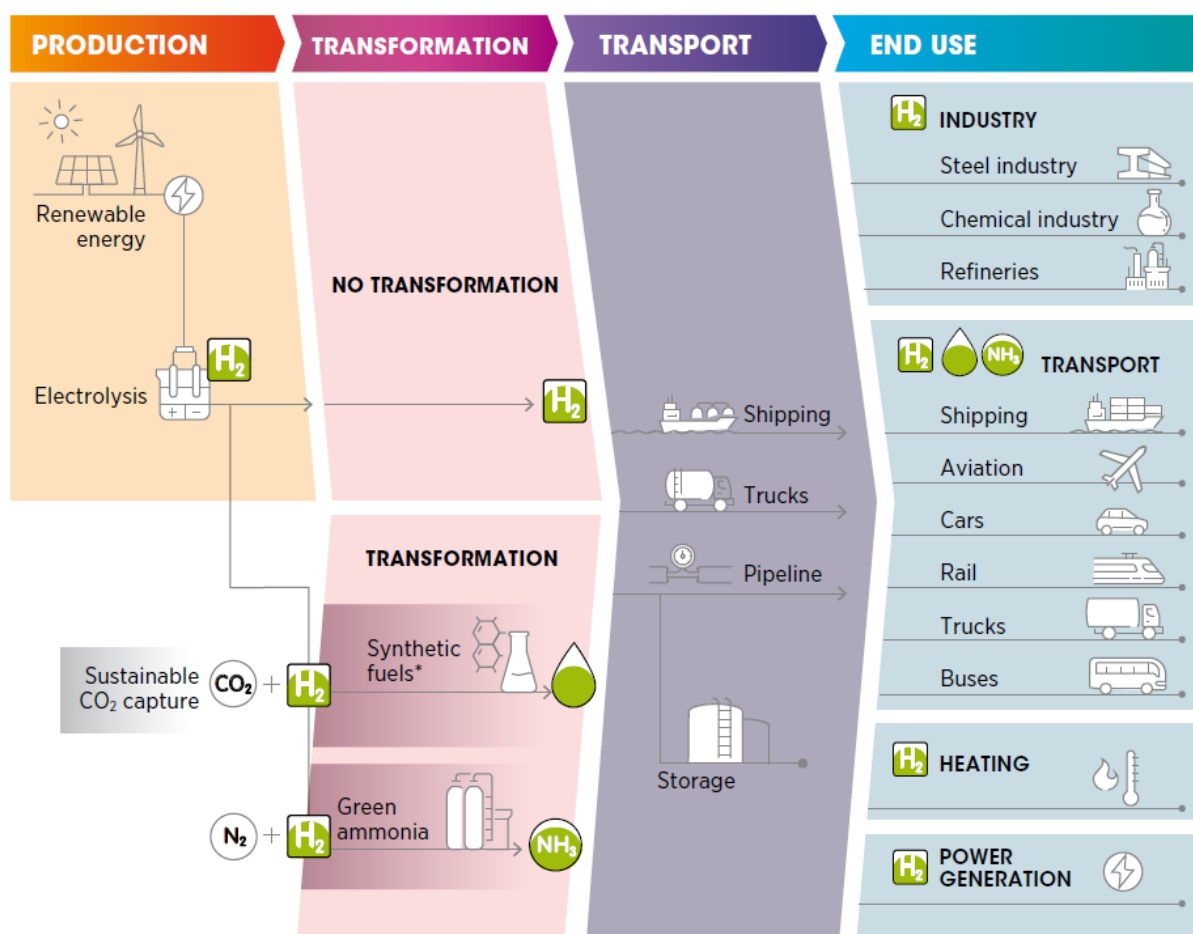


Figure 13: Green hydrogen production, conversion and end-uses across the energy system [100]

It is important to understand that, even though the utilisation of green hydrogen has great potential, it is not the only decarbonisation alternative. An example of this could be the transport sector, for which the declining cost and technological improvement of batteries have made electric powered vehicles an attractive solution for the decarbonisation of said sector [100].

Below, a picture that show how green hydrogen acts as a complement to alternative ways of generating a carbon-free future.










	RENEWABLES 	DIRECT ELECTRIFICATION 	ENERGY EFFICIENCY 	GREEN HYDROGEN 
HEATING 	<ul style="list-style-type: none"> Solar water heaters, direct geothermal use, biomass (low-grade heating) 	<ul style="list-style-type: none"> Heat pumps 	<ul style="list-style-type: none"> Retrofit of buildings Technological advancement 	<ul style="list-style-type: none"> High-grade heating
INDUSTRY 	<ul style="list-style-type: none"> Solar drying, biomass (productive uses) 	<ul style="list-style-type: none"> Electric industrial application (e.g. arc furnaces) 	<ul style="list-style-type: none"> Use of best available technologies 	<ul style="list-style-type: none"> Steelmaking refineries Chemical industry
LAND TRANSPORT 	<ul style="list-style-type: none"> Biofuels 	<ul style="list-style-type: none"> Battery electric vehicles 	<ul style="list-style-type: none"> Performance standards Travel avoidance Engine design 	<ul style="list-style-type: none"> FCEVs
SHIPPING 	<ul style="list-style-type: none"> Biofuels Wind energy 	<ul style="list-style-type: none"> Short-distance shipping 	<ul style="list-style-type: none"> Ship design Operation optimisation Travel avoidance 	<ul style="list-style-type: none"> Green ammonia Methanol
AVIATION 	<ul style="list-style-type: none"> Biojet fuels 	<ul style="list-style-type: none"> Short-distance aviation 	<ul style="list-style-type: none"> Plane design Travel avoidance 	<ul style="list-style-type: none"> Hydrogen and synthetic fuels for aviation

Figure 14: Hydrogen as a complement to alternative ways to decarbonise end uses [100]

1.3: Economic indicators

1.3.1: Levelized Cost Of Energy/Hydrogen

To understand the feasibility of an investment it's possible to utilise economic indicators which can help predict the best course of action. Since this master's thesis work focuses on the energy field, the first tool that comes to mind is the Levelized Cost Of Energy (LCOE). This indicator is defined as the ratio between the costs necessary to build and operate a power generating asset (e.g. a power plant) over its lifetime, and the total energy output of said plant, over its lifetime [33].

The LCOE can be expressed by the following formula:

$$LCOE = \frac{\text{Total costs}_{lifetime}[EUR]}{\text{Energy produced}_{lifetime}[kWh]} = \sum_n \frac{C_n + O_n + M_n + F_n}{(1+r)^n} / \sum_n \frac{E_n}{(1+r)^n} \quad (1.10)$$

The values C_n , O_n , M_n , F_n respectively indicate the capital, operating, maintenance and fuel cost, while the E_n value represents the energy produced. The subscript “n” indicates that said variables they are calculated over a year, while the sum \sum_n indicates that both the numerator and denominator are calculated over the whole lifetime of the asset. Finally, the r value is the discount rate; the $(1+r)^n$ term indicates how much this rate (assumed to be constant, but this can vary) influences the various costs and the energy production over the lifetime of the asset.

The LCOE is useful to compare different methods of energy production of a potential plant, in order to see which one would be the most profitable/least expensive over the considered time period. Even though it does not represent the actual cost of the energy (electricity), it is a useful tool from an investment point of view, as long as the assumptions made for the cost used to calculate it are acceptable.

Even though the E in the LCOE acronym stands for “Energy”, it’s mainly associated to “Electricity”, since that’s usually the main end-product of power plants. However this tool can be used in the same way for other end-products, such as heat or hydrogen. An example of the latter (Levelized Cost of Hydrogen, LCOH) can be found in Chapter 5 of IRENA’s 2019 report, “Hydrogen: A Renewable Energy Perspective” [34]. IRENA, which stands for International Renewable ENergy Agency, is an intergovernmental organisation that supports countries in their transition to a sustainable energy future, by promoting the widespread adoption of all forms of renewable energy [34].

The competitiveness of green H₂ in the energy market mainly depends on three factors: the electrolyser capital costs, the LCOE of the renewable energy necessary to use it, and its load factor (number of yearly operating hours). It has been shown that, even with a low enough renewable LCOE, green H₂ is currently not as competitive as blue/grey H₂. However, considering the expected decrease of electrolyser capital costs and renewable electricity, IRENA’s projections (Figure 15, next page) show that green H₂ could become a very competitive product, especially considering the increase of not captured CO₂ prices, which would noticeably elevate the price of grey H₂ [34].

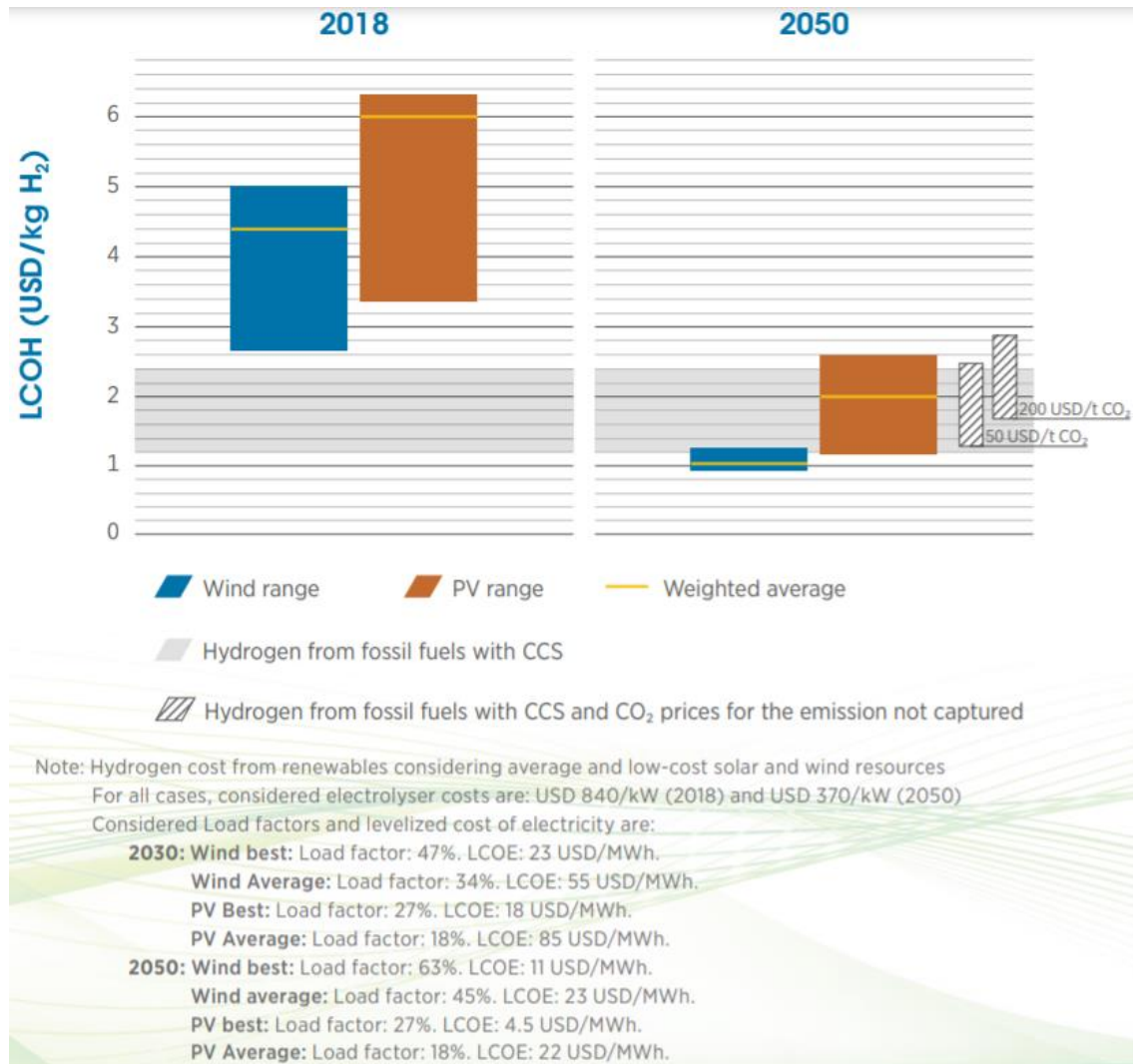


Figure 15: Irena's LCOH comparison between the current scenario (2018) and the 2050 projection [34]

1.3.2 PayBack Period and Discounted PayBack Period

The PayBack Period (PBP) is defined as the time required to earn back the amount of money expended in an investment, or at least to reach the break-even point, which is defined as the moment in which total costs and revenues are equal, all the predicted expenses are paid, and there is no profit nor loss [35]. The PBP is measured in years, and the method to calculate it is the ratio between the expected costs/investments of a project and its annual revenues.

$$PBP [\text{year}] = \frac{\text{Expected costs [EUR]}}{\text{Annual revenues [EUR/year]}} \quad (1.11)$$

The cases in which both the expected costs and the annual revenue are constant are simple to calculate, e.g. an investment of a machinery with negligible operating costs that brings a constant revenue each year. Of course both the expected costs and the annual revenues can vary throughout the years; this however doesn't affect the PBP calculation method.

The main advantage of the PBP tool is that it's simple and intuitive, thus gives important information about an economic scenario in an easy to understand way. That being said, it suffers from the following drawbacks:

1. The tool does not take into consideration the investment's lifespan: even if the PBP of a certain asset is low (hence, advantageous), if its lifespan is relatively short it won't be a good investment, even if it could seem so by looking only at the PBP itself.
2. Additional cash flows may arise from an investment after a full payback/break-even point has been reached, and those are not considered by the PBP.
3. The formula is too simplistic to account for the various cash flows that can arise within the acquisition of an asset, e.g. a multi-stage investment process.
4. The tool does not take profitability into consideration: the PBP of a certain asset might be short, but if the overall revenue that can be gained from it is relatively low, it could be better to invest into an asset which has a bigger PBP but also higher long term profitability.
5. The PBP does not consider the time value of money, since the revenue generated in later times might be worth less (or more) than current period earnings.

The notion of time value of money is based on the widely accepted assumption that money has different value according to the period in which one owns it [36]. To put it in another way, it's more advantageous to obtain a certain sum of money today than in two years, since its potential interest value could make it so that in two years said sum could be bigger.

This concept is extremely important when considering an investment, which is the reason why an improvement to the PBP tool was created, the Discounted PayBack Period, or DPBP. The difference between the two tools is simple: the latter takes into consideration the time value of money, which means that the considered cash flows are discounted back to their present value before the calculation [35]. Since this discounting mechanism is not applied for the PBP, the DPBP will always be higher than its corresponding PBP.

The steps necessary to calculate the DPBP are the following:

- 1) The starting point will be the considered investment cost, or expected cash outflow, which will be assigned to the "year 0" (zero), since no amount of time passed and nothing was gained yet. This value, conventionally, is negative.
- 2) Each subsequent year, the investment will generate a certain amount of money, which can be called expected cash inflow. These values, conventionally, are positive.
- 3) For each year (except year 0), the expected cash inflow must be multiplied by the applicable discount rate, thus generating the annual discounted cash flow.
- 4) The discounted cash flow is accumulated, which means that the more time will pass, the more the sum of the initial investment (expected cash outflow) and the accumulated discounted cash inflow will grow, getting closer to zero.
- 5) After a certain number of years, the sum described in step 4) will become positive: the corresponding year for which this happened can be considered the DPBP value

The DPBP is a slightly more precise tool to evaluate an investment, but it only resolves the last (5.) of the previously described drawbacks.

1.3.3 Net Present Value and Internal Rate of Return

As mentioned in the previous chapter, the concept of time value of money is very important in economics, since it takes into consideration the potential of having a certain sum of money in the present rather than in the future. It's possible to measure this potential by utilizing the present value (PV), which is defined as the worth of a certain cash flow at the moment of its assessment [36]. As mentioned before, the PV is usually lower than its future value (FV), due to the interest-earning potential of money; an exception to this are periods of zero/negative interest rates. The formula to calculate the PV is below.

$$PV = \frac{C}{(1 + r)^n} \quad (1.12)$$

The C value represents the cash flow, while r is the discount rate (or return), and n is the number of years after which the sum will be obtained.

An example of this would be the knowledge of obtaining 500 € in six years; assuming to have a return of 15%, the PV can be computed like so:

$$PV = \frac{500}{(1 + 0.15)^6} = 216.16 \text{ €}$$

When planning an investment it's fair to assume that, for each year of the considered time period, there is going to be an overall cashflow, derived from the various expenditures and earnings of that year. Knowing this, it's possible to calculate the PV of each one of said cashflows. The Net Present Value (NPV) is defined as the sum of the beforementioned present values, and the formula to calculate it is the following [37]:

$$PV_n = \frac{C_n}{(1 + r)^n} \Rightarrow NPV = \sum_{n=0}^N \frac{C_n}{(1 + r)^n} = \sum_{n=1}^N \frac{C_n}{(1 + r)^n} - C_0 \quad (1.13)$$

In the NPV formula (Equation 1.13, previous page), N is the number of years considered for the investment; for $n = 0$, $(1 + r)^n = 1$, while C_0 is almost always a negative value, since it represents the typical large negative cash flow of a capital investment.

The NPV can be seen as an indicator of the added value of an investment. If the calculated NPV is higher than zero, it means that the considered investment would bring a profit, assuming that relevant factors (such as its risk) were appropriately evaluated. If, instead, the NPV is lower than zero, it means that the investment won't be profitable. A NVP equal to zero represents an investment that brings no monetary value, and thus the decision to accept it or not should be based on other factors.

The role of the discount rate in the NPV calculation is crucial. There are various ways to set it: some companies utilize a weighted average cost of capital, a rate that companies are expected to pay (on average) to their holders to secure their assets; some companies set higher discount rates in order to adjust for risk and other variables [38].

CHALMERS UNIVERSITY OF TECHNOLOGY
Gothenburg, Sweden, December 2021
www.chalmers.se

The return value can also be set in a way that external factors such as risk and inflation are excluded from the calculation; this is done by utilising the Internal Rate of Return (IRR), whose name (“internal”) underlines said exclusion. The IRR is defined as the discount rate for which the NPV is equal to zero, as it’s shown in the following equation:

$$\sum_{n=0}^N \frac{C_n}{(1+r)^n} = 0 \quad \Rightarrow \quad r = IRR \quad (1.14)$$

The IRR is useful when comparing the profitability of possible new investments; as a rule of thumb, the higher the IRR, the more desirable is to undertake the project. The difference between this tool and NPV is that the former is a measure of a project’s profitability, while the latter measures the added value of a potential new asset.

The IRR calculation is essentially the mathematical problem of finding the n roots of the equation $NPV(r) = 0$. Since n can get quite high, there are various numerical methods that can be used to estimate it; said methods are often built-in functions implemented in softwares such as Microsoft Excel.

2. The HSY Ämmässuo eco-industrial centre

2.1 Overview

The Ämmässuo eco-industrial centre is a circular economy site where the Helsinki Region Environmental Services Authority arranges the treatment of waste for producing landfill gas, biogas and compost, as well as the disposal of municipal waste. The biogas is produced via anaerobic digestion, and it's utilised in a biogas power plant; there are also present a gas power plant that utilises landfill gas, a station used to accept and sort various types of waste (Sortti Station), and sites used to treat ash and slag [39].

The Helsinki Region Environmental Services Authority's Finnish name is Helsingin Seudun Ympäristöpalvelut; it will be later referred to as regional authority, municipal federation, or simply HSY.

The eco-centre began its operations in 1987 as a waste treatment centre, and it has been managed by HSY since then. Thanks to the regional authority, the centre has been continuously developing its equipment and processes: a new composting facility was completed in 2007, a landfill gas power plant was installed in 2010, and a biogas plant was built in 2015. The Ämmässuo waste treatment centre is the largest in the Nordic countries, and among the largest in Europe [40].

Currently, Ämmässuo has two landfills; the oldest one's growth has been completely stopped, while the filling of the second one is very scarce. Even though the landfill gas has been an important resource to the eco-centre for many years, the recent shift towards waste-to-energy has dramatically reduced the amount of municipal waste landfilled and consequentially utilized to produce the gas. Also, the recent legislation regarding landfills, specifically the ban of landfilling organic and plastic waste that came into force in 2016 [41], has reduced the quantity of municipal waste that can be accumulated in this manner.

The beforementioned reduction can be seen from the picture next page (Figure 14), which shows the amount of gas generated in Ämmässuo between 2007 and 2020 from both the old and the new landfill (the green line represents the cumulative amount). It's interesting to notice that, around 2008, the quantity of gas was so high (more than $4,000 \text{ m}^3/\text{h}$) that the centre by itself could produce more than one third of the natural gas generated in the entire country of Finland [42].

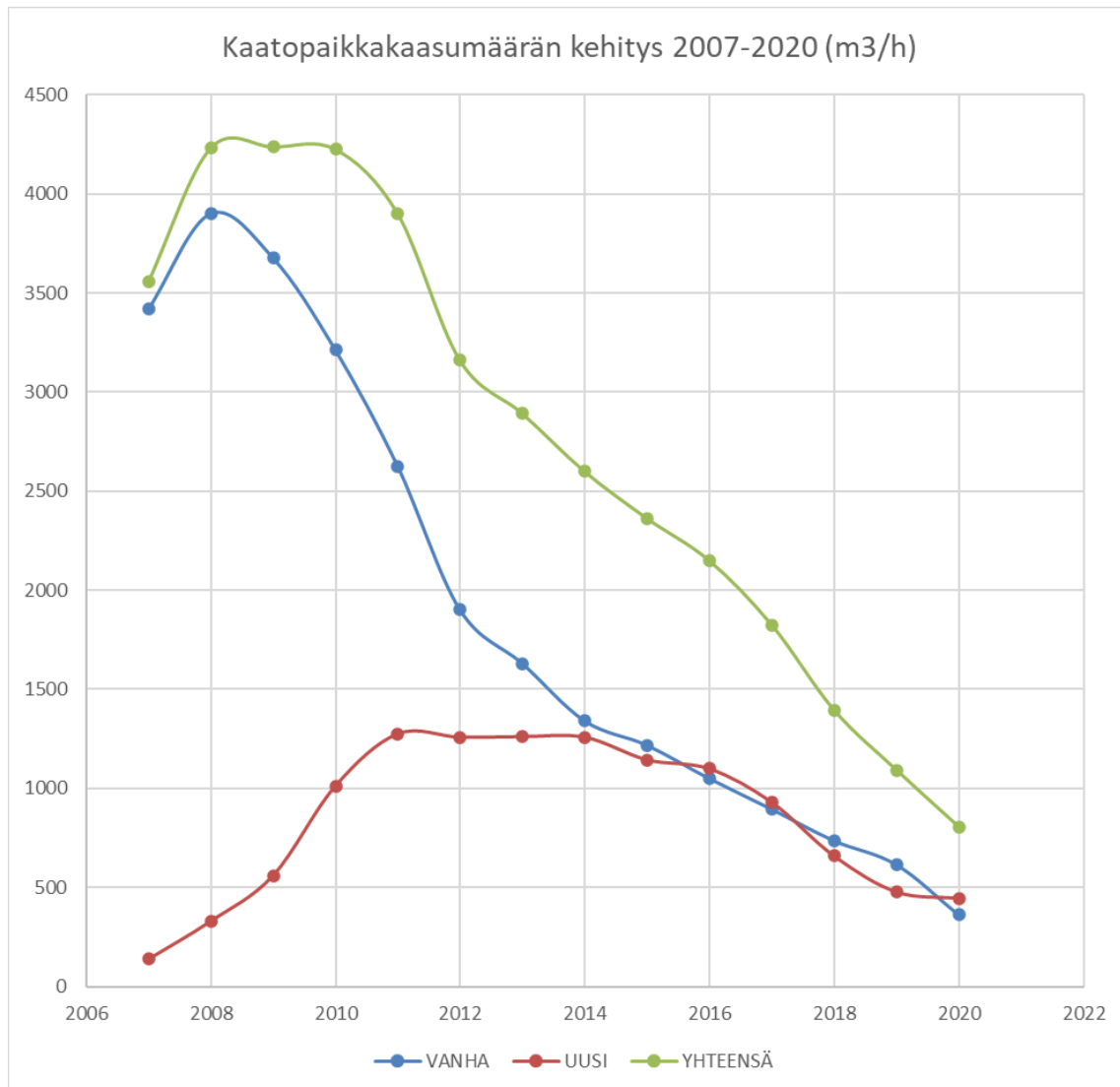


Figure 16: Amount of landfill gas [m³/h] produced in Ämmässuo between 2007 and 2020 [42]
Blue line: old landfill. Red line: new landfill. Green line: cumulative amount

Data such as the energy obtained from this resource will be analysed more in detail in the following chapters. This picture, however, can be helpful to visualize the future situation in which the landfill gas won't be a reliable resource of energy for the eco-centre. Even though the amount produced is still not negligible, this situation leaves the site with a gap which menaces its energy self-sufficiency. The main goal of this work will be to analyse possible scenarios in which this future energy gap can be filled utilizing renewable energy sources.

2.2 Current resources

2.2.1 Landfill gas and biogas production

As mentioned in the previous chapter, two of the main resources of the Ämmässuo eco-centre are landfill gas and biogas. The products are very similar: landfill gas is defined as the raw high methane content gas generated from landfill processing (as the name implies), while biogas is defined as the unfiltered and un-purified methane gas produced by the breakdown of organic matter.

The process used to produce them is essentially the same (anaerobic digestion); the key difference between the two is the amount of trace impurities, which is usually higher in landfill gas. One of the most common harmful trace compounds is siloxane, which can cause problems to gas engines due to the hard deposit that it generates within the engines [43].

The collection of landfill gas in Ämmässuo began around 1990 to reduce emissions in the area. Originally the gas was simply burned, but from 2004 it started being used to produce district heating, utilising the Kivenlahti power plant. In 2010 HSY built a cogeneration plant in the area, in order to utilise the landfill gas to produce electricity and heat for the centre [44][45].

The combined heat and power (CHP) landfill gas-power plant originally utilised four MWM TCG 2032 16V gas engines, for a total rated output of 15.4 MW. Currently, due to the landfill gas reduction, only one of the engines is running, and not even at full capacity. Considering that, regardless of its pace, this reduction will continue in the following years, HSY is considering selling or scrapping the engines, even though an official decision has not already been made [44]. The table below summarizes the characteristics of the beforementioned engines [46].

Table 4: Characteristics of the MWM TCG 2032 16V gas engines installed at Ämmässuo [46]

Biogas, Landfill Gas, and Sewage Gas Applications, $\text{NO}_x \leq 500 \text{ mg/Nm}^3$ *			
Engine type		TCG 2032 V16 X = Optimized for operation with biogases	
		50 Hz	60 Hz**
Electrical output	kW	3770	3510
Mean effective pressure	bar	17.0	17.0
Thermal output $\pm 8\%$	kW	3196	2880
Electrical efficiency	%	43.0	43.3
Thermal efficiency	%	41.9	40.6
Total efficiency	%	84.9	83.9
Power to heat ratio***		1.03	1.07

The Ämmässuo biogas power plant was commissioned in 2016; it has two engines, and it utilizes the biogas generated in the anaerobic digestion process to produce electricity and heat. Currently, the amount of biogas produced is enough for operating only one of the two engines, and so the second one is in reserve [44]. Since this is the second combined heat and power plant of the centre, from now on it will be referred as CHP2, while the landfill gas power plant will be referred as CHP1.

In order to increase the efficiency of both CHP power plants, an Organic Rankine Cycle (ORC) was implemented in their system. The mechanism of this cycle allows to recover waste heat from the exhaust gases of the main cycle. To increase the performance of the ORC, the organic liquid hexamethyldisiloxane is utilised instead of water as the circulating medium, allowing to profit from low-temperature heat sources.

The ORC starts with the circulating medium is pumped to the evaporator using a pump, passing through a regenerator. There, the working fluid receives the heat from the exhaust gases from the main thermodynamic cycle, changing phase from liquid to gaseous in the process. The fluid is then sent to a turbine, which is used to generate electricity. After the turbine expansion, the working fluid passes through the regenerator again, transferring its heat to the branch going in the evaporator, thus increasing the efficiency of the ORC. Finally, the condensation of the working fluid at the condenser closes this secondary cycle, where low temperature heat can be collected with an appropriate cogeneration system. Most of the heat produced in the Ämmässuo biogas power plant is led to the district heating network, and part of it is also fed directly into the internal cycle of the composting plant's treatment operations. Below, a representation of the described ORC [47].

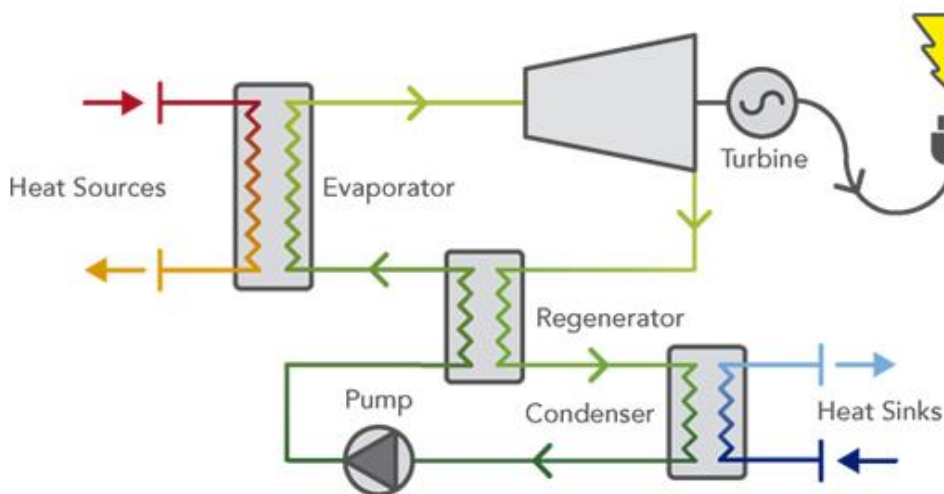


Figure 17: Organic Rankine Cycle (ORC) representation [47]

According to HSY's annual statistics for waste management in the Helsinki metropolitan area [48], the amount of landfill gas and biogas produced from 2016 to 2020 in the eco-centre was the following:

*Table 5: Landfill gas and biogas produced and utilised in the Ämmässuo eco-centre from 2016 to 2020 [48]
 Nm^3 = cubic meters at normal conditions (temperature of 20 °C, pressure of 1 atm)*

	2016	2017	2018	2019	2020
Landfill gas [kNm^3] = $10^3 \cdot [Nm^3]$					
Produced	37980	31980	24320	19140	14100
Utilised	34800	27280	23240	18630	13540
Biogas [kNm^3] = $10^3 \cdot [Nm^3]$					
Produced	4140	5090	4240	5100	4630
Utilised	3440	4530	3890	4830	4550

The landfill gas data from Table 5 confirms the trend shown in Figure 14 (Chapter 2.1 of this work). The data about the biogas (lower section of Table 5) shows instead a production (hence consumption) trend which is essentially stable, even if there is a slightly oscillating pattern. This information about the landfill gas and the biogas confirms the future unreliability as an energy source of the former, and the reliability of the latter, even if the biogas amount was substantially lower in the considered years.

2.2.2 Electricity production

The Ämmässuo eco-centre currently utilises its two gas-powered power plants (CHP1, CHP2) to produce energy. CHP2 was commissioned in 2016, so it started generating energy from 2017 onward; before that, CHP1 was the main source. Regarding electricity, a connection to the grid allows the eco-centre to purchase it, as well as sell it if there is a surplus. Using the data requested from the HSY municipal federation, which has also been used by Lehteva V. in his work, it's possible to visualize (next page, Figure 18 and 19) the electricity production of the eco-centre [49].

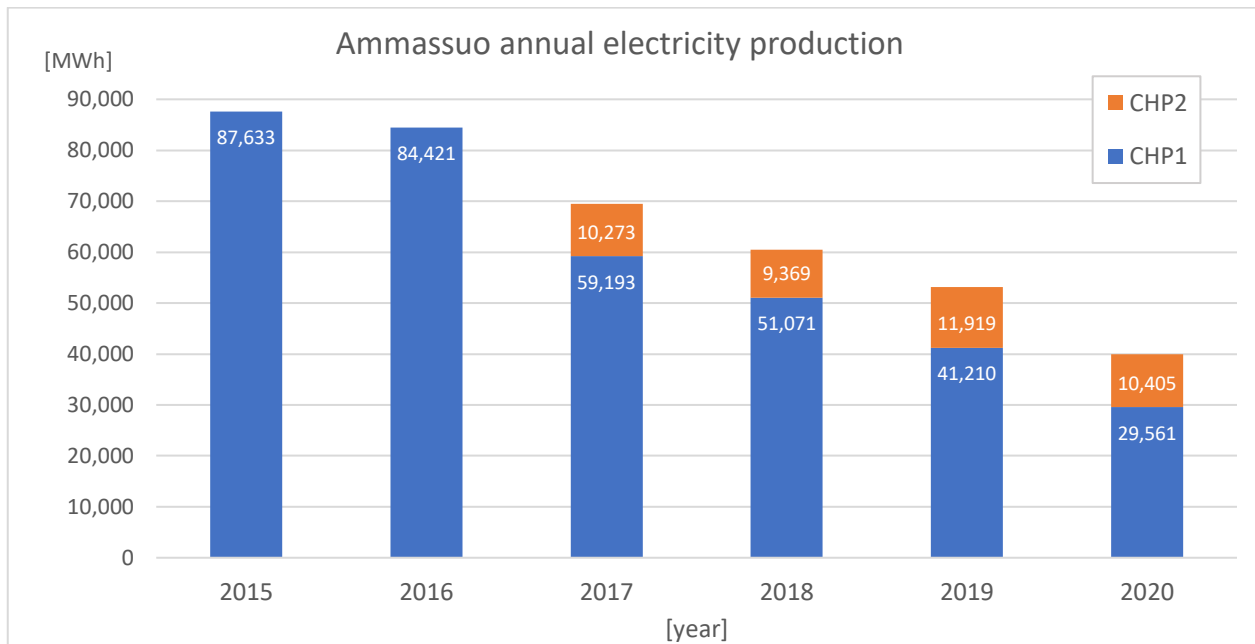


Figure 18: Ämmässuo annual electricity production, from 2015 to 2020 [49]

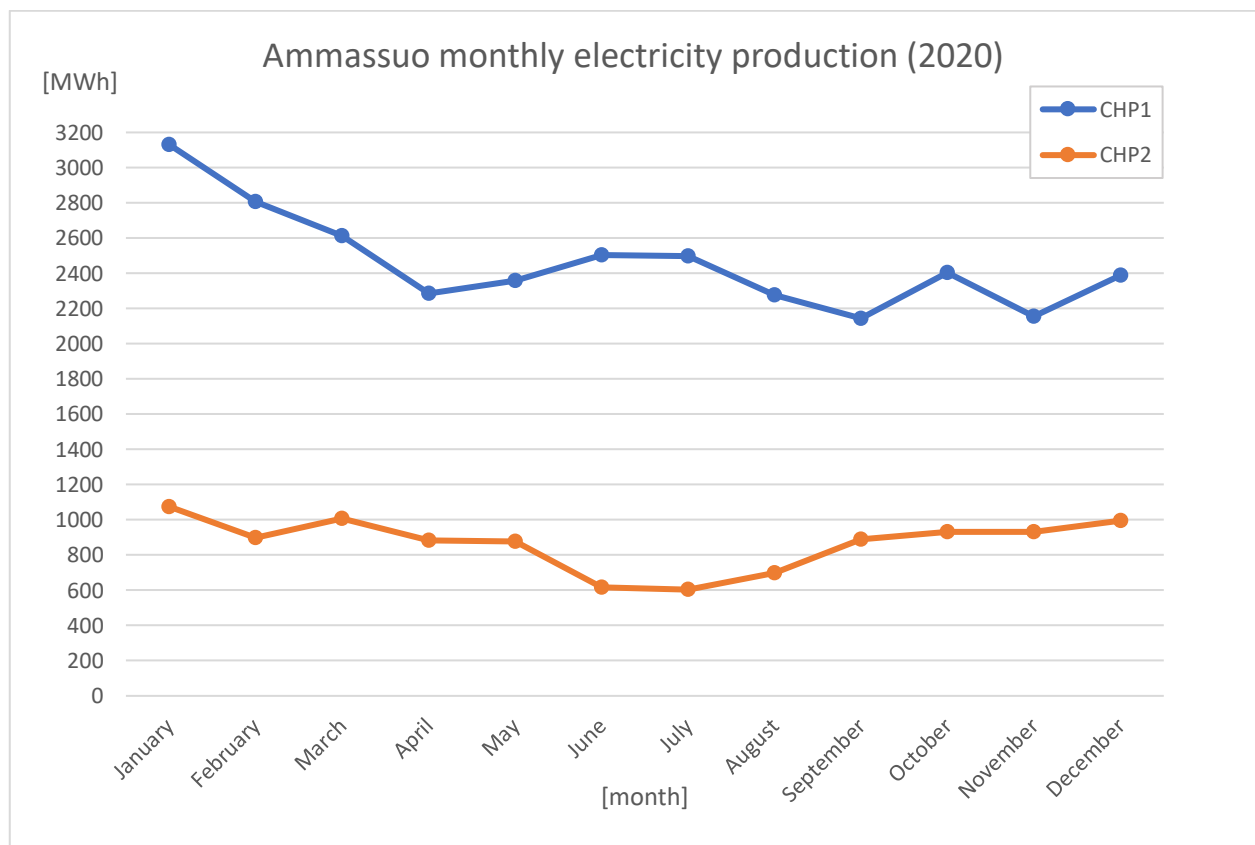


Figure 19: Ämmässuo 2020 monthly electricity production [49]

It's possible to see from Figure 18 the CHP1 energy production decline over the years, as mentioned before. CHP2 instead has been generating a relatively constant amount of energy: about 10,000 MWh per year, since it was commissioned. Exceptions to this trend appear in 2018, when CHP2 produced a slightly lower amount of electricity (9,369 MWh), and 2019, when CHP2 produced a noticeably higher amount of electricity (11,919 MWh).

HSY is considering investing in renewable energy sources (i.e. wind turbines, solar panels), in order to simultaneously increase the energy at disposal of the eco-centre and offset its CO₂ production. The technical and economic characteristics of said investments will be analysed in the following chapters.

2.2.3 Heat production

The Ämmässuo eco-centre's main sources of heat are still the two gas-powered plants CHP1 and CHP2; due to their nature, they provide the centre with both electricity and heat. The difference with this form of energy is that an excess of heat, even if it could potentially be stored with the appropriate technology, cannot be sold to a "grid" like its electricity counterpart.

Using again the data requested from the HSY regional authority it is possible to visualize (below and next page, Figure 20 and 21) the heat production of the eco-centre [49].

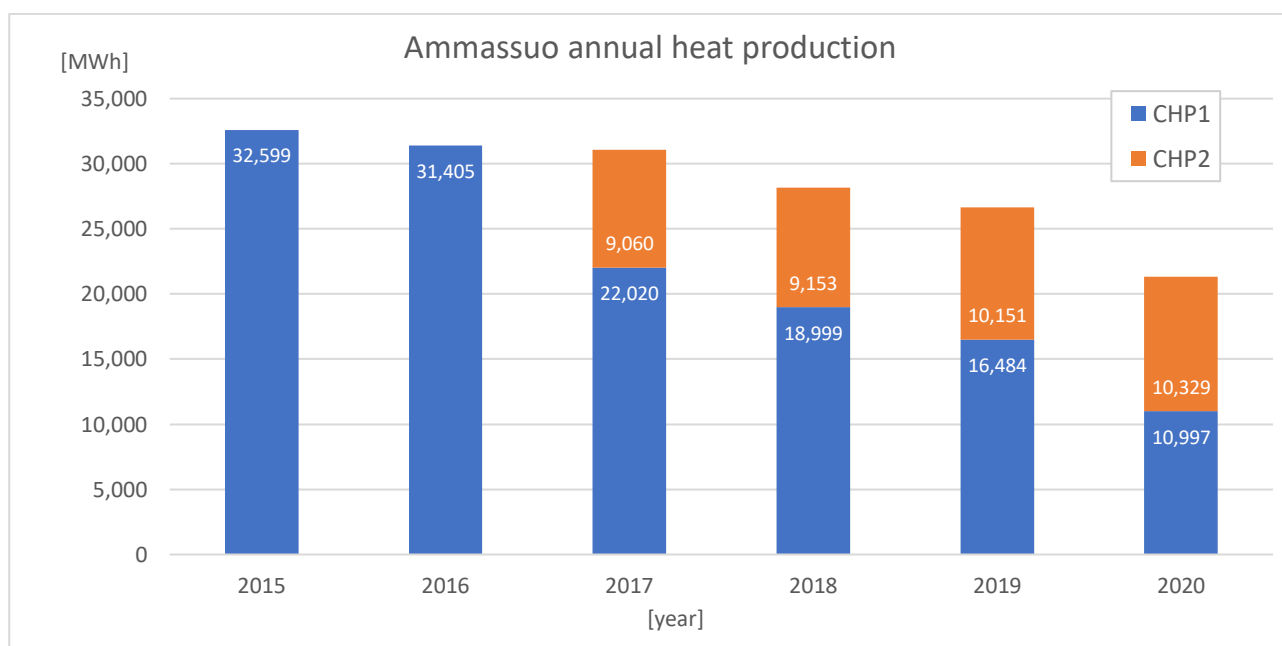


Figure 20: Ämmässuo annual heat production, from 2015 to 2020 [49]

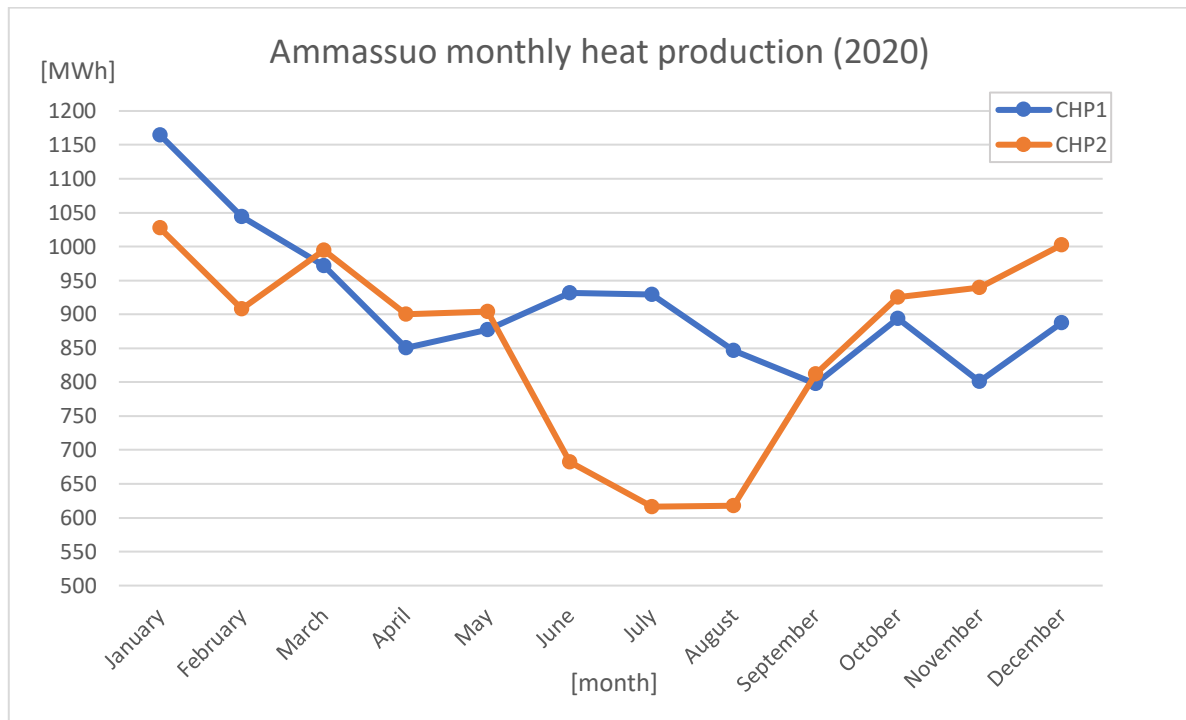


Figure 21: Ämmässuo 2020 monthly heat production [49]

Looking at Figure 20 it is possible to make the same considerations regarding the landfill gas decline and the biogas reliability derived from Figure 16; Figure 19 instead shows that CHP1 and CHP2 did generate a comparable amount of heat in 2020, with the exception of the summer period, for which however a decrease in heating demand is to be expected.

2.3 Energy consumption and self-sufficiency

2.3.1 Electricity consumption

According to the 2021 Sweco report [50], the electricity consumption of the eco-centre can be subdivided in the following categories:

- CHP1 and CHP2 consume respectively around 3,300 MWh and 660 MWh per year;
- The landfill collection requires circa 1,700 MWh per year;
- The biowaste management sector demands about 6,500 MWh per year, including the PIMA hall, which consumes around 350 MWh yearly, and the biogas pump, which consumes around 150 MWh yearly;
- Sortti station and the offices consume about 500 MWh per year;
- Other consumptions, such as ash treatment and area lightning, consume about 450 MWh per year.

The total measured amount was roughly 13,000 MWh in 2020; the picture below summarizes the data.

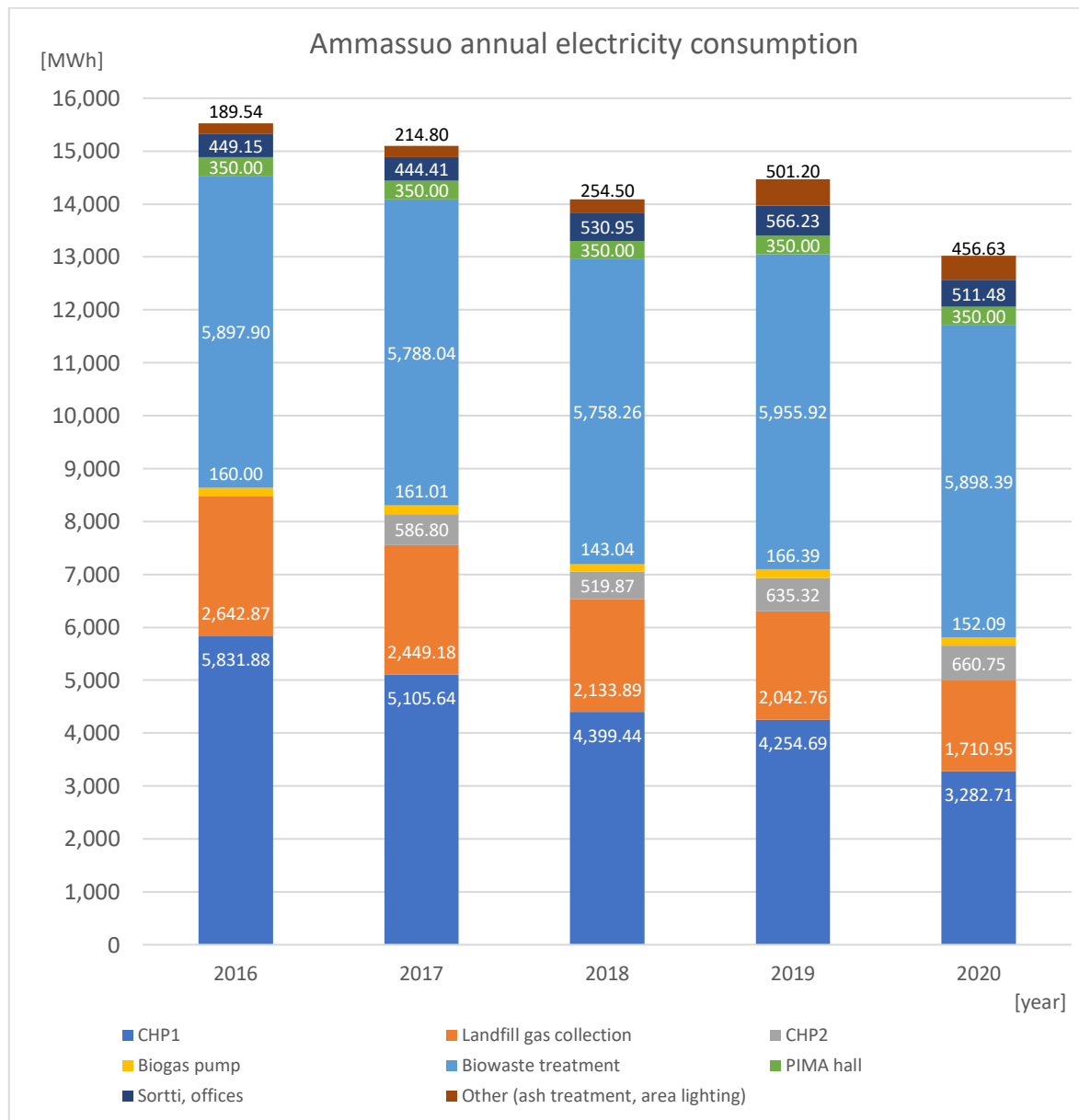


Figure 22: Ämmässuo annual electricity consumption, from 2015 to 2020 [49]

The main contributors to the electricity demand of the centre are the energy used by the landfill gas powered plant (CHP1), the energy used for the landfill gas collection, and the energy used for the biowaste treatment. With the exception of the latter, it's possible to see a decrease of these consumption contributors; this is due to the reducing amount of landfill gas accumulated, which brings down both the energy production and the energy demand linked to it.

It's possible to monitor the self-sufficiency of the eco-centre by utilizing the ratio between the energy produced and the energy consumed, for both electricity and heat. The picture below shows a representation of this proportion.

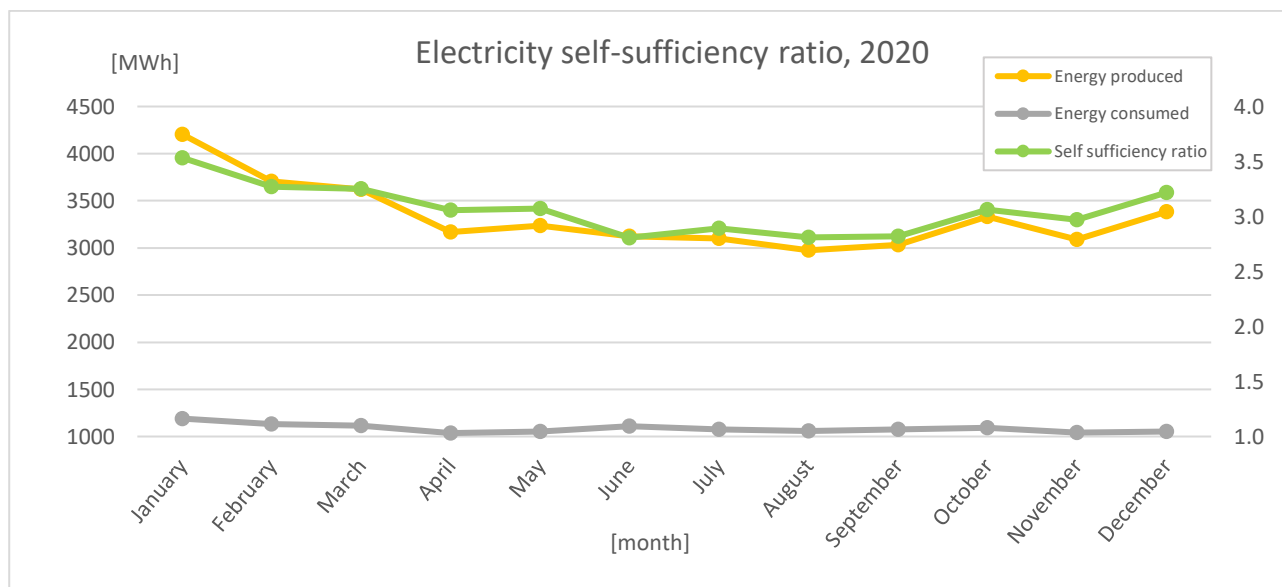


Figure 23: Electricity self-sufficient ratio for the year 2020 [49]

Figure 23 shows that, electric energy-wise, the self-sufficiency of the centre is greatly achieved. In a situation in which no investments will be made in the following years, the electricity production would noticeably decrease in the future, since there won't be the landfill gas contribution anymore. However, the electricity consumption would decrease as well, since the demand for CHP1 and the landfill gas collection (Figure 20, blue and orange bars on the chart) will not be present.

It's possible to imagine a case for which the landfill gas-related electricity production and consumption would be zero, while the other factors would be the same as in 2020. In this situation the electricity self-sufficiency ratio would be the following:

$$10405 \text{ MWh} / (456.63 + 551.48 + 350 + 5898.39 + 152.09 + 660.75) \text{ MWh} = 10405 / 8069.34 = 1.29 > 1$$

The assumptions related to this calculation are imprecise, since there is no guarantee that the factors unrelated to the landfill gas would remain the same in the future; in fact, Chapter 4 of this work will provide data showing an increase of the future energy demands of the eco-centre. Knowing this, the calculation above shows how the electricity self-sufficiency of the eco-centre is not in immediate jeopardy, while its heat self-sufficiency, as it will be shown in the next chapter of this work (2.3.2), is more at risk.

2.3.2 Heat consumption

According to the 2021 Sweco report [50], the heat consumption of the eco-centre is formed by the energy needed by the two composting plants (old and new), the energy needed by the two gas-powered plants (CHP1, CHP2), the energy needed by the PIMA hall and the support hall, and other consumptions such as the energy required by the Sortti station and the offices. The picture below summarizes the data.

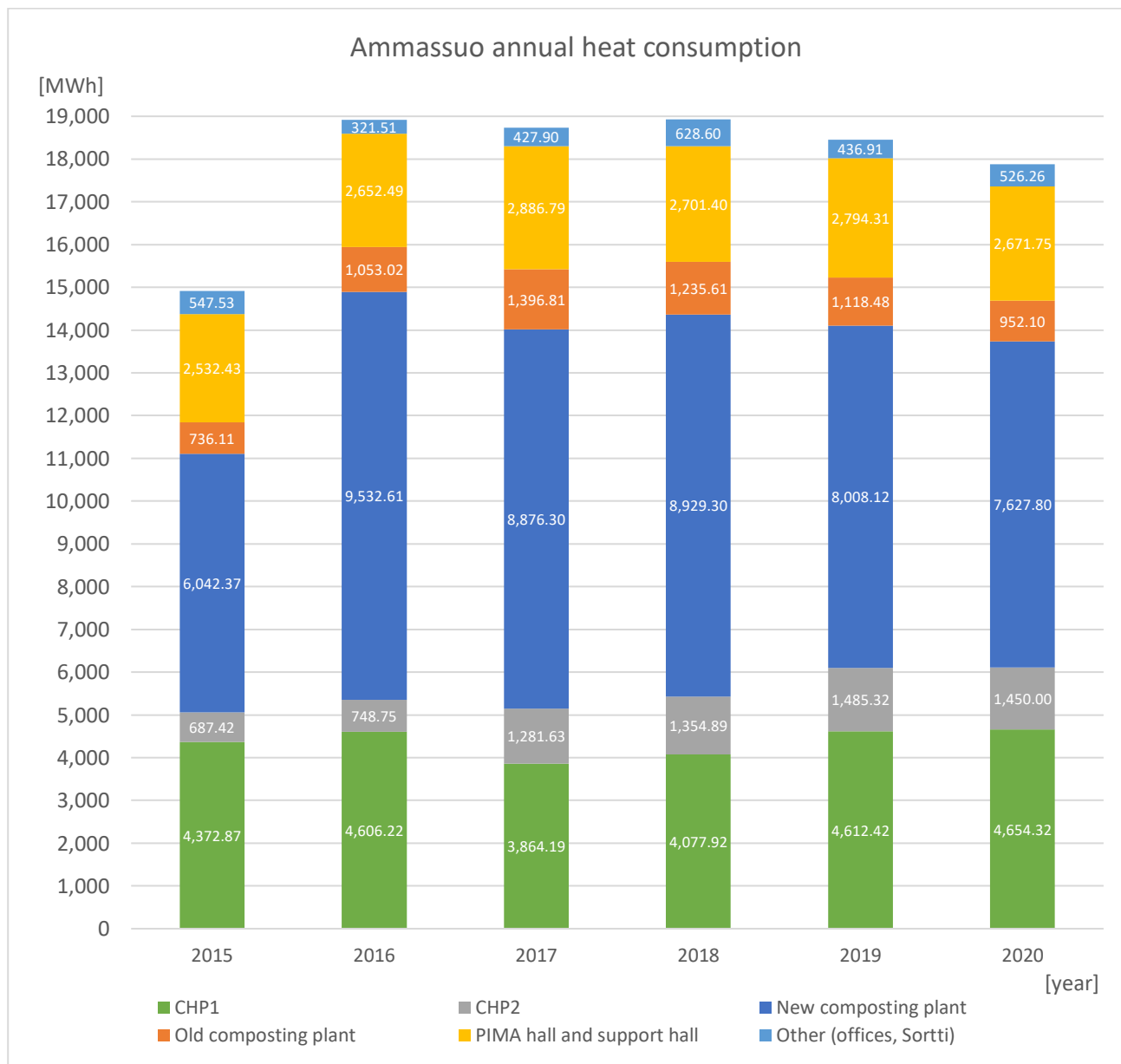


Figure 24: Ämmässuo annual heat consumption, from 2015 to 2020 [49]

Figure 24 (previous page) shows that the total measured amount of heat consumed in 2020 was roughly 18,000 MWh; the highest contributor to the eco-centre heat demand was the energy used by the new composting plant (7,628 MWh in 2020), followed by the energy utilized by the CHP1 (4,654 MWh in 2020).

As it was previously done for electricity, it is possible to monitor the heat self-sufficiency of the eco-centre by utilizing the ratio between the energy produced and the energy consumed. The results are summarized by the graph below.

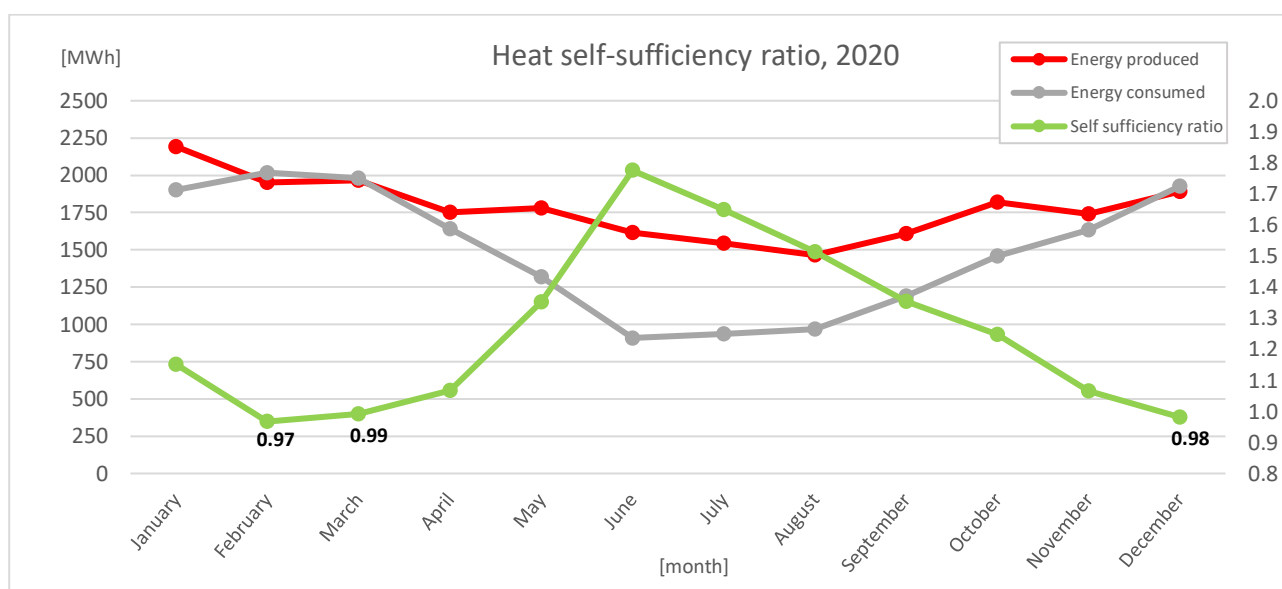


Figure 25: Heat self-sufficient ratio for the year 2020 [49]

It's possible to see from Figure 25 that, as opposed as the electricity case, the heat self-sufficiency of the centre can be considered at risk even in current years, mainly due to the higher heating demand of the winter months.

The situation will become increasingly dire in the future if no investment will be made to contrast it. Following the same reasoning used for the assumption made in the previous chapter (2.3.1), it's possible to consider the ratio between the heat energy produced and consumed in 2020, leaving out any landfill gas contribution. The result of said assumption would be this:

$$10329 \text{ MWh} / (1450.00 + 7627.80 + 952.10 + 2671.75 + 526.26) \text{ MWh} = 10329 / 13227.91 = 0.78 < 1$$

As it was mentioned in the previous chapter (2.3.1), the assumptions made for this calculation are imprecise, since they state that the rest non landfill-based values will remain the same as 2020, and the month-by-month variation of the production/demand is not considered as well. However it helps understanding the necessity to invest in alternative energy solutions, especially considering that, from the heat energy point of view, there is an evident reduction of the resources, and the energy self-sufficiency is at stake.

2.3.3 Methanol demand

Methanol (CH_3OH) is an important resource for the HSY municipal federation; among other chemicals, it's a compound used for wastewater treatment. The chemical process utilized for said industrial treatment is called denitrification. Specific details about this process are beyond the scope of this thesis, but as an overview, the excess nitrate (NO_3^-) present in the water is converted into molecular nitrogen (N_2) through various intermediate gaseous nitrogen oxide products; in the end, the N_2 is vented through the atmosphere [51].

HSY has currently two wastewater treatment plants at its disposal: Viikinmäki and Suomenoja [52]; the data about the methanol consumption of the two plants can be seen below.

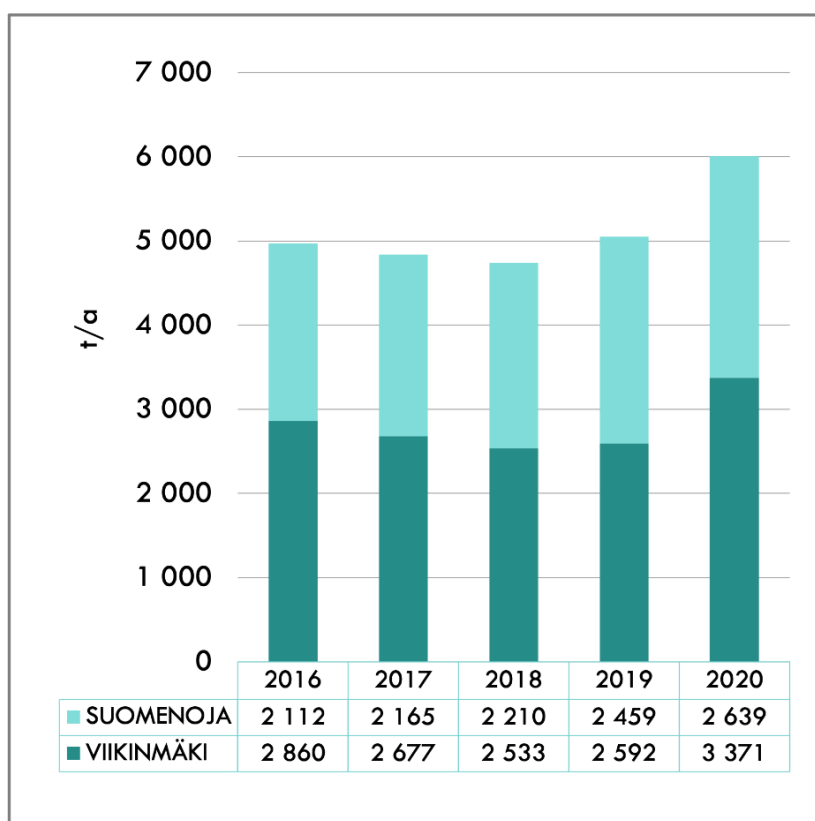


Figure 26: Suomenoja and Viikinmäki annual methanol consumption (tons/year), from 2016 to 2020 [52]

Adding the two values shown in Figure 26 together, the annual methanol consumption for 2020 was 5,910 tons. To understand the quantity of the compound that the regional authority will need in the following years, it's necessary to take into consideration the future plans of HSY for wastewater treatment, which include the development of a new plant, Blominmäki.

During summer 2022, the new Blominmaki plant will substitute the Suomenoja one, since it has exceeded its design load. There will be a brief period in which both the plants will be active simultaneously, hence three wastewater treatment plans will be utilized, but from a certain point onwards only the Viikinmaki and Blominmaki plants will be active. The precise data about the new plant is still not available, but the HSY municipal federation is aiming to have around 10,000 tons per year of methanol at its disposal [52].

Knowing the methanol demand of the regional authority is important to the scope of this work because, if it were to be produced internally, HSY could avoid having to buy it. A method to achieve this is a process called CO₂ hydrogenation, for which methanol can be generated using hydrogen and carbon dioxide. This would also remove the CO₂ produced from the biogas combustion from the system, thus generating a negative emission cycle. More details about this possibility will be described in the following chapters.

2.4 Production vs consumption energy summary

The tables below and next page (Table 6 and 7) summarize the various energy inputs and outputs of the situations analysed in this the previous chapters. The table refers to the most recent data available, which is related to the year 2020 [49]; any landfill gas contribution (for both energy production and consumption) is marked in red.

Table 6: 2020 Ämmässuo electricity production vs consumption [49].

*Estimated total refers to a situation for which the landfill gas is no longer a resource

Sources	Electricity production [MWh]	Electricity consumption [MWh]
CHP1	29,561	3,283
CHP2	10,405	661
Landfill gas collection		1,711
Biowaste treatment		5,898
Biogas pump		152
PIMA hall		350
Sortti, offices		511
Other		457
TOTAL	39,966	13,023
Estimated total*	10,405	8,029

Table 7: 2020 Ämmässuo heat production vs consumption [49]

**Estimated total refers to a situation for which the landfill gas is no longer a resource*

Sources	Heat production [MWh]	Heat consumption [MWh]
CHP1	10,997	4,654
CHP2	10,329	1,450
New composting plant		7,628
Old composting plant		952
PIMA hall		2,672
Other		526
TOTAL	21,326	17,882
Estimated total*	10,329	13,228

2.5 Ämmässuo weather data

The implementation of renewable energy sources will be key for the following chapter of this work. Knowing this, it's important to understand the characteristic of the Ämmässuo weather. Using the Renewable Ninja website tool [53], it has been possible to gather weather data about the area. Next page (Figure 27), various graphs describe useful information about the Ämmässuo zone.



Figure 27: Weather information about the Ämmässuo area, referred to the year 2019 [53]

In order: Daily mean top of atmosphere solar irradiance (a), daily mean top of atmosphere solar irradiance (a), Daily mean ground-level solar irradiance (b), daily mean air temperature (c), daily mean electrical power that could be obtained by a Vestas V150 4000 turbine with a hub height of 92m

3. Potential investments

3.1 Overview and technical characteristics

3.1.1 Wind Turbine

In order to increase the energy production and keep the Ämmässuo eco-centre self-sustainable, the first renewable based investment that HSY is considering is a wind turbine. The model in question is a V150-4.2MW turbine; its technical characteristics can be seen on the table below.

Table 8: Vestas V150-4.2MW Wind Turbine main technical characteristics [54]

OPERATING DATA		ROTOR	
Rated power	4,000 kW/4,200 kW	Rotor diameter	150m
Cut-in wind speed	3m/s	Swept area	17,671m ²
Cut-out wind speed	22.5m/s	Air brake	full blade feathering with 3 pitch cylinders
Re cut-in wind speed	20m/s		
Wind class	IEC IIIB/IEC S		
Standard operating temperature range from -20°C* to +45°C with de-rating above 30°C (4,000 kW)		ELECTRICAL	
*subject to different temperature options		Frequency	50/60Hz
		Converter	full scale
SOUND POWER		GEARBOX	
Maximum	104.9dB(A)*	Type	two planetary stages and one helical stage
*Sound Optimised modes dependent on site and country			

As its name and operational data imply, the turbine is designed to generate 4.0-4.2 MW of power. Of course said power generation can vary, considering that the wind speed is not constant due to its nature. With appropriate assumptions it's possible to predict the yearly energy production of the turbine; manufacturers often include an Annual Energy Production (AEP) curve for each one of their product series. The AEP curve and power curve for the Vestas V150-4.2MW turbine are shown next page (Figure 28 and 29).

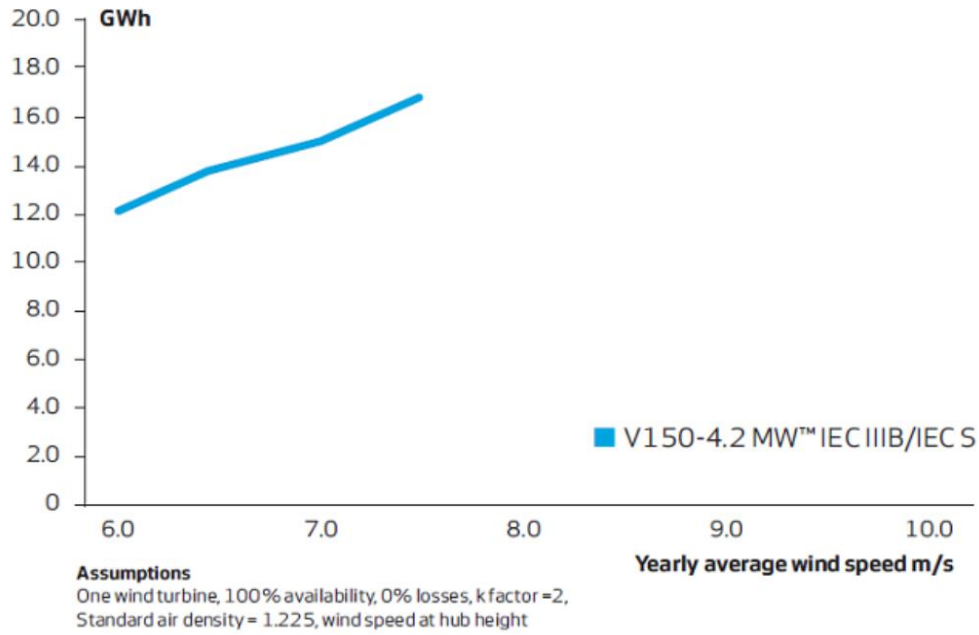


Figure 28: V150-4.2 MW AEP curve [54]

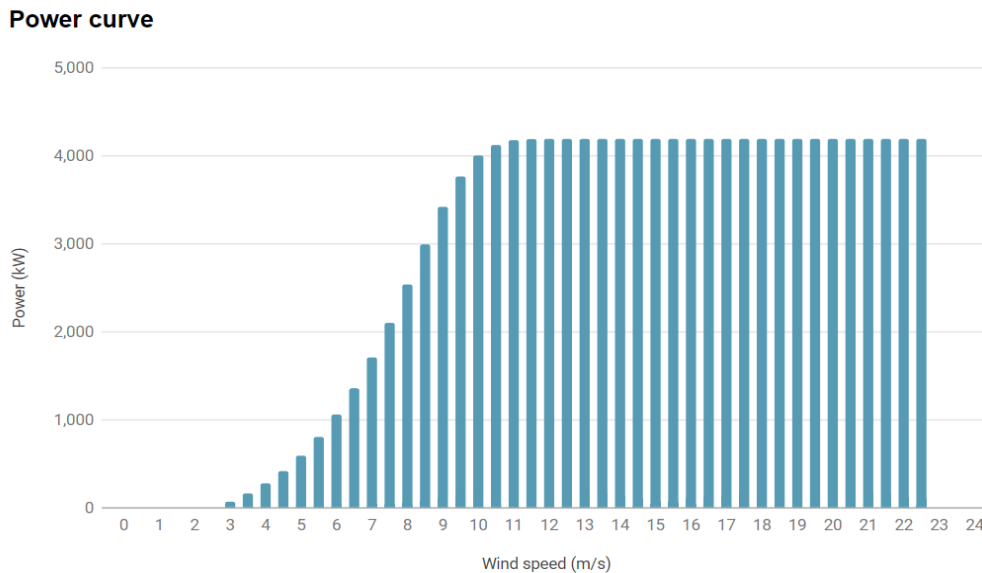


Figure 29: V150-4.2 MW power curve [55]

The power that passes through a wind turbine can be expressed like so [56]:

$$P_{in} = \dot{m} \cdot E_k = (\rho A v_{\infty}) \cdot \left(\frac{1}{2} v_{\infty}^2 \right) = \frac{1}{2} \rho A v_{\infty}^3 \quad (3.1)$$

A represents the blade swept area ($A = \pi r^2$, where r is the length of the turbine blades), ρ represents the air density, while v_{∞} represents the wind speed. Looking at Figure 27, the dependency on v_{∞}^3 can be noticed until a certain point: after that, the power generated becomes constant.

This constant trend is caused by the fact that a wind turbine cannot harvest all the power available in the wind [56]; this concept can be expressed using the power coefficient c_p , which represents the overall turbine efficiency:

$$c_p = \eta_t \cdot \eta_m \cdot \eta_e = \frac{P_{out}}{P_{in}} = \frac{P_{out}}{\frac{1}{2} A v_{\infty}^3} \quad (3.2)$$

The terms η_t η_m η_e represent, respectively, the blade (aerodynamic), mechanical (gearbox) and electrical (generator) efficiency.

The wind speed for which the power generated starts to become constant (11 m/s for the V150-4.2 turbine, as can be seen of Figure 29) is called rated speed; the wind speeds for which the wind turbine starts and stops generating power are called, respectively, cut-in speed and cut-out speed [56]. For the V150-4.2 turbine their values, as listed in Table 8, are respectively 3 m/s and 22.5 m/s.

The notation ‘IEC IIIB/IEC S’ on Figure 26 indicates the wind speed class considered for the turbine. Wind speed classes determine some wind characteristics that the manufacturers must take into consideration while designing a turbine in relation to a specific site. Said characteristics are the annual mean wind speed at hub height, the higher wind speed, the extreme gusts (sudden increase of speed) that could happen over a period of 50 years, and the average turbulence.

These wind classes are defined as an International Standard published by the International Electrotechnical Commission (IEC) [57][58]. The table below summarizes said standards.

Table 9: IEC wind speed classes [57]

Wind turbine class		I	II	III	S
V_{ave} (m/s)		10	8.5	7.5	User defined
V_{ref} (m/s)		50	42.5	37.5	
$V_{50,gust}$ (m/s)		70	59.5	52.5	
I_{ref}	A	0.16			
	B	0.14			
	C	0.12			

In the table (IEC61400-1: 2005):

1. Rayleigh distribution is assumed, i.e. $k = 2$.
2. V_{ave} is the annual mean wind speed at hub height; V_{ref} is the 50-year extreme wind speed over 10 minutes; $V_{50,gust}$ is the 50-year extreme gust over 3 seconds; I_{ref} is the mean turbulence intensity at 15 m/s.
3. A, B and C are the categories of higher, medium and lower turbulence intensity characteristics respectively.

- Section 1: Vertical insulation walls, $7,000 \text{ m}^2$. The surface area provides a solid base, but the vertical installation of the panels would reduce the annual electricity production. Other disadvantages include shading and dusting due to area operations.
- Section 2: Southern slope of the old landfill, $23,000 \text{ m}^2$. The landfill gas collection (near the slope) and the soil composition must be taken into account.
- Section 3: South-eastern slope of the old landfill. Same considerations as section 2 apply, however the area is smaller ($20,500 \text{ m}^2$), and a mild shading might happen in the last hours of sunlight.
- Section 4: Northern slope of the old landfill. The location and size are suitable for the power plant, but the slope is steeper than the lower slopes and gravel-based, which may affect the design of the installation. The impact of landfill gas collection as well as the possible low ground level subsidence must be considered too.
- Section 5: composting plant roof. The area is about $4,740 \text{ m}^2$ flat roof. The almost unobstructed view in all directions provides a good base for the panels' installation. Disadvantages include the bird populations in the area (that may contaminate the panels) and the fact that the building frame structures for solar panel scaffolding must be mapped, which may create additional costs.

The most appropriate location was deemed to be Section 2.

The space requirements for a solar power plant depend on the nominal power and the installation geometry chosen; the panels can be mounted vertically or horizontally, and in one or more rows of racks. The panels used in large power plants usually have an output of $250\text{--}265 \text{ W}_p$. Assuming to be working with 250 W_p solar panels, their length can be estimated to 1 meter per panel; a row composed of 10 panels would then be 10 meters long, for a panel power of $250 \cdot 10 = 2500 \text{ W}_p = 2.5 \text{ kW}_p$ [59].

The term kW_p stands for kilowatt-peak of a system, meaning the power that a solar panel will generate at peak performance, essentially on a sunny day around noon. Since the electrical energy harvested is measured in kilowatt-hours, a solar panel with a peak power of 250 kW_p working in its best conditions for an hour will generate 250 kWh in that time frame [60]. In order to determine their peak power (kW_p), solar panels are usually rated under Standard Test Conditions (STC): irradiance of 1000 W/m^2 , temperature of 25°C and a solar spectrum of AM 1.5 [61].

A picture of the IV-curve, an essential tool for understanding how much power can be obtained from solar cells, is shown below. The blue line represents the current and voltage output of a PV cell; their product is equivalent to the power delivered by the cell. The span of the IV characteristic ranges between the solar cell short circuit current, I_{sc} , and its open circuit voltage, V_{oc} [62].

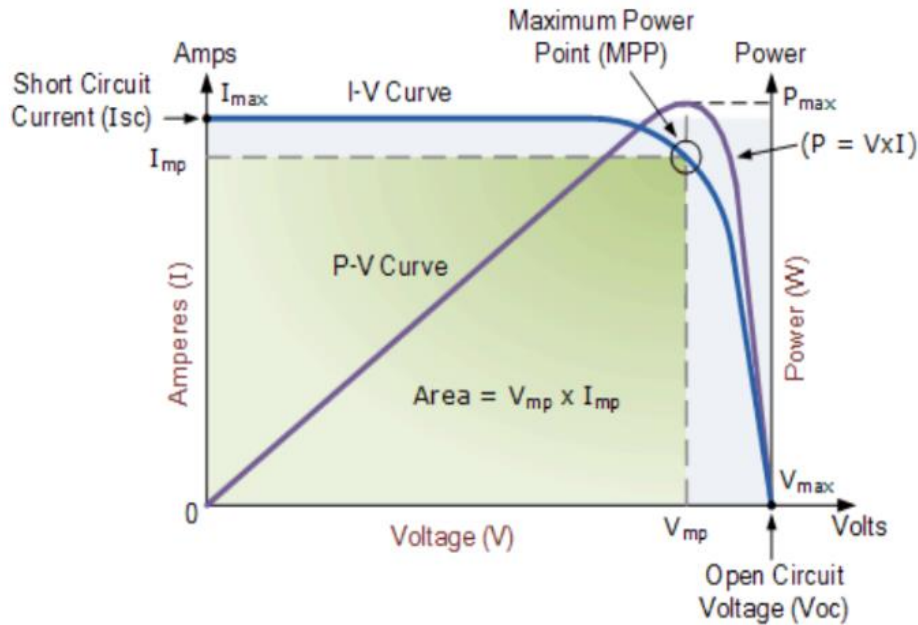


Figure 31: Solar cell current-voltage (IV curve) characteristics [62]

When the solar cell is short circuited (hence its positive and negative leads are connected) its current is at his maximum and is equivalent to I_{sc} , while its voltage is at his minimum, hence zero. On the contrary, when the solar cell is open circuited (not connected to any load) its voltage is at his maximum and is equivalent to V_{oc} , while its current is at his minimum, hence zero. The optimal current-voltage combination for which the power reaches its highest value is called maximum power point, or MPP; the ideal operation of a photovoltaic panel is defined to be at the MPP, when its current and voltage value are, respectively, I_{mp} and V_{mp} . The green area in Figure 31 represents these conditions [56][62].

Next page (Figure 32) the IV-characteristics of a 250 W_p solar PV module [63].

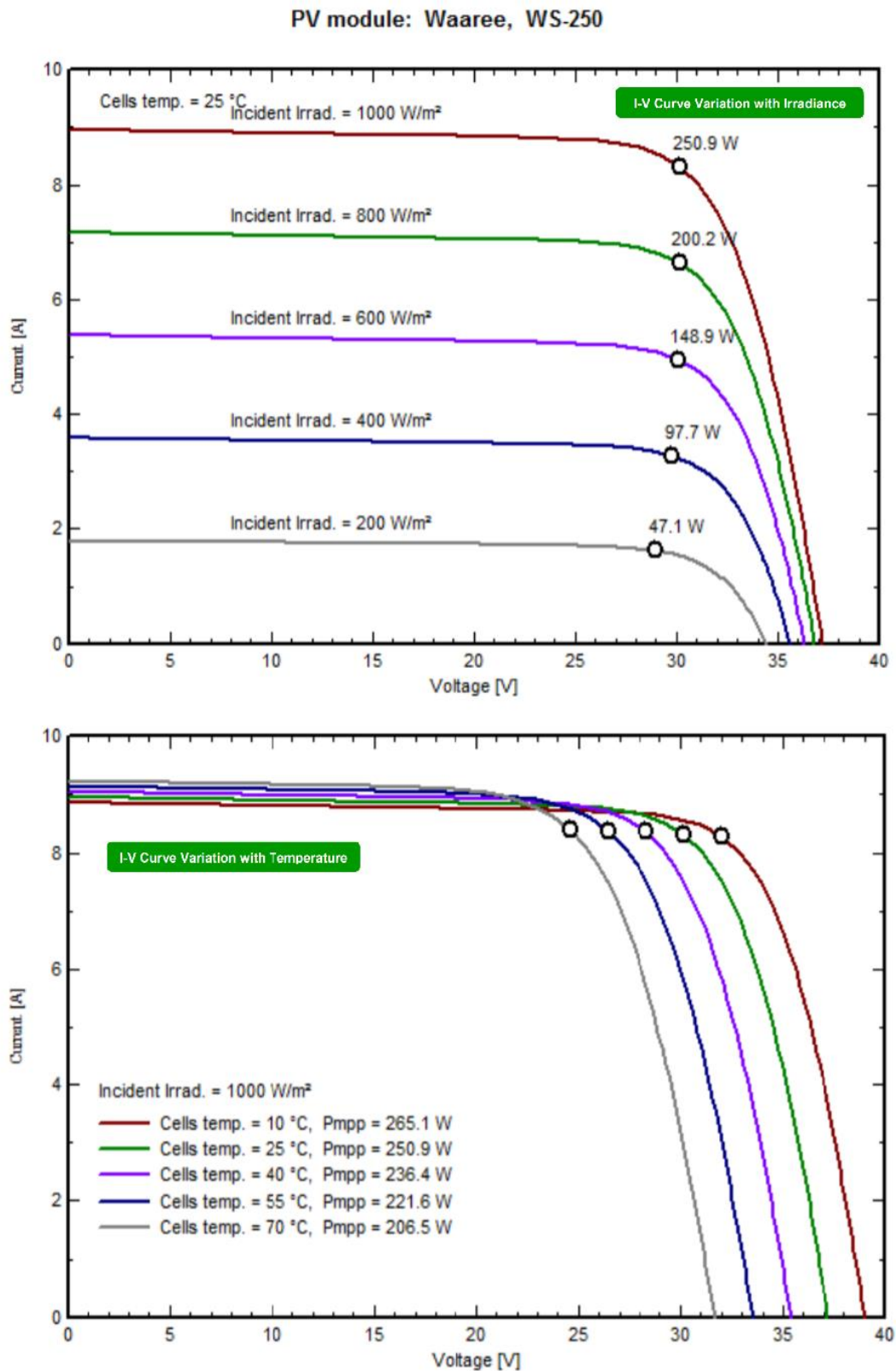


Figure 32: IV-characteristics of a 250 Wp solar PV module [63]
Above: IV-curve variation with irradiance; below: IV-curve variation with temperature

It's possible to calculate how much power can be obtained from a solar panel/module using the following equation [56]:

$$P [W] = \eta \cdot I \left[\frac{W}{m^2} \right] \cdot A [m^2] \quad (3.3)$$

A represents the panel/module area, I represents the solar irradiance, while η represents the panel efficiency, which can be calculated using the equation below:

$$\eta = \frac{P_{max}[W]}{1000 \left[\frac{W}{m^2} \right] \cdot A [m^2]} = \frac{I_{mp}[A] \cdot V_{mp}[V]}{1000 \left[\frac{W}{m^2} \right] \cdot A [m^2]} \quad (3.4)$$

As mentioned before, 1000 W/m^2 corresponds to the STC irradiance, the typical maximum irradiation value on earth's surface. In order to harvest the most solar energy possible, the spacing between the installed solar panels is an important parameter. A reasonable amount of spacing was found to be 3.6 m, while the optimal spacing (in order to completely avoid shading) was found to be 6m. Below, a representation of the solar panel configuration [59].

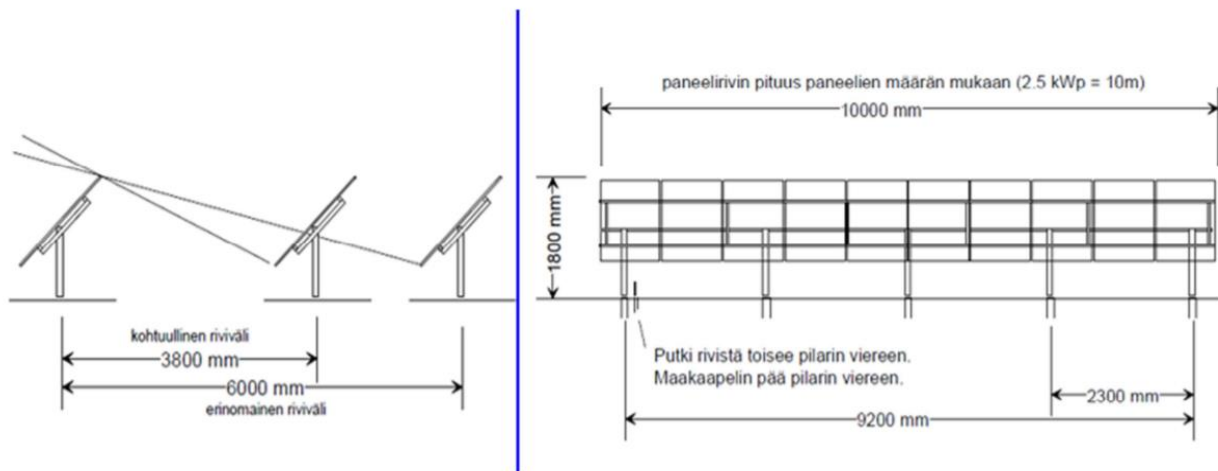


Figure 33: 2.5 kW_p solar panels configuration [59]

A promising arrangement was found to be an extension of one of the previously described configurations, shown in Figure 33. By installing a block of four 50 meter-long panels, it's possible to obtain a solar module of $4 \cdot 50 \cdot 250 = 50,000 \text{ W}_p = 50 \text{ kW}_p$ nominal power. Considering the 6 meter spacing (which is reasonable, due to the width of the whole area), the installation would occupy about 50 meters in length and $6 \times 3 = 18$ meters in width, amounting to a total of circa 900 m^2 .

Figure 34 (next page) illustrates the space required by the described PV module [59].



Figure 34: Placement of a 50 kW_p solar module in the Ämmässuo area [59]

The chosen section's width, as previously described and shown on Figure 28, is around 23,000 m². It is possible to install various 50 kW_p modules in order to utilise the whole area at disposal: the configuration that would allow to do so is shown below (Figure 35). The amount of nominal power of the system was estimated to be $50 \times 27 = 1,350 \text{ kW}_p = 1.35 \text{ MW}_p$.



Figure 35: Optimal configuration of the 50 kW_p solar modules in the Ämmässuo area [59]

When planning to invest in a solar power plant it is necessary to consider the amount of solar irradiation that is possible to get in the relative site. Ämmässuo is located in the southern part of Finland; the picture below shows how much radiant energy it's possible to obtain each month on that country zone (I-II) [64].



Figure 36: Monthly radiant energy [kW/m²] in Southern Finland (zones I-II) [64]

The PV plant can be an important asset to help maintaining the HSY eco-centre energy self-sufficiency. However, it suffers from the same problem of its wind counterpart: unreliability due the intermittency of its energy source. Possible solutions are the same as the ones mentioned for the wind turbine: accurate weather data and an energy storage system.

3.1.3 Additional renewable energy production summary

By using the Ämmässuo weather data gathered for Chapter 2, the information from Vestas [54] and the data from the Elomatic report [59], it's possible to estimate the amount of additional renewable electrical energy that can be produced using the energy sources that HSY is considering. Representative graphs are shown below and next page (Figure 37, 38).

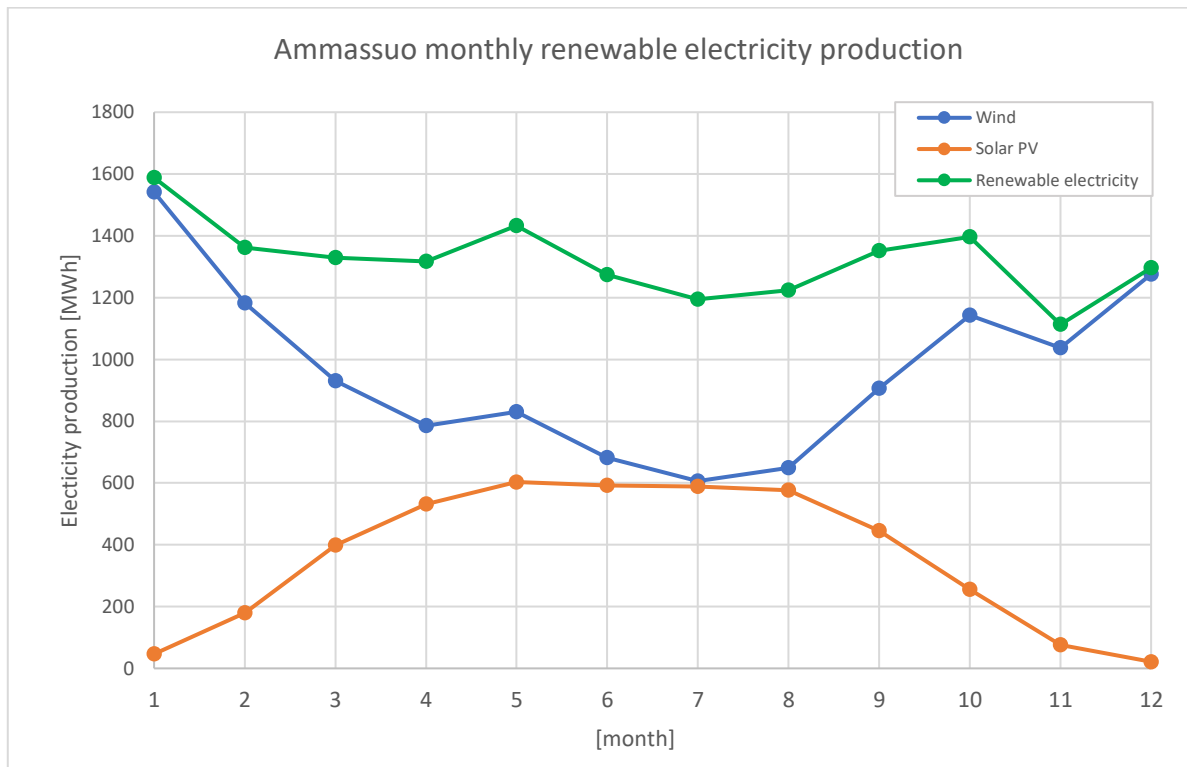


Figure 37: Ämmässuo monthly renewable electricity production [54][59]

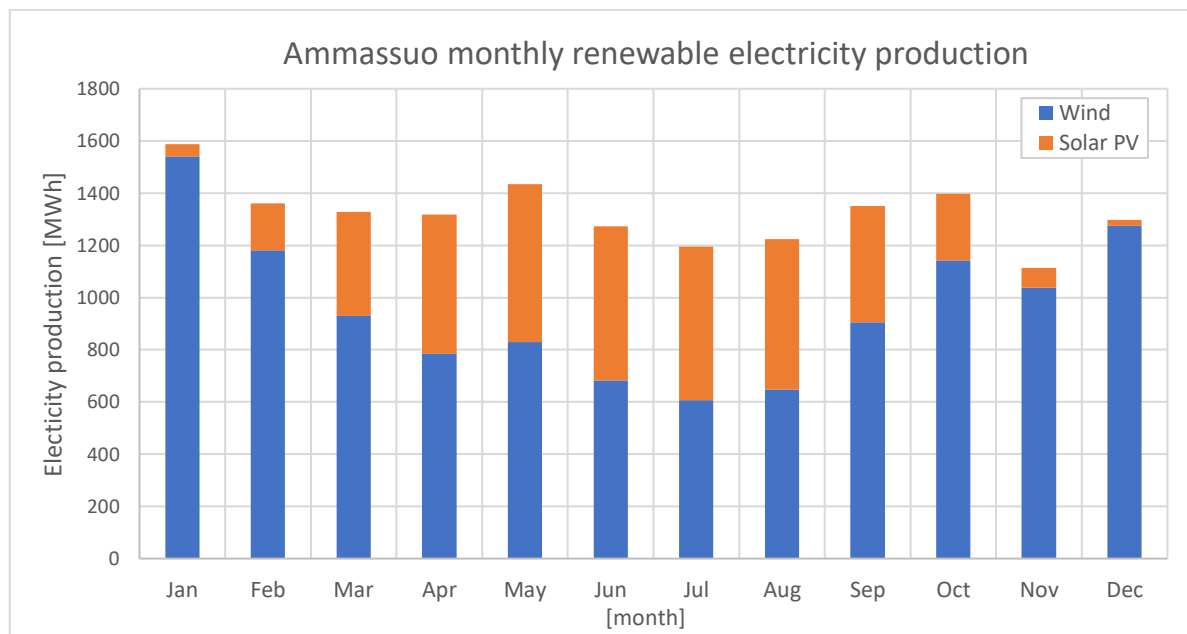


Figure 38: Ämmässuo monthly renewable electricity production (bar graph) [54][59]

The cumulative amount of electricity that can be obtained used renewable sources was estimated to be 15,879 MWh per year, with a minimum monthly value of 1,113 MWh and a maximum monthly value of 1,433 MWh. For the solar calculations, the total panel area was set to 23,000 m^2 , while the panels efficiency was estimated to be 15% [59].

It is possible to update the electricity production vs consumption table, used in Chapter 2 of this work, with the newfound data about the renewable energy sources:

Table 10: Ämmässuo electricity production vs consumption [54][59]

*value referring to a situation where the landfill gas is no longer used and the renewable sources have been installed

Sources	Electricity production [MWh]	Electricity consumption [MWh]
CHP1	29,561	3,283
CHP2	10,405	661
Landfill gas collection		1,711
Biowaste treatment		5,898
Biogas pump		152
PIMA hall		350
Sortti, offices		511
Other		457
Wind	11,565	
Solar	4,314	
TOTAL	39,966	13,023
Estimated total*	26,284	8,029

3.1.4 Heat pump

During Chapter 2's analysis of the current energy self-sufficiency of the Ämmässuo eco-centre, it has been shown that its heat self-sufficiency is more at risk than its electricity self-sufficiency. In fact, the self-sufficiency ratio (energy produced against energy consumed) of the former has been measured to be lower than 1 (0.78) due to 2020's colder months, while the ratio of the latter has been measured to be way higher than 1 in 2020, and it was assumed that it would be higher than 1 (1.29) even when the landfill gas won't be a resource for the eco-centre.

Because of this situation, a promising solution would be to invest in a heat pump system, which would, to put it simply, increase the heat production of the centre while consuming only a fraction of the electricity at its disposal, for which it has been established that the self-sufficiency is not at an immediate risk.

The two prevailing heat pump technologies are called ground source heat pumps (GSHP) and air source heat pumps (ASHP). The main difference between the two is the source from where they absorb heat; as the name implies, GSHP absorb heat from the ground, where ASHP absorb heat from the air. A schematic of the technologies can be seen next page (Figure 39) [65].

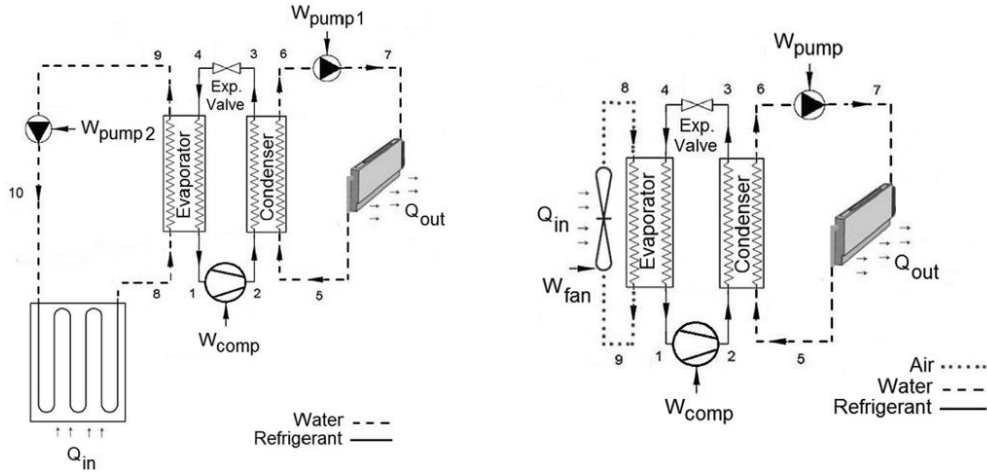


Figure 39: Heat pump schematics: GSHP on the left, ASHP on the right [65]

It's possible to notice the main difference between the two technologies from Figure 39, since the only variation between the cycles is the leftmost part: their central and rightmost parts are the same. For the former, the refrigerant receives heat from the working fluid on the left (water or air, depending on the technology) through the evaporator, then transfers it to the water, on the right, through the condenser. For the latter, after receiving heat from the refrigerant through condenser and being pumped, the water yields the heat accumulated towards the system for which heat is needed (Q_{out}).

The coefficient of performance (COP) of a heat pump is calculated by dividing the amount of heat that it generates by the amount of work required by it; the COP can be identified as a measurement of the heat pump efficiency. It can be expressed using the following equation:

$$COP = \frac{Q_{out}}{W_{in}} \quad (3.5)$$

Considering the processes described by Figure 37 (previous page):

$$COP_{ASHP} = \frac{Q_{out}}{W_{pump1} + W_{pump2} + W_{comp}} \quad COP_{GSHP} = \frac{Q_{out}}{W_{pump} + W_{fan} + W_{comp}} \quad (3.6, 3.7)$$

Usually the COP of GSHPs is higher than the one of ASHPs, mainly for two reasons. First of all, the specific heat capacity of water is about four times higher than the one of air: $4182 \text{ [J/kg} \cdot \text{K]}$ against $1005 \text{ [J/kg} \cdot \text{K]}$ [66]. Considering the working fluid that the technologies use as a medium, is to be expected for GSHPs to have higher efficiency. Secondly, due to the natural fluctuations of the weather, ASHPs consume low amounts of energy during the summer, since the air used as a medium is already at a high temperature; in turn, however, they require a considerably higher amount of energy during the winter (a season during which the heating needs are clearly higher), which causes the efficiency to drop. This issue is not present for GSHPs, since the water that they use as a medium runs underground, and its temperature is considerably more stable during the year.

The main reason why ASHPs can be advantageous is their lower capital cost: apart from the relatively smaller size, GSHPs require the additional groundwork and ground arrays installation. ASHPs, however, have higher operating costs than GSHPs, as well as a lower lifetime: ASHPs tend to last about 10 years due to their exposure to external elements, while GSHPs are a closed system, protected from environmental damage. GSHPs need little maintenance, and their design life last about 20 years, while the buried ground array can last over 100 years [67].

According to Lehteva V.'s work [49], a possible source of heat would be eco-centre composting plants: a heat pump that harnesses thermal energy from the exhaust air could be utilised. The designed capacity of the ASHP would be 2,000 kW, and its electrical power would be 400 kW, thus its COP value would be equal to 5. Assuming that the heat pump would run at full capacity all the time (for the whole year), it would consume $400 \cdot (60 \cdot 60 \cdot 24 \cdot 365 \cdot 1 / 1000) = 12,614,400 \text{ MJ} = 3,504 \text{ MWh}$ of electricity, which would in turn produce $3504 \cdot 5 = 17,520 \text{ MWh}$ of heat.

With this information is possible to update once more the heat production vs consumption table used in Chapter 2 of this master's thesis:

Table 11: Ämmässuo heat production vs consumption [49]

* value referring to a situation where the landfill gas is no longer used and the heat pump has been installed

Sources	Heat production [MWh]	Heat consumption [MWh]
CHP1	10,997	4,654
CHP2	10,329	1,450
New composting plant		7,628
Old composting plant		952
PIMA hall		2,672
Other		526
Heat pump	17,520	
TOTAL	21,326	17,882
Estimated total*	27,849	13,228

3.1.5 Alkaline water electrolyser

A brief summary on how electrolysis works was provided at the beginning of Chapter 1.2.2 of this work; it was also mentioned that alkaline water electrolysis (AEL) is the most mature technology of the ones developed for this chemical process. This implies AEL's reliability; considering how much this factor is key to maintaining the self-sustainability of the HSY eco-centre, it's safe to assume that investing in a AEL is the best choice between the available electrolyzer options.

A typical process flow for hydrogen production (and oxygen production) via alkaline water electrolysis is shown below.

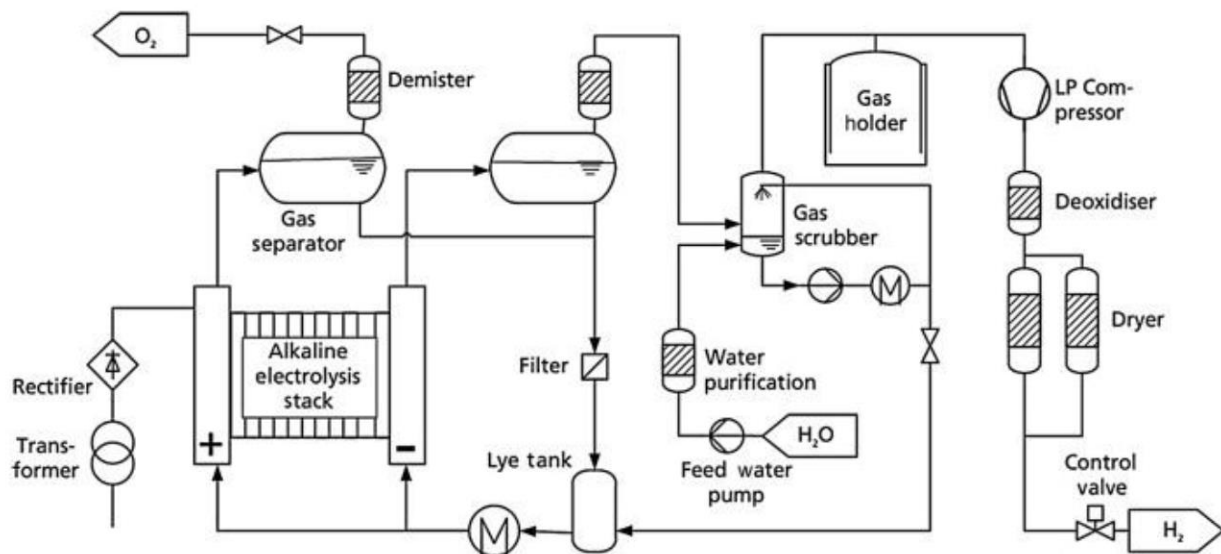


Figure 40: Process flow for H₂ and O₂ production via alkaline electrolysis [68]

Figure 40 shows that the process starts by sending the water (H₂O) towards a purification site using a feed water pump. After this, H₂O is sent towards a scrubber; part of it is used in the wet gas scrubber, to clean the H₂ exiting from the electrolyser. The water then goes through the lye tank, in order to generate the alkaline solution KOH, used as the electrolyte. The water is then sent towards the electrolyser, which is attached to a power supply, and is separated into H₂ and O₂. After the liquid-gas separation, the hydrogen and oxygen produced are treated before being utilised or stored; the anodic and cathodic electrolytes from the liquid-gas separation are mixed, and then recycled.

It is important to understand how much hydrogen can be produced from this investment. Logically, the bigger the machine, the higher the quantity of product that can be obtained (but also the higher the capital cost). Next page (Table 12), the technical characteristics of three AEL models produced by the manufacturer NEL, ordered from smaller to larger [69].

Table 12: NEL alkaline water electrolyser technical characteristics [69]

SPECIFICATIONS	A300	A1000	A3880
Net Production Rate	150-300 Nm ³ /h	600-970 Nm ³ /h	2,400-3,880 Nm ³ /h
Production Capacity Dynamic Range	15-100% of flow range	15-100% of flow range	3.75-100% of flow range
Power Consumption at Stack ¹	3.8-4.4 kWh/Nm ³	3.8-4.4 kWh/Nm ³	3.8-4.4 kWh/Nm ³
Purity – with optional purification	99.99-99.999%	99.99-99.999%	99.99-99.999%
O ₂ -Content in H ₂	< 2 ppm v	< 2 ppm v	< 2 ppm v
H ₂ O-Content in H ₂	< 2 ppm v	< 2 ppm v	< 2 ppm v
Delivery Pressure	1-200 barg	1-200 barg	1-200 barg
Dimensions			
Footprint	~200 m ²	~225 m ²	~770 m ²
Container 1 – W x D x H	NA	NA	NA
Container 2 – W x D x H	NA	NA	NA
Container 3 – W x D x H	NA	NA	NA
Ambient Temperature	5-35° C	5-35° C	5-35° C
Electrolyte	25% KOH aqueous solution	25% KOH aqueous solution	25% KOH aqueous solution
Feed Water Consumption	0.9 l/Nm ³	0.9 l/Nm ³	0.9 l/Nm ³

By looking at the NEL data [69], it is possible to see that the power consumption is within the range of 3.8 – 4.4 kWh/Nm³ for every model. In order to understand how much hydrogen could be obtained, let's assume that the power consumption value is $\alpha = 4.1$ kWh/Nm³, and that the power load sent towards the AEL is 500 MWh per month. The following equation can describe how much H₂ can be obtained in a year:

$$V_{H_2, year} [Nm^3] = E_{el, year} [kWh] \cdot \frac{1}{\alpha} \left[\frac{Nm^3}{kWh} \right] = \frac{(12 \cdot 500) \cdot 1000}{4.1} = 1,463,414.63 m^3 \quad (3.8)$$

It's necessary to mention that the hydrogen obtained is in normal conditions (its density is 0.08375 kg/m³), and so it has to be compressed in order to become a useful end product.

Regarding the AEL oxygen production, the quantity of O₂ moles generated will be half of the quantity of H₂ moles generated, considering the chemical reaction that governs electrolysis. In order to calculate the actual O₂ quantity generated, is necessary to use the following equation:

$$m_{O_2} [kg] = \frac{1}{2} \cdot m_{H_2} [kg] \cdot \frac{MM_{O_2} [kg/mol]}{MM_{H_2} [kg/mol]} \quad (3.9)$$

Another important aspect of this investment is the coupling of the AEL with renewable sources of energy, in order to produce green hydrogen. An experimental study conducted by Alfredo Ursúa et al for the Public University of Navarre (UPNa) [70] showed the possibilities of the beforementioned coupling: both a wind power based energy system and a PV-based energy system were connected to a 1 Nm³/h AEL located in UPNa.

The parameters measured were the hydrogen production rate, the energy efficiency, the electrical performance and the gases' purity. The ranges of temperature, pressure and operating current were set to 35-65°C, 5-25 bar, 40-120 A (respectively).

For the wind power simulation, the turbine model utilised as a reference was a Bornay 6000 [71], with a rated power of 6,000 W, as its name implies. Below, two graphs representing the parameters measured during the experiment.

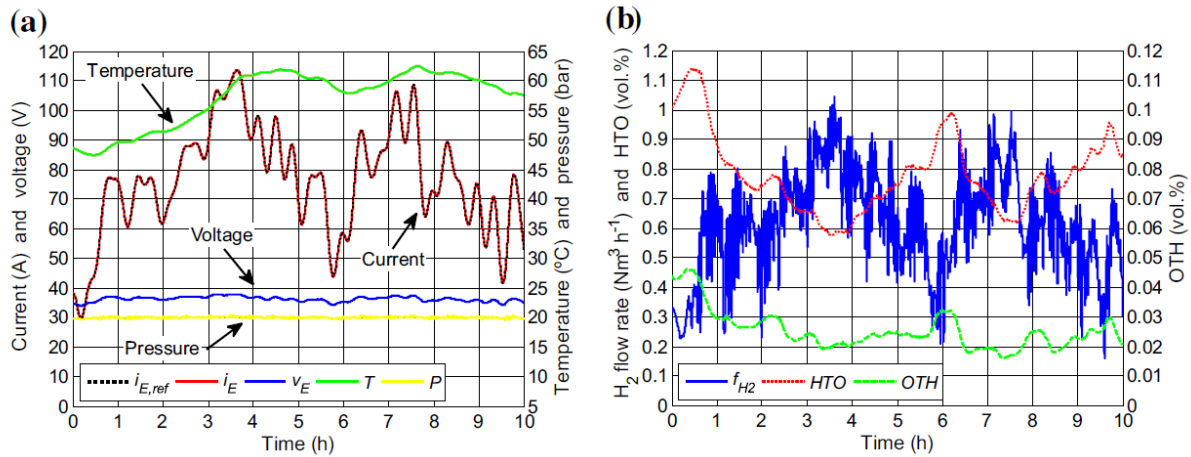


Figure 41: Experimental wind power emulation on the alkaline electrolyser.
On the left (a), reference current evolution ($i_{E,ref}$), current supplied to the electrolyser (i_E), voltage of the electrolysis module (v_E), operating temperature (T) and pressure (P).
On the right (b), hydrogen production rate (f_{H2}), hydrogen percentage transferred to the oxygen current (HTO), oxygen percentage transferred to the hydrogen current (OTH) [70]

The solar simulation was based on a PV installation on the roof of one of the buildings of UPNa, composed of 60 BP585 modules [72], produced by the former company BP solar. Each module has a peak power of 85 W, for a total peak power of $85 \cdot 60 = 5,100$ W. Below, two graphs representing the parameters measured during the experiment.

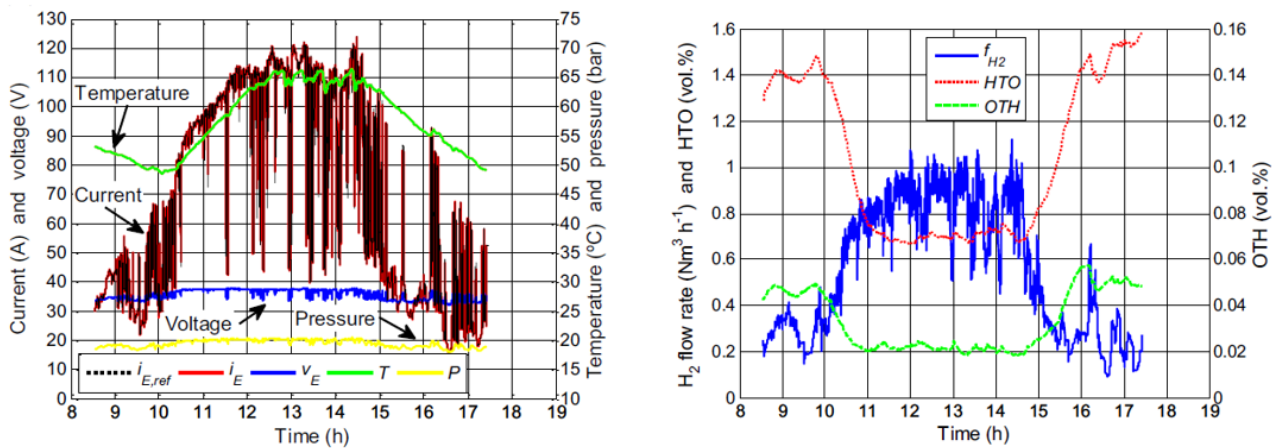


Figure 42: Experimental solar power emulation on the alkaline electrolyser.
On the left (a), reference current evolution ($i_{E,ref}$), current supplied to the electrolyser (i_E), voltage of the electrolysis module (v_E), operating temperature (T) and pressure (P).
On the right (b), hydrogen production rate (f_{H2}), hydrogen percentage transferred to the oxygen current (HTO), oxygen percentage transferred to the hydrogen current (OTH) [70]

The intermittent nature of renewable energy sources can pose a challenge for the electrolyser coupling, but there are mainly three ways for which this connection can be accomplished [73].

The first method implies connecting the electrolyser to the power grid to which the wind turbine(s) and PV plant(s) deliver electricity to (indirect connection). This makes the electrolyser operate in continuous mode, but since not all the electricity supplied to the machine is surely generated using renewable energy sources, the hydrogen produced cannot be considered 100% green.

The second method implies connecting the wind turbine(s) and solar plant(s) directly to the electrolyser, in order to produce only green H₂ and sell the surplus energy to the grid. This configuration however would require an electrolyser technology that can operate in a non-continuous mode. The quantity of hydrogen produced would also be not constant, even though there could be prediction methods to compute how much H₂ can be produced, to a certain degree.

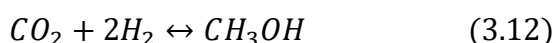
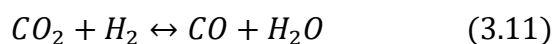
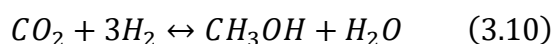
The third method implies a coupling between the renewable sources and the power grid, for which the electrolyser is intended to comply with the forecast of renewable power generated, by acting as a controlled load to consume more or less electricity from the grid, based on previously established strategies.

Considering that the AEL technology is best suited to work with continuous loads, and that the knowledge of available resources is of key importance for this study, the most suitable configuration for a renewable coupled electrolyser in the Ämmässuo eco-centre would be the first one.

3.1.6 Methanol production

It was mentioned in Chapter 2 that a very relevant synergy regarding the usage of H₂ would be the production of methanol, useful for wastewater treatment, an operation that the HSY regional authority conducts. The quantity of product that the municipal federation is going to need has been estimated to around 10 kt (10,000 tons) per year.

The production of methanol via carbon dioxide hydrogenation is primarily regulated by three chemical reactions: CO₂ hydrogenation (Equation 3.10), reverse water-gas shift (Equation 3.11), CO hydrogenation (Equation 3.12). Said reaction rates are dependent on the used catalyst, as well as the operating conditions, which usually range between 50 - 100 bar for pressure and 200 - 300 °C for temperature [74]. Said chemical reactions are shown below.



A crucial part for CH_3OH generation is the choice of the synthesis reactor, as well as the distillation equipment, considering the impurities that would impede the usage of raw methanol as an end product. The typical process configuration can be seen below [75].

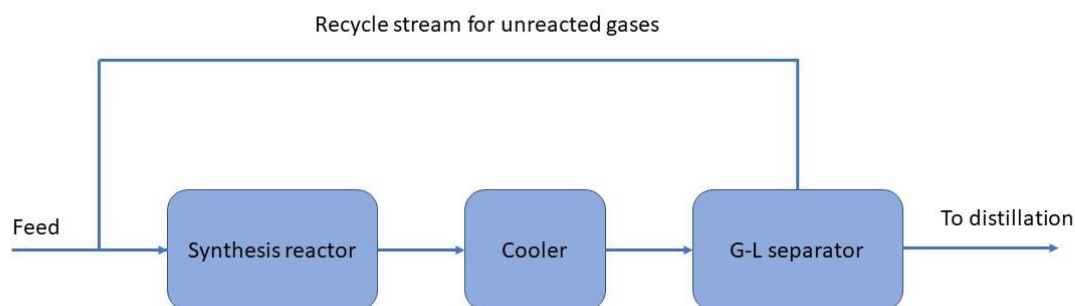


Figure 43: Simplified process configuration for methanol synthesis [75]

The crude methanol outlet stream needs to be cooled down before going towards distillation. Due to the limitation of chemical equilibrium, the conversion is often incomplete, thus the unreacted products are separated after the process, as shown by the recycle stream represented by the upper arrow in Figure 43. Said separation is usually performed in a gas-liquid (G-L) flash separator: the liquid impure CH_3OH is sent towards distillation, while the unreacted gases (mainly H_2 , CO , CO_2) are sent back to the feed [76].

There are various ways to classify methanol synthesis reactors. The first distinctive characteristic is the bed design, which can be fixed-bed or fluidized-bed, even though the former is the most employed type in industry [74]. Another possible classification is thermodynamic, since methanol reactors can be either adiabatic or quasi-isothermal. The difference between the two is the method of heat removal; for quasi-isothermal reactors, the average reaction temperature of the catalyst bed is lower than the adiabatic reactors' one, resulting in longer catalyst lifetime. Since less catalyst is needed to produce the same amount of CH_3OH , isothermal reactors have higher efficiency than adiabatic ones [77]. Yet another possible classification is the cooling technique, which can be gas based or water based [76].

Combination of methanol synthesis reactor technologies has shown to be possible. A well implemented example of this is the Lurgi MegaMethanol two-stage process design, where a water-cooled reactor is followed by a gas-cooled reactor, in order to improve heat integration, decrease the recycle ratio and optimize the use of the water boiling unit [78]. A representation of said two-stage process is shown next page (Figure 44).

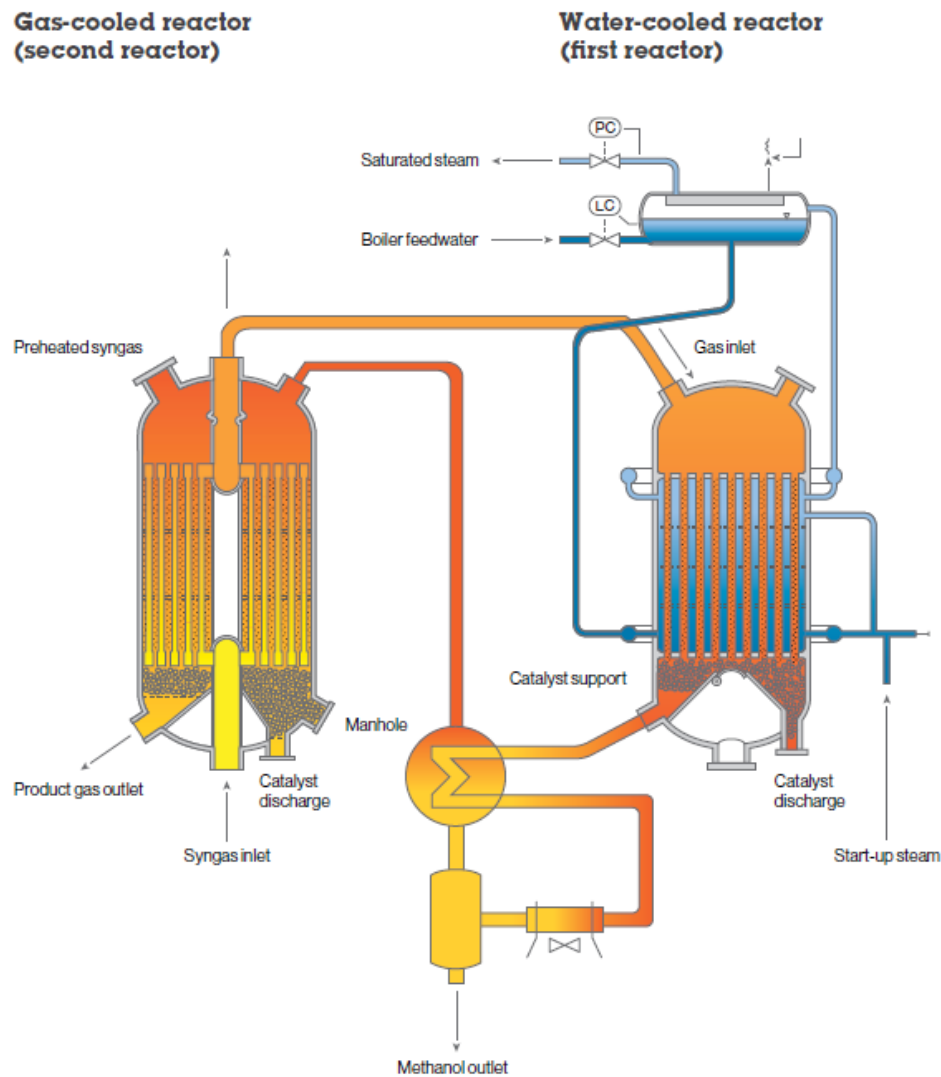


Figure 44: Lurgi MegaMethanol two-stage process design [78]

As mentioned before, distillation is also a very important part of the methanol production process. The required purity has a significant influence on the distillation process; for fuel-grade CH_3OH is sufficient a single column system, while chemical-grade CH_3OH requires higher purity, thus a multiple column system is necessary for distillation, as well as a higher amount of energy, approximately three times the energy required for fuel-grade methanol [77]. A two-column distillation system can be seen next page (Figure 45).

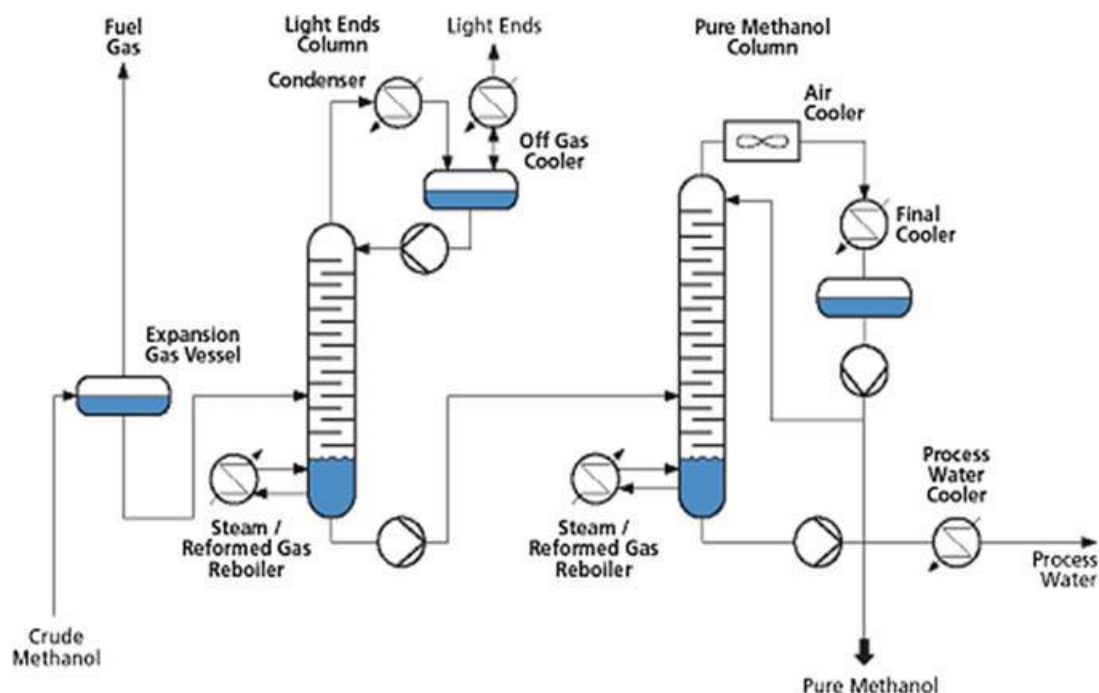


Figure 45: Lurgi two-column methanol distillation system [77]

Unfortunately the analysis of the current and future energy resources at disposal of the HSY eco-centre has shown that producing methanol internally is not feasible. Assuming to have an electrolysis power requirement of 47.8 kWh/kg for the H₂ production [69] (4.0 kWh/Nm³ ÷ 0.08375 kg/Nm³), the methanol production would require more than 90,000 MWh per year. Calculations are shown in the table below:

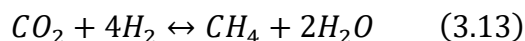
Table 13: Unfeasibility of the internal methanol production [69]

MeOH requirement				10000000 kg			
Electrolysis power requirement, NEL				47.8 kWh/kgH ₂			
N = mole amount							
M = molar mass							
m = mass in reaction equation							
	N, mol	M, g/mol	m, g	m _i /m _{MeOH}	m _i , kg	m _i , ton	E, MWh
H ₂	3	2.02	6.05	0.19	1887640	1887.6	90229
CO ₂	1	44.01	44.01	1.37	13735799	13735.8	
CH ₃ OH	1	32.04	32.04	1.00	10000000	10000.0	

The estimated amount of yearly electrical energy at disposal of the eco-centre is 26284 – 8029 = 18,225 MWh. Considering the Table 13 data, even with the inaccurate assumption to not have any other additional electricity consumptions, using all the electrical energy at disposal of the eco-centre would cover only (18225/90229) · 100 = 20.23 % of the energy necessary to produce all the methanol needed by HSY.

3.1.7 Methane production

Another versatile end-product that can be obtained from CO₂ is methane. The chemical process to obtain CH₄ from CO₂ is called methanation, and it can be represented by the following chemical reaction:



The conversion can be obtained directly through CO₂ hydrogenation, or through the intermediate conversion of CO₂ to CO. Below, a representation of the two paths.

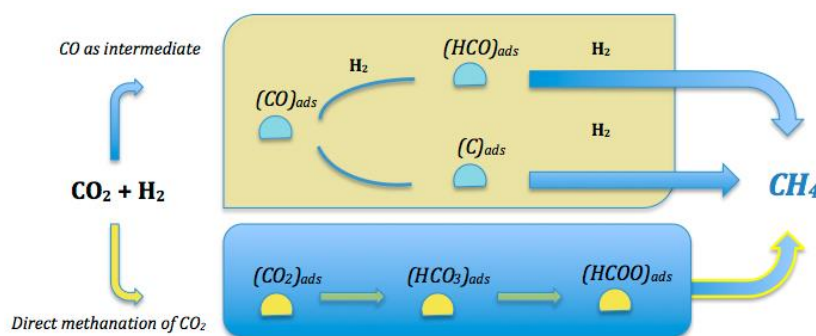


Figure 46: Simplified reaction mechanisms of CO₂ methanation [79]

Methanation can be distinguished into thermochemical methanation and biological methanation. The former is defined as the conversion represented by Figure 44 paths, facilitated by the presence of a catalyst, usually nickel based. Typical operating pressures and temperatures range between 1 - 100 bar and 300 - 550 °C respectively. Thermochemical methanation can be subdivided in respect to its process design: fixed bed methanation, fluidized bed methanation, three-phase methanation [80].

The latter consist in a process in which a biocatalyst facilitates the conversion of hydrogen and carbon dioxide into methane. Biological methanation operates at relatively low temperatures (40 - 70 °C), which makes the process simple to implement, especially for small plant applications. This type of methanation can also generate better grade CH₄, since the micro-organisms have high tolerance for the gas impurities typically found in methanation feed gases, such as sulphur and ammonia. The technical implementation of this process however is still an issue, especially because of the nature of the reaction site: since H₂ is poorly soluble in liquids, the aqueous solution where the chemical reaction occurs makes it so that the supply of hydrogen is the biggest problem of the process, due to mass transfer limitations [80].

An interesting pathway to generate CH₄ could be the conversion of the biogas produced by the eco-centre CHP2. The biogas composition can be assumed to be 65 % CH₄, 35% CO₂ plus trace amounts of other gases [81], so the chemical conversion from biogas to CH₄ could be potentially more feasible than the CO₂ hydrogenation of the gas engine exhaust CO₂, which would also require a CCS or CCU system. This process will be analysed in more detail in Chapter 4.

A 2019 study from Moiola et al [82] shows an interesting configuration of a combined methanol-methane synthesis process; its representation is showed below.

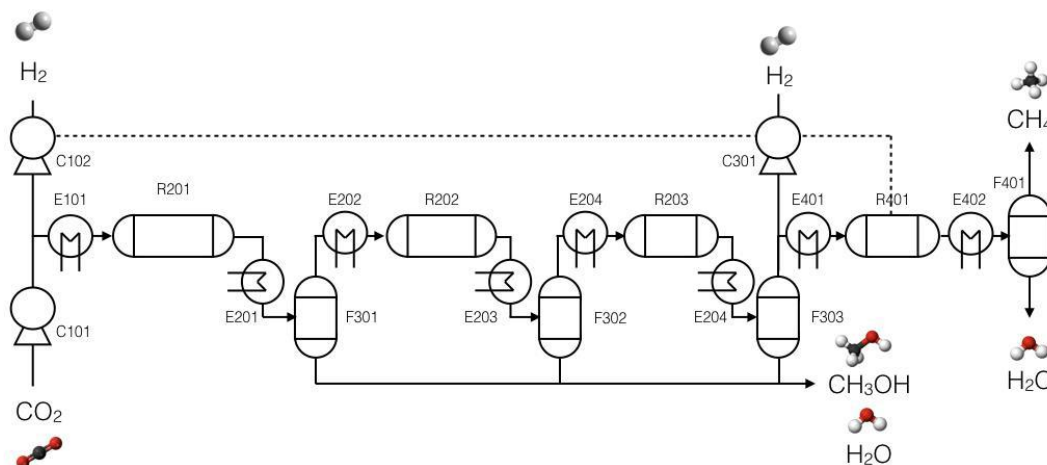


Figure 47: Diagram of a combined methanol-methane synthesis process [82]

The process can be divided in four steps: preparation, methanol production, methanol separation, methane production. The units' symbols represent, respectively, reactors (R), heat exchangers (E), flashers (F), compressors (C). The units' numbers represent the unit number followed by the respective step: R203, for example, represents the second reactor in the third step.

During the first step the reactants are delivered at the appropriate stoichiometric, temperature and pressure conditions. For the second step, H₂ and CO₂ are compressed and sent towards the cascade reactors and flashers configuration (which can improve the chemical conversion process). For the third step the unreacted gases are separated from the flow. For the fourth step, methane is generated with the remaining unused product from the previous steps (R401, F401).

3.1.8 Electric powered buses and hydrogen powered buses

A viable use for some end products of the HSY eco-centre can be alternative fuel for public transportation. Since the electricity self-sufficiency of the centre is not at risk, it might be possible to have a surplus of electricity once the renewable energy sources are implemented; said resource could be used to power electric vehicles, such as electric powered buses (E-buses). A similar strategy could be implemented for the generated H₂ via electrolysis, for fuel cell powered buses (H-buses).

Since resource management is key in this analysis, the most important thing to understand is the consumption of the said vehicles.

Regarding E-buses, a report from the company ViriCiti analysed data from more than 100 buses in Netherlands, over a period of 10 months (Jun 2019 – March 2020) [83].

The characteristics of the analysed data were the following:

- The buses were divided into two categories, according to their length: 12 meter long (12m) buses and 18 meter long (18m) buses
- To gather as much representative as possible data, buses that drove for less than 40 km per day were excluded, and buses that drove for less one third of the days included in the analysis period were excluded
- Temperature affects the performance of the buses, so it was taken into consideration and split into three categories: cold ($-10/14$ °C), normal ($15/19$ °C), hot ($20/29$ °C)

The average distance run by the buses was found to be 218.02 km/day for 12m buses and 164.32 km/day for 18m buses. The average fuel consumption was found to be 1.15 kWh/km for 12m buses and 1.63 kWh/km for 18m buses. Below, two graphs showing the correlation between fuel consumption and temperature, for both bus lengths.

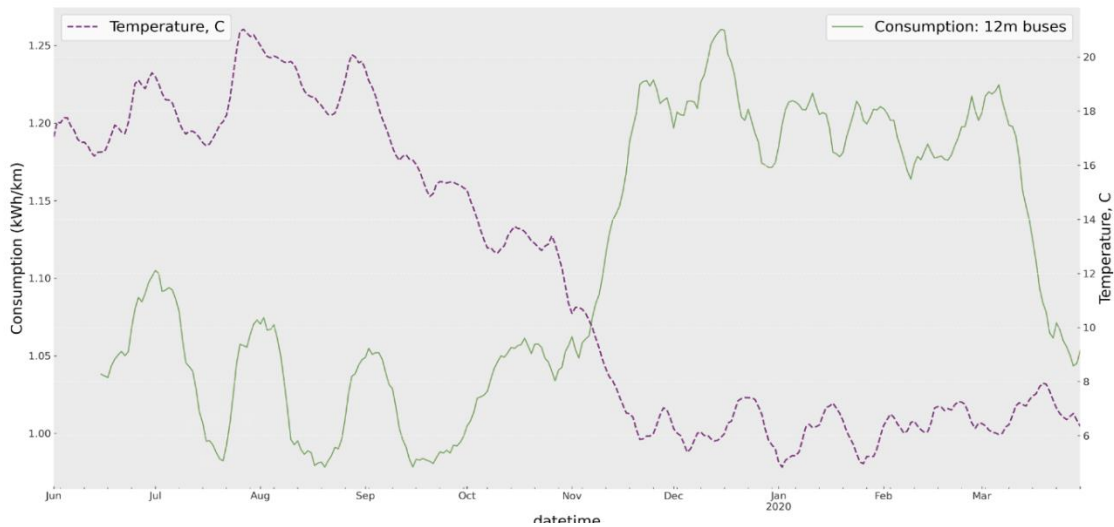


Figure 48: Correlation between temperature and daily average consumption of 12m buses [83]

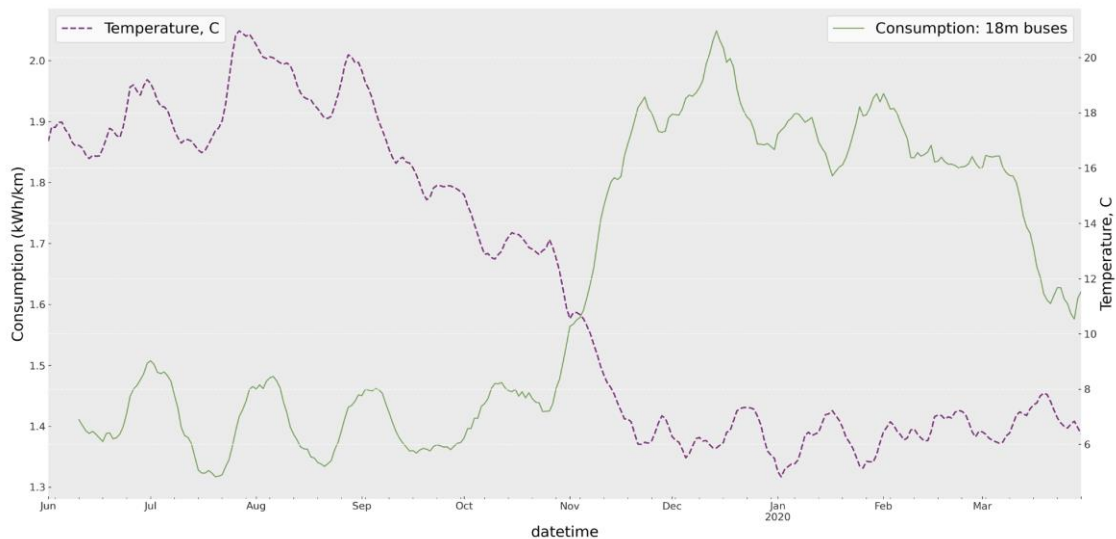


Figure 49: Correlation between temperature and daily average consumption of 18m buses [83]

CHALMERS UNIVERSITY OF TECHNOLOGY
Gothenburg, Sweden, December 2021
www.chalmers.se

Figure 48 and 49 (previous page) show how the temperature affected the fuel consumption. On average, cold temperatures increased by 14% the 12m buses consumption and by 21% for 18m buses consumption; hot temperatures increased by 9% the 12m buses consumption and by 12% for 18m buses consumption.

Another study from Xylia M. et al [84] showed similar results: the consumption assumed for the modelled infrastructure of electric buses in Stockholm showed an average value of 1.50 kWh/km .

Regarding H-buses, a report from Lozanovski A. et al [85] presented an evaluation of the performance of fuel cell buses throughout the European Economic Area. Said buses are from different manufacturers and cities, thus have different characteristics, which are listed on the table below.

Table 14: Characteristics of the fuel cell buses (H-buses) [85]

Bus Manufacturer	APTS	EvoBus Mercedes-Benz	New Flyer	Van Hool	Wrightbus
Number of buses	Cologne: 2	Aargau: 5 Bolzano: 5 Hamburg: 4 Milan: 3	Whistler: 20	Cologne: 2 Oslo: 5	London: 8
Overall length [m]	18.5	12	12.5	13.2	11.9
Net weight [t]	20.6	13.2	15.4	15.7/16.1	10.3–11.3
Passenger capacity [no.]	96	76	60	101/76	49
Number of axles	3	2	2	3	2
Drive power [kW]	240	$2 \times 120 \text{ max}$	$2 \times 85 \text{ max}$	$2 \times 85 \text{ max}$	$2 \times 67 \text{ max}$
Fuel cell manufacturer	Ballard	AFCC	Ballard	Ballard	Ballard
Fuel cell system power [kW]	150	120	150	150	75
Electricity Storage Type	NiMH battery + Supercaps	Li-Ion battery	Li-Ion battery	Li-Ion battery	Supercaps
Electricity storage Power [kW]	Max. 200	250	N/A	120/100	105
Electricity storage capacity [kWh]	Supercaps 2 Battery 26	26.9	47	24/17.4	20
Hydrogen cylinders (@350 bar) [no.]	8	7	8	8/7	4
Hydrogen storage capacity [kg]	40	35	56	40/35	31

The consumption of the H-buses was found to be, on average, $12 \text{ kg}_{\text{H}_2}/100\text{km}$; only considering the 12 meter long buses, the average value was found to be $9 \text{ kg}_{\text{H}_2}/100\text{km}$. This data can be seen from the table, below.

Table 15: Average consumption of the fuel cell buses (H-buses), in respect to their length [85]

Site	Bus Length [m]	Number of Vehicles [No.]	At Each Site	Average Fuel Consumption	
				All 54 FC Buses	Only 12 m Solo Buses (25 out of 54)
				[kg H ₂ /100 km]	
Cologne	18.5	2	16.5	12.0	9.0
Whistler	12.7	20	14.9		
Cologne	13.2	2	14.4		
Oslo	13.2	5	13.2		
Hamburg	12.0	4	8.7		
Aargau	12.0	5	8.0		
Bolzano	12.0	5	8.6		
London	11.9	8	9.6		
Milan	12.0	3	9.9		

3.2 Economic point of view

In this sub-chapter the costs of the various investments will be shown. According to the 2020 IRENA Renewable Power Generation Costs report [86], 2010-2020 has been a decade of falling costs for renewable energy sources. The picture below shows said trend for renewable based technologies.

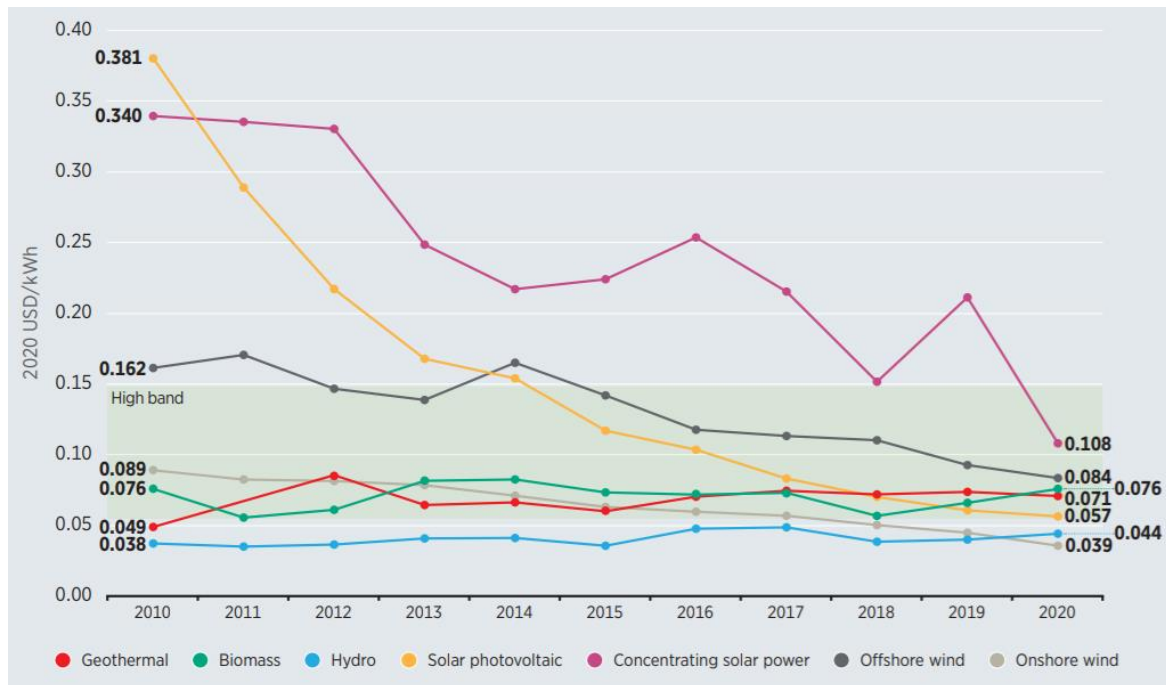


Figure 50: Global weighted-average LCOE by technology, 2010-2020 [86]

The table below shows cost estimates of the technologies analysed in this work. The costs for the buses were not included, since said information is not relevant for this master thesis' analysis.

Table 16: Cost estimates of the technologies analysed in this work.

*LCOX has been used since "X" can represent various parameters (electricity, heat, hydrogen, etc.)

¹Europe weighted average price, IRENA [86] ; ²World weighted average price, IRENA [86]

³Heat pump prices, Nera A. ; GREBE [87][88] ; ⁴Hydrogen price in Europe, European Commission [89]

⁵Methanol production prices for a 10 kt/a plant, Nyari J. [90] ; ⁶Methane production costs [89]

		CAPEX [€/kW]	OPEX [€/kW/a]	LCOX*
Wind	Onshore	1322 ¹	19.50 ²	0.034 €/kWh _{el} ²
	Offshore	2961 ¹	65.60 ²	0.073 €/kWh _{el} ²
Solar	PV	771 ²	8.80 ¹	0.050 €/kWh _{el} ²
Heat pump	ASHP	715 – 736 ³	11.70 ³	0.066 €/kWh _{heat} ³
	GHSP	1319 – 1420 ³	11.70 ³	0.052 €/kWh _{heat} ³
Electrolyser	AEL	628 – 1955 ⁴	2-5%(CAPEX) ⁴	0.115 – 0.335 €/kWh _{H₂ LHV} ⁴
CO ₂ + H ₂	Methanol	22420000 € ⁵	8000000 €/a ⁵	1.035 €/kg _{MeOH} ⁵
	Methane	530 – 600 ⁶	5-10%(CAPEX) ⁶	0.28 – 0.41 €/kg _{CH₄} ⁶

4. Future energy scenarios

4.1 Methodology

The focus of this chapter will be the analysis of potential future energy scenarios for the HSY Ämmässuo eco-centre. According to Letheva V.'s work [49], the electricity and heat energy consumption of the centre will increase in the following years, mainly due to new sectors being developed in the Ämmässuo area, such as the introduction of a sorting and processing hall for waste disposal.

The electricity consumption estimate can be seen below (Figure 51), while the heat consumption estimate can be seen next page (Figure 52).

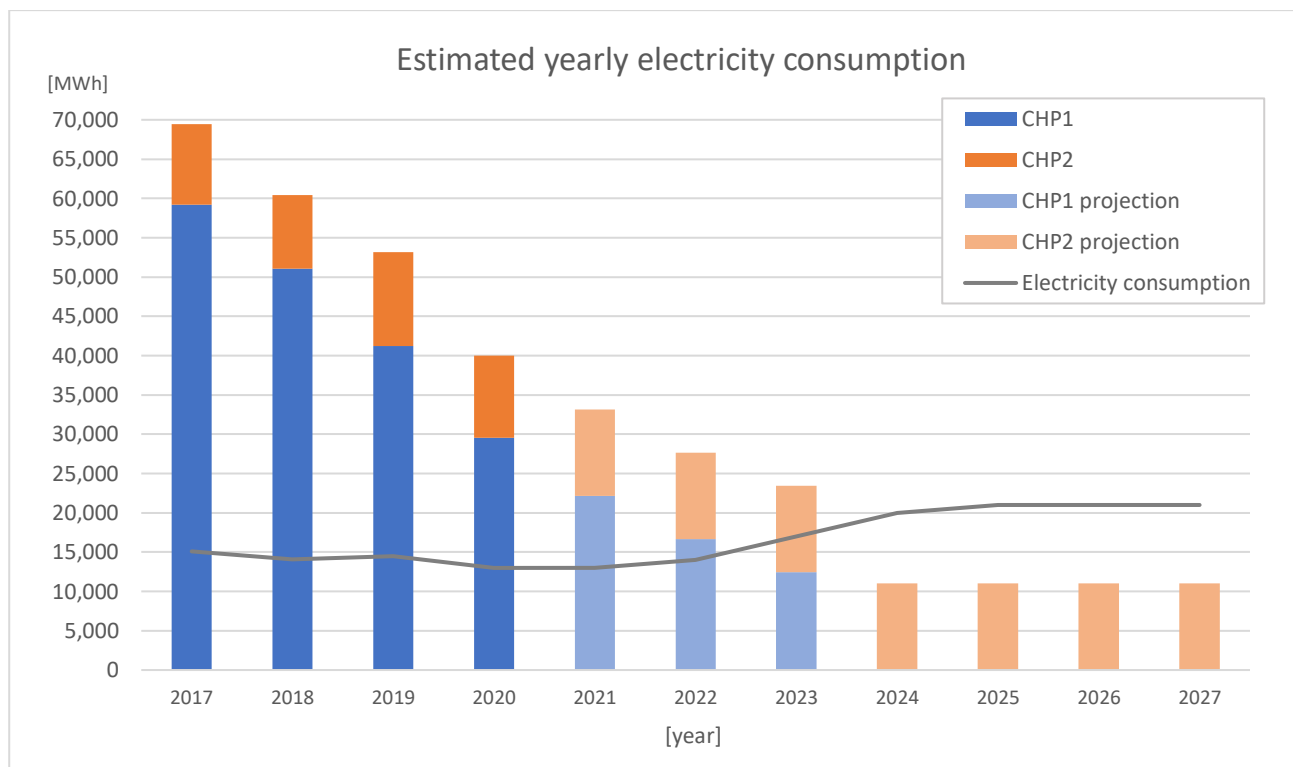


Figure 51: Estimated yearly electricity consumption for the Ämmässuo eco-centre [49]

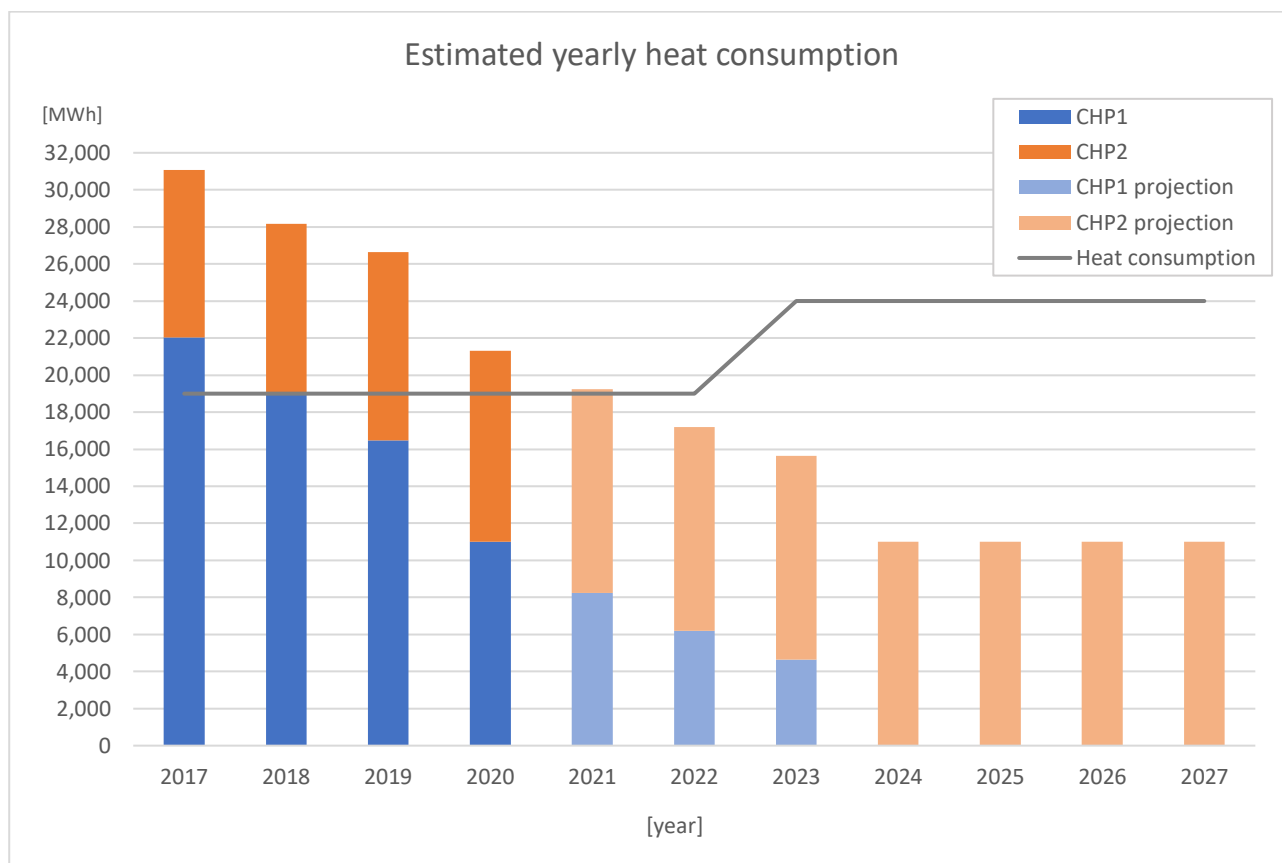


Figure 52: Estimated yearly heat consumption for the Ämmässuo eco-centre [49]

According to these projections, the 2025 electricity and heat yearly requirements of the centre will be 21,000 MWh and 24,000 MWh respectively. The year 2025 is relevant for two reasons: firstly, it will be the year in which the wind turbine obtained by HSY will be operative; secondly, in 2025 the landfill gas engines will be no longer be functional, thus the landfill gas will no longer be a resource for the eco-centre.

The methodology of the future scenarios' analysis will be to understand how to cover the energy requirements of the eco-centre, using both the current resources and the resources provided by the possible investments. There will be scenarios in which the energy produced will be more than the energy required: in that case, the surplus energy will be either sold (when possible) or utilized to generate useful end products, such as H₂.

Each scenario will consider the same investments of the previous one plus additional ones, gradually increasing the level of complexity of the energy system, as well as the resources that can be generated. This, of course, will also increase the overall costs.

Considering the intermittent nature of renewable energy sources, the relative energy analysis will be mostly a monthly one. For the economic point of view analysis, the method that will be mainly utilised is the DPBP (discounted payback period, as described on Chapter 1.3). Most of the calculations will be done using Microsoft Excel.

4.2 Power-to-X perspectives

As mentioned before, when the energy produced will be more than the energy required in the analysed scenarios, the surplus can be utilized to produce hydrogen. This concept can be viewed as the definition of Power-to-X: the energy carriers and chemical products that can be generated using excess energy can provide significant versatility for the energy sector, especially regarding the storage, which is key to solve the intermittency issue linked to renewable sources.

Electrolysis is the core of P2X technologies, since the hydrogen produced can be further converted using processes such as hydrogenation, as mentioned in Chapter 1.2.3 of this master's thesis.

Even though the Ämmässuo eco-centre is not a site specialized for hydrogen production, a particularly attractive pathway is the internal generation of methanol: not only the chemical compound is utilised by the regional authority HSY for wastewater treatment, but since CO₂ can be used to produce it, the process would remove it from the system, potentially creating a negative CO₂ cycle.

However this idea presents vast flows. First of all, as discussed in Chapter 3.1.6 of this work, internal methanol production is not doable with the potential amount of surplus electricity at disposal of the eco-centre. Secondly, capturing the CO₂ would require installing a carbon capture and utilisation (CCU) system, something that is not feasible for the eco-centre. Finally, even assuming to have solved the two previously described obstacles, the costs to set up the whole system would be so high that buying the methanol would still result to be the better option.

Shifting away the focus from Ämmässuo towards a more general discussion, the benefits of renewable P2X is increasingly well-recognized by governments and industries around the globe. According to Daiyan, R. et al report [101], various P2X projects of different scale can be hypothesized and classified in three categories, according to their capacity.

The first wave of deployment (kW capacity) would entail the usage of P2X on a individual/household level, which may include utilization of green H₂ as an energy storage for domestic and office purposes. The second wave of deployment (MW capacity) would entail the generation of products for utilization as feedstock for industry, such as ammonia and synthetic hydrocarbons. The third wave of deployment (hundreds of MW – GW capacity) would entail the production of bulk volumes of green H₂, which would be expected to make a significant contribution to a country's energy mix.

A picture of the previously described P2X roadmap can be viewed next page (Figure 53).

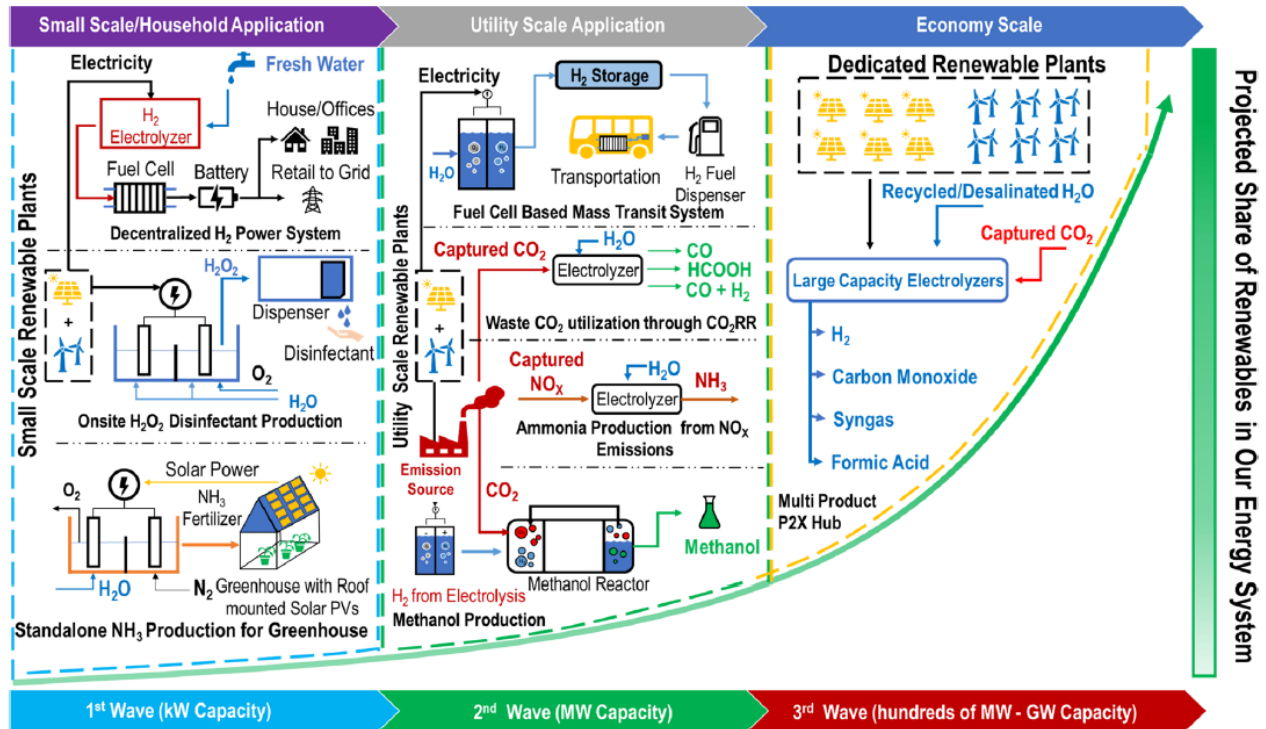


Figure 53: P2X deployment roadmap [101]

4.3 Scenario 1: Heat pump acquisition, doubling of the biogas engine utilization factor

In order to achieve energy self-sustainability, the HSY eco-centre needs to have access to a certain amount of both electricity and heat, as previously described. The acquisition of a heat pump can be considered one of the most important investments in this sense. Considering that the machine's function is to convert electricity into heat with an efficiency greatly superior to 100% (heat pumps' COP can easily be higher than 4.0), it effectively reduces the resources needed for self-sustainability from two to one: if enough electricity is available, the heat pump can essentially provide all the heat that the eco-centre requires.

As it was mentioned in chapter 3.1.4 of this work, a possible investment for the eco-centre would be a ASHP that harnesses thermal energy from the exhaust air of the composting plants. The heat pump would be designed to have a capacity of 2 MW, while its (electrical) consumption would be 400 kW. Knowing this,

$$COP = \frac{Q_{out}}{W_{in}} = \frac{2,000 \text{ kW}}{400 \text{ kW}} = 5.0 \quad (4.1)$$

Assuming that the ASHP runs at full capacity all year, the annual electricity required and annual heat produced are, respectively:

$$E_{HP_{in}} = 400 [kW] \cdot (60 \cdot 60 \cdot 24 \cdot 365) \left[\frac{s}{year} \right] \cdot \left(\frac{1}{1000} \right) \left[\frac{MW}{kW} \right] \cdot \left(\frac{1}{3600} \right) \left[\frac{MWh}{MJ} \right] = 3,504 \frac{MWh}{year}$$

$$Q_{HP_{out}} = E_{HP_{in}} \cdot COP = 3504 \cdot 5 = 17,520 \frac{MWh}{year} \quad (4.2, 4.3)$$

Regarding the electrical energy production, once the landfill gas engines (CHP1) go out of commission, the primary source of electrical energy will be the combined heat and power biogas engines (CHP2). To produce energy, the anaerobic digestion (AD) reactor utilizes biowaste (and sludge) to generate biogas, but then digestate is also produced, which is sent to the composting plants to be processed and turned into compost.

Currently the utilisation rate of the biogas reactors is about 50%; this is due to fact that, even with the second HSY composting plant installed at Ämmässuo, their capacity is insufficient to handle very large amounts of digestate. Knowing that CHP1 will be gradually shut down, bringing the utilisation rate of the biogas reactors up to 100% can be key, since it would double the amount of electricity produced by the biogas engines.

To deal with the increased amount of digestate, mainly two solutions were proposed. Firstly, the utilization of digestate in agriculture as a fertilizer was investigated. In a survey conducted by Taitosuuli in 2021, twenty Uusimaa farmers were interviewed; everybody expressed interest but emphasized that the product would have to be tested first [49]. Secondly, a pyrolysis plant could receive and process the digestate, in order to produce biochar. A pilot plant was commissioned in 2021, in order to understand whether a full scale plant for the Blominmäki wastewater treatment (WWT) sludge would be feasible; a decision regarding said investment is scheduled to happen in 2022 - 2023. The full scale plant would not bring major changes for the energy requirements of the eco-centre, since it would be self-sufficient; the produced thermal energy would mainly be used to dry the sludge [49].

Another energy source for the Ämmässuo eco-centre is the ORC (Organic Rankine Cycle, as described in Chapter 2.2), a system that produces thermal energy from the exhaust of the biogas plant, thus recovering waste heat. The energy produced by this system is included in the CHP2 data. Next page (Figure 54), a representation of the scenario.

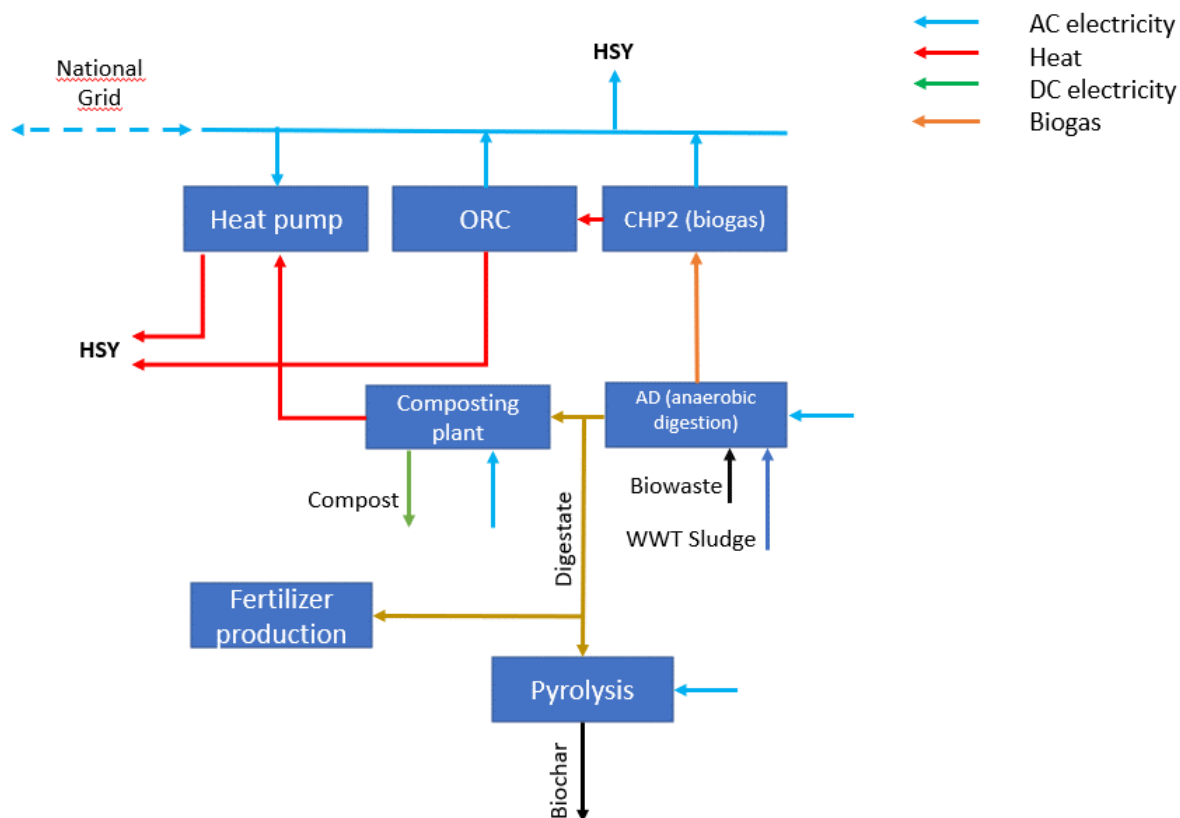


Figure 54: Scenario 1

Assuming to have two times the electrical energy produced by the CHP2 plant with the utilisation rate of the biogas reactors up to 100%, the situation in 2025 would be the following:

Table 27: Scenario 1 energy balance

Ämmässuo (2025)	Produced [MWh]	Required [MWh]	Difference [MWh]
<i>before the heat pump:</i>			
Electricity	$11,000 \cdot 2$	21,000	1,000
Heat	$11,000 \cdot 2$	24,000	-2,000
<i>using the heat pump:</i>			
Electricity	$11,000 \cdot 2$	$21,000 + 400$	600
Heat	$11,000 \cdot 2 + (5 \cdot 400)$	24,000	0

The calculations show that, with the heat pump and the biogas reactors utilization up to 100%, HSY would have 600 MWh leftover energy each year. Assuming to have an average electricity price of 0.1767 €/kWh [91], the regional authority could gain $0.1767 \cdot 1000 \cdot 600 = 106,020$ €/year.

Assuming to have a PBP of five years for the capital cost of the ASHP, the municipal federation would have to pay $(294400 / 5) = 58880$ €/year, for 5 years. Adding the annual earnings and costs, in this situation HSY's balance would be $(106020 - 4680 - 58880) = + 42,460$ €/year for five years, then $(106020 - 4680) = + 101,340$ €/year.

By doubling the CHP2 utilisation factor, deploying the heat pump and selling the surplus electricity to the grid, the self-sufficiency of the eco-centre can be secured. However it can be attractive to explore other possibilities, as it will be shown in the following chapters.

It was mentioned in Chapter 2 of this work that HSY is investing in a wind turbine, in order to face the threat to the eco-centre self-sufficiency brought by the future decision of not utilising the landfill gas in the future. A picture of the scenario can be seen below:

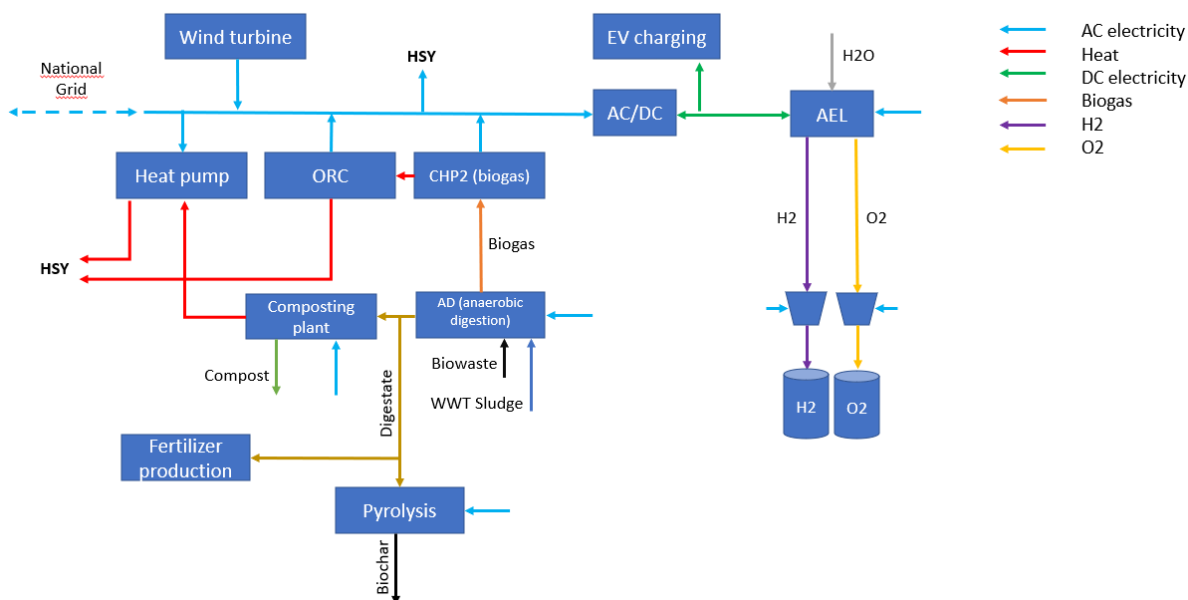


Figure 55: Scenario 2

The amount of electrical energy required by the eco-centre each month will be compared with the amount of electrical energy that the wind turbine can provide monthly. This comparison can be seen next page (Table 18).

Table 18: Scenario 2: electricity, before using the heat pump

Electr. [MWh]	Jan	Feb	Mar	Apr	May	Jun	Jul	Aug	Sep	Oct	Nov	Dec
Produced												
CHP2*	2149	1798	2012	1766	1756	1234	1207	1395	1776	1861	1866	1991
Wind power	1541	1182	930	785	830	682	606	648	906	1142	1037	1275
Required*	1919	1826	1795	1671	1699	1793	1730	1706	1733	1757	1676	1695
Difference	1771	1154	1147	880	887	123	83	337	949	1246	1227	1571

Regarding the electricity produced by CHP2 and the electricity required by the eco-centre, marked with an asterisk on Table 18 (previous page), since the 2025 monthly data was not available, approximations were made. For the former, the 2020 monthly data was doubled, in order to fit the assumption that the power generation would be doubled if the utilisation rate of the biogas reactors will be brought to 100%. For the latter, this equation was utilised:

$$\frac{E_{req,2025} = 21,000 \text{ MWh}}{\sum_1^{12}(E_{month,2020})} = k \Rightarrow E_{month,2025} = k \cdot E_{month,2020} , \forall \text{ month} \quad (4.4)$$

A graph representing the electricity situation can be seen below.

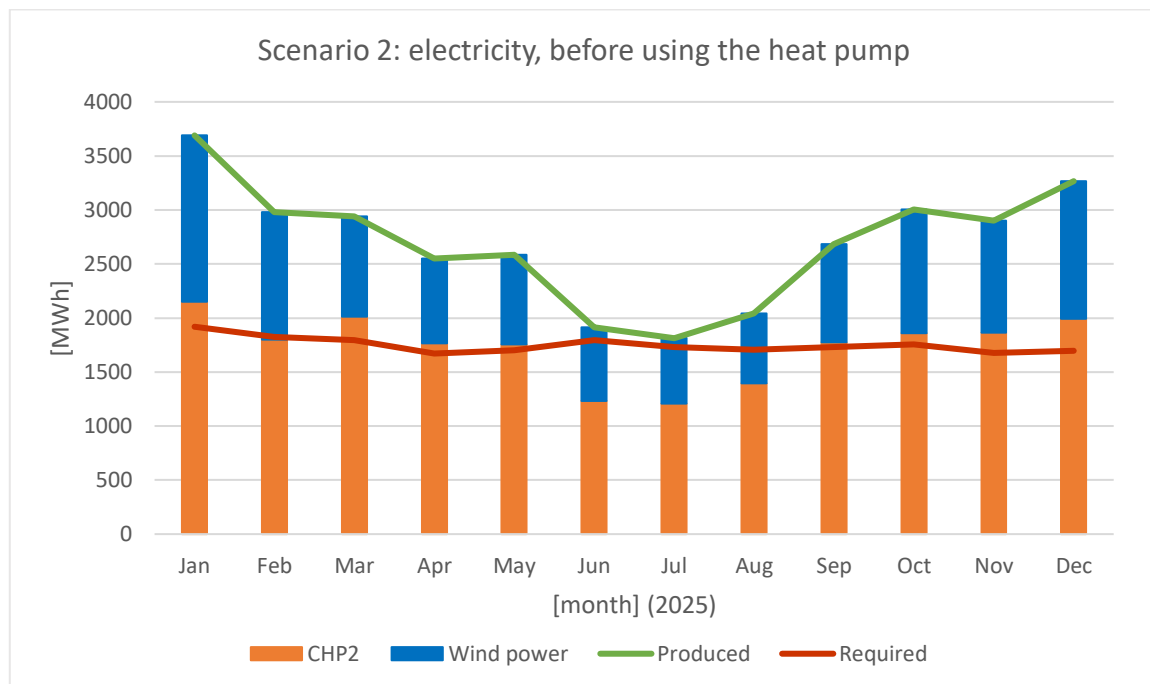


Figure 56: Scenario 2: electricity, before using the heat pump

The “Difference” row in Table 18 (previous page) represents the monthly surplus electrical energy at disposal of the Ämmässuo eco-centre. It is necessary to analyse how the situation for heat would be in this scenario, in order to understand how to utilise the extra energy.

The comparison described by Table 18, but for heat energy, can be seen below (Table 19); the same assumptions were utilised, however $Q_{req,2025} = 24,000 \text{ MWh}$ instead.

Table 19: Scenario 2: heat, before using the heat pump

Heat [MWh]	Jan	Feb	Mar	Apr	May	Jun	Jul	Aug	Sep	Oct	Nov	Dec
Produced												
CHP2*	2055	1815	1988	1801	1808	1365	1233	1235	1624	1850	1879	2005
Required*	2554	2708	2660	2203	1768	1220	1257	1298	1595	1958	2193	2585
Difference	-499	-893	-672	-402	40	145	-24	-63	29	-108	-314	-580

It’s possible to see that each month, with May June and September as exceptions, there is a deficiency that prevents the eco-centre to achieve heat self-sufficiency. By utilising the heat pump and the surplus electrical energy shown in Table 18 (previous page), it is possible to achieve said self-sufficiency. Assuming that the ASHP utilisation rate can be modulated monthly (and in general), the electricity required by the heat pump would simply be the ratio between the heat needed by the centre and its COP: $E_{HP_{cons}} = Q_{HP_{diff}}/COP \text{ [MWh/month]}$.

Knowing this, it’s possible to visualise the situation after utilising the heat pump, summarized by the table below and the picture next page (Figure 57).

Table 20: Scenario 2: heat, after using the heat pump

Heat [MWh]	Jan	Feb	Mar	Apr	May	Jun	Jul	Aug	Sep	Oct	Nov	Dec
Produced												
CHP2*	2055	1815	1988	1801	1808	1365	1233	1235	1624	1850	1879	2005
Required*	2554	2708	2660	2203	1768	1220	1257	1298	1595	1958	2193	2585
Difference	-499	-893	-672	-402	40	145	-24	-63	29	-108	-314	-580
Heat pump												
El. consumed	100	179	134	80	0	0	5	13	0	22	63	116
Heat produced	499	893	672	402	0	0	24	63	0	108	314	580
Difference	0	0	0	0	40	145	0	0	29	0	0	0

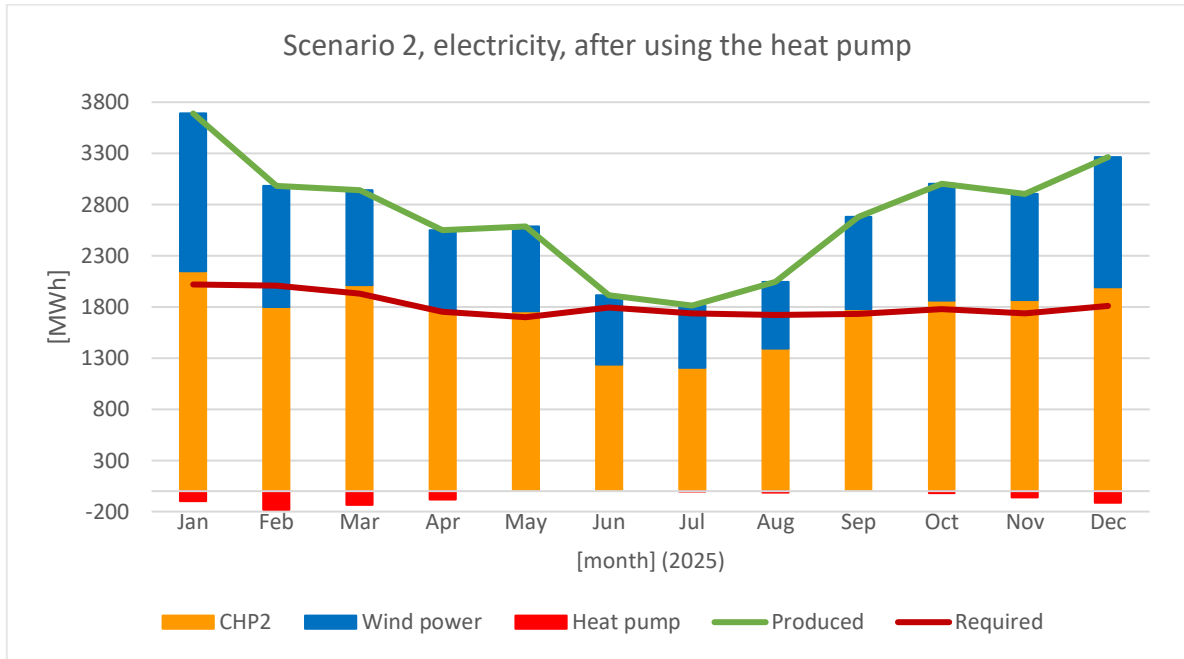


Figure 57: Scenario 2, electricity, after using the heat pump

Equation 4.2 (page 74) regulates the energy balance of the heat pump; a more generic version can be seen below:

$$E_{HP_{cons}} \left[\frac{MWh}{month} \right] = P_{el} [kW] \cdot t_{month} \left[\frac{s}{month} \right] \cdot \left(\frac{1}{1000} \right) \left[\frac{MW}{kW} \right] \cdot \left(\frac{1}{3600} \right) \left[\frac{MWh}{MJ} \right] \quad (4.5)$$

From Equation 4.5 (above), since $E_{HP_{cons}}$ is regulated by the heat needed by the eco-centre monthly, the two variables are P_{el} and t_{month} . If P_{el} is kept at 400 kW and cannot be changed, each month the ASHP will be active the amount of time necessary for it to consume $E_{HP_{cons}}$ and thus produce the exact amount of heat needed. Alternatively, the heat pump could run all year (t_{month} is kept at its maximum value), while P_{el} is modulated, thus keeping the utilisation rate of the heat pump under 100% all the time.

In both cases, the ASHP would not run/be in standby mode in May, June and September, which means that the small amount of surplus heat of these months would be wasted. Regardless, the eco-centre heat self-sufficiency would be achieved.

Graphs representing the heat situation can be seen next page (Figure 58 and 59).

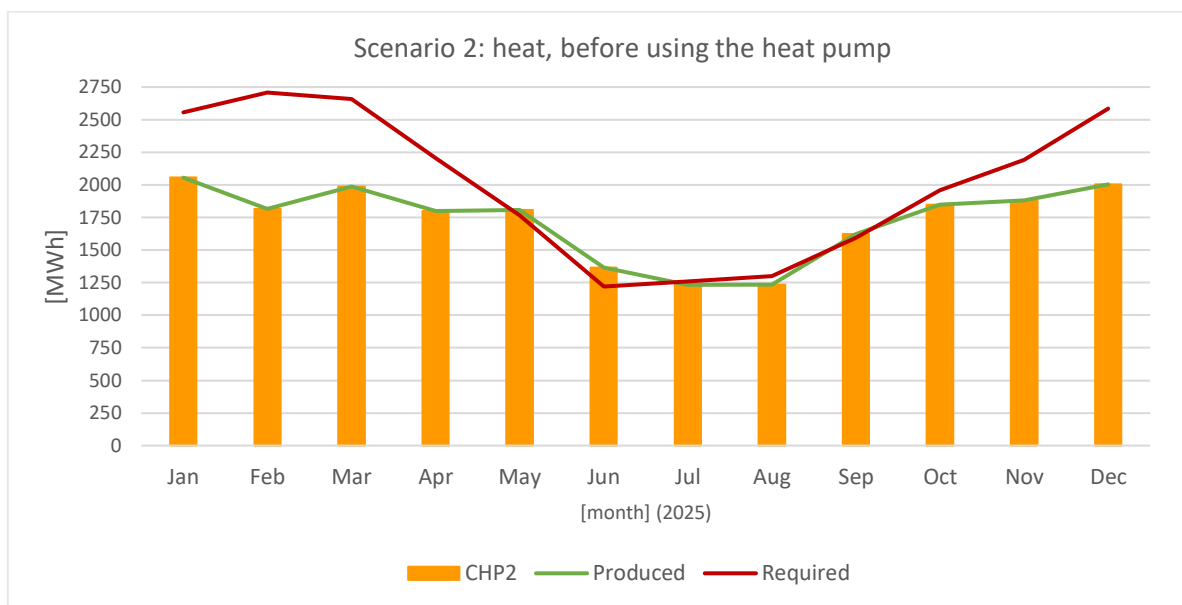


Figure 58: Scenario 2: heat, before using the heat pump

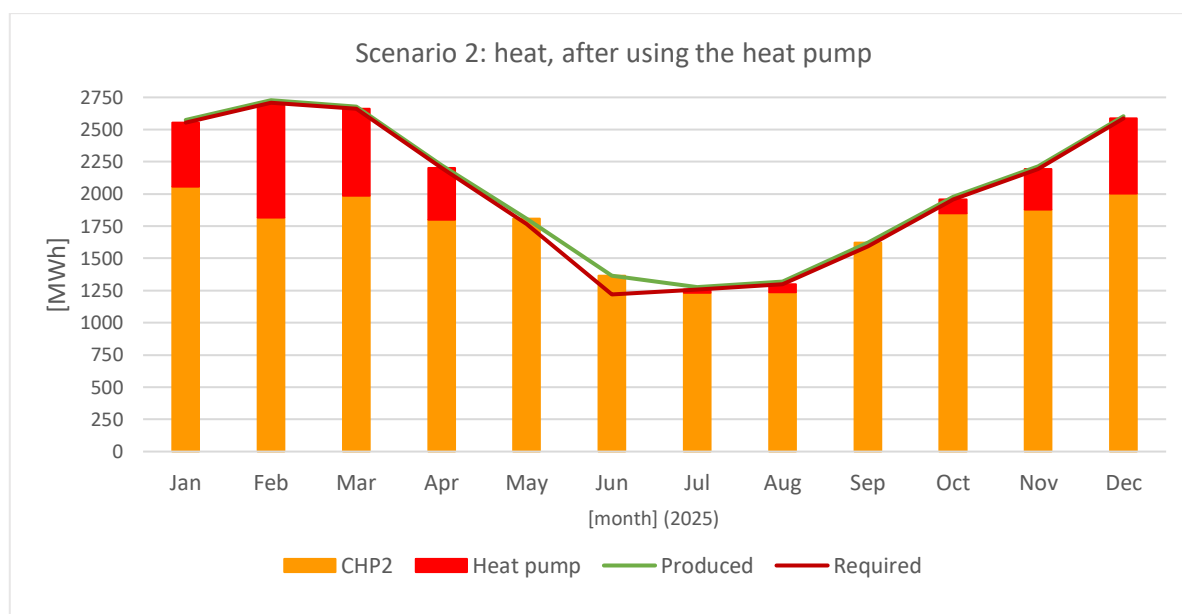


Figure 59: Scenario 2: heat, after using the heat pump

Since it has been established how much electricity will be needed for the heat pump, it is possible to calculate the leftover surplus electrical energy. The results are shown on Table 21, next page; the assumptions made for the Table 18's data (page 77) are again applied for the entries marked with an asterisk.

Table 21: Scenario 2, electricity, after using the heat pump

Heat [MWh]	Jan	Feb	Mar	Apr	May	Jun	Jul	Aug	Sep	Oct	Nov	Dec
CHP2*	2149	1798	2012	1766	1756	1234	1207	1395	1776	1861	1866	1991
Wind power	1541	1182	930	785	830	682	606	648	906	1142	1037	1275
Heat pump	-100	-179	-134	-80	0	0	-5	-13	0	-22	-63	-116
Produced	3690	2980	2942	2551	2586	1916	1813	2043	2682	3003	2903	3266
Required*	2019	2005	1929	1751	1699	1793	1735	1719	1733	1779	1739	1811
Difference	1671	975	1013	800	887	123	78	324	949	1224	1164	1455

The last line of Table 21 indicates how much surplus electrical energy will be at disposal of the eco-centre each month. This energy could be either sold to the grid for a profit (according to the market price) or used to generate hydrogen with an alkaline water electrolyser (AEL). In order to utilise the electrolyser, an AC/DC inverter is necessary (as shown in Figure 4), since the AEL operates using direct current. Utilising the average Finnish market price of electricity [91], the yearly profit would be:

$$\begin{aligned}
 & 0.1767 \frac{\text{€}}{\text{kWh}} \cdot 1000 \cdot \left(\sum_{\text{year}} E_{\text{surplus}_{\text{month}}} \right) \\
 & = 0.1767 \cdot 1000 \cdot 10663 = 1,884,152 \left[\frac{\text{€}}{\text{year}} \right] \quad (4.6)
 \end{aligned}$$

A compromise between the two beforementioned possibilities could be achieved: part of the extra electricity could be sold, while part of it could be sent towards electrolyser. Speaking of which, even though it has been shown to be possible for the AEL to operate with an intermittent load (Chapter 3.1.5 of this master's thesis), it would be best to utilise a constant load.

Assuming to send 850 MWh of electricity per month towards the AEL, each month it would be either necessary to buy some electricity from the grid to match this level, or possible to sell to the grid the surplus electricity that exceeds 850 MWh. The situation can be represented by Figure 60, next page.

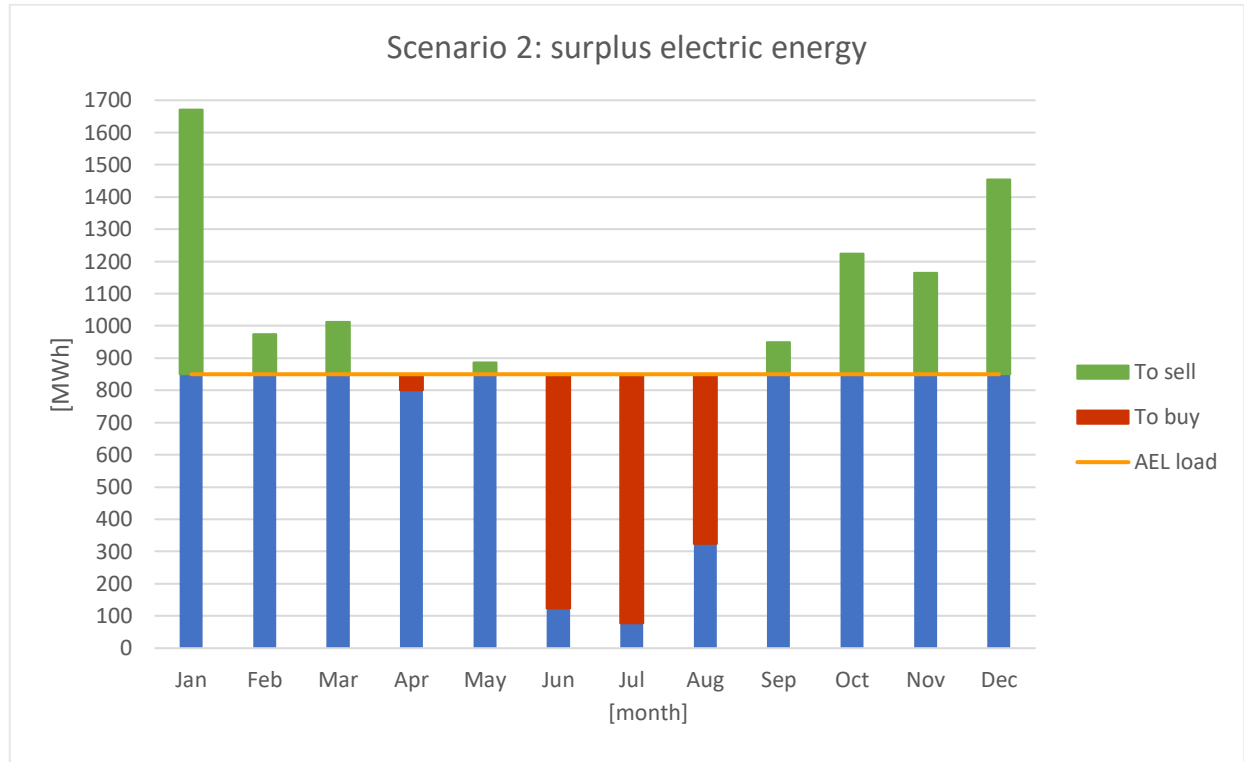


Figure 60: Scenario 2: surplus electricity, AEL monthly load = 850 MWh

In this situation, assuming that the price to sell electricity to the grid is the same as the price to buy it from the grid, the energy sold would be 2,538 MWh, while the energy bought would be 2,075 MWh. Knowing this, a profit would be earned each year:

$$0.1767 \text{ EUR/kWh} \cdot (2538 - 2075) \text{ MWh} \cdot 1000 \text{ kWh/MWh} = 81,812 \text{ €/year} \quad (4.7)$$

Regarding the hydrogen production, it's possible to use the data from NEL [69] to calculate it. Since the power consumption for NEL AEL ranges from 3.8 and 4.4 kWh/Nm³ it can be assumed to have a factor of 4.1 kWh/Nm³; knowing that the monthly energy sent to the AEL is 850 MWh, the H₂ produced would be the following quantity:

$$H_2 [\text{Nm}^3] = (12 \cdot 850 \cdot 1000) [\text{kWh}] \cdot \frac{1}{4.1} \left[\frac{\text{Nm}^3}{\text{kWh}} \right] = 2,487,804.88 \text{ Nm}^3 \quad (4.8)$$

The higher the production rate, the lower the hours for which the electrolyser would have to be active in order to produce said amount of hydrogen. For a production rate of 785 Nm³/h (NEL A1000 alkaline water electrolyser, operating range 600 - 970 Nm³/h):

$$h = 2487804.88 [\text{Nm}^3] / 785 \left[\frac{\text{Nm}^3}{h} \right] = 3,169 \text{ h} \quad (4.9)$$

The amount of energy to be bought from the grid is relatively high in the summer, while the number of hours that the A1000 electrolyser needs to generate the amount of H₂ that can be obtained with the monthly energy of 850 MWh is relatively low. Knowing this, another configuration to be used can be to keep the AEL in standby mode from June to August, in order to substantially reduce the electrical energy to be bought, thus increasing the profit without affecting in a noticeable manner the AEL operations. In this situation, the load could be increased to 1100 MWh.

A representation of the case described on the previous page can be seen below.

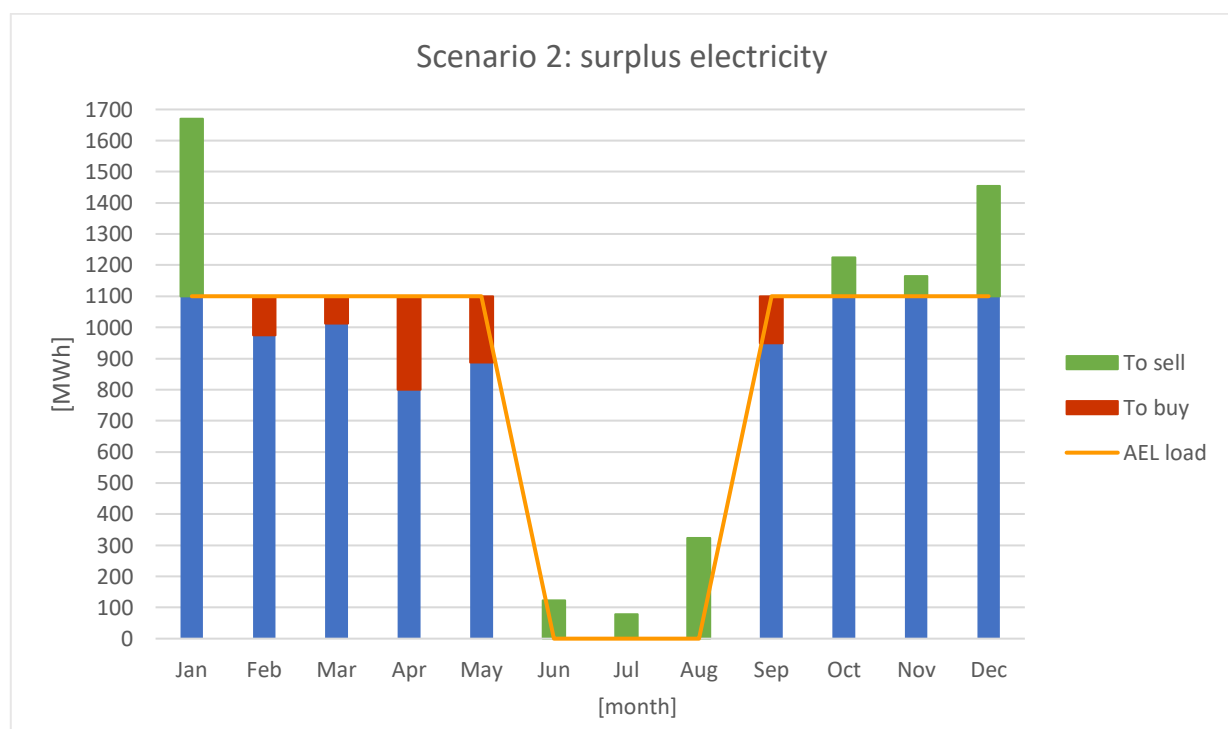


Figure 61: Scenario 2, AEL monthly load = 1100 MWh, summer interruption

The table below shows a comparison between the previously described situations.

Table 22: Scenario 2, surplus electricity utilisation comparison

*the price to buy electricity and sell electricity from/to the grid is assumed to be the same, 0.1767 €/kWh [91]

**the power consumption is assumed to be 4.1 kWh/Nm³ (NEL AELs power consumption: 3.8-4.4 Nm³/h [69])

***the production rate is assumed to be 785 Nm³/h (NEL A1000 AEL production rate: 600-970 Nm³/h [69])

	AEL load [MWh/ month]	Electricity sold [MWh]	Electricity bought [MWh]	Profit* (electricity) [€/year]	H ₂ produced** [Nm ³]	Operating hours*** [h]
No AEL	0	10,663	0	1,884,152	0	0
Continuous load	850	2,538	2,075	81,812	2,487,804.88	3,169
Jun-Aug standby	1,100	1,639	876	13,4882	2,414,634.15	3,076

Table 22 (previous page) shows that the continuous load generates slightly more hydrogen, while the Jun-Aug standby case generates more surplus electricity. Also, the AEL operating hours are relatively low in both cases. Considering that there are 8760 hours each year and 6480 hours every 9 months, the percentage of utilised hours each year would be, respectively, 36.18% and 47.47%. This can be solved by lowering the AEL utilisation rate or by increasing the load towards the electrolyser.

Alternatively, it could be possible to invest in an electrolyser with a lower H₂ production rate, such as the NEL A485, for which the rate is 300 - 485 Nm³/h; this would also lead to lower capital costs (and operating costs, which are a percentage of the CAPEX), considering that the AEL would have a smaller size.

As discussed in Chapter 1.2.3 of this work, one of the main issues with hydrogen is the very low density of the compound. Even though the electrolyser itself could release its products up to a pressure of 200 bar (according to the NEL site [69]), it still is not a satisfying pressure for the H₂ density to be an acceptable level. Knowing this, it's necessary to invest in compressors, shown in the Scenario 2's representative picture (Figure 55).

As explained in chapter one, the AEL produces oxygen as well. Using the proportion from Equation 3.9 (shown in Chapter 3), it is possible to understand how much O₂ can be obtained. Looking at the "Continuous load" case from Table 22, and assuming to have a density of $\rho_{H_2} = 0.08375 \text{ kg/Nm}^3$ for the hydrogen (normal conditions),

$$\begin{aligned} m_{O_2} [kg] &= \frac{1}{2} \cdot m_{H_2} [kg] \cdot \left(\frac{MM_{O_2} [kg/mol]}{MM_{H_2} [kg/mol]} \right) = \frac{1}{2} \cdot \left(\rho_{H_2} \left[\frac{kg}{Nm^3} \right] \cdot V_{H_2} [Nm^3] \right) \cdot \left(\frac{MM_{O_2} [kg/mol]}{MM_{H_2} [kg/mol]} \right) \\ &= 0.5 \cdot (0.08375 \cdot 2487804.88) \cdot (31.99 \cdot 10^{-3} / 2.106 \cdot 10^{-3}) = 1,653,083.71 \text{ kg} \end{aligned} \quad (4.10)$$

The same method can be used for the Jun-Aug standby case, resulting in 1,604,463.61 kg of produced oxygen.

Scenario 2 really shows how much difference is the wind turbine capable of making for the self-sustainability of the centre, especially when paired with the heat pump, to the point of not only achieving self-sufficiency, but also generating hydrogen, oxygen and revenue due to the electricity surplus.

4.5 Scenario 3: Addition of solar panels

Scenario 3 is very similar to Scenario 2: the addition of solar panels can increase the energy gained from renewable sources, but it doesn't change the pattern of the energy system by much. This can be seen by looking at Scenario 3's picture next page (Figure 62).

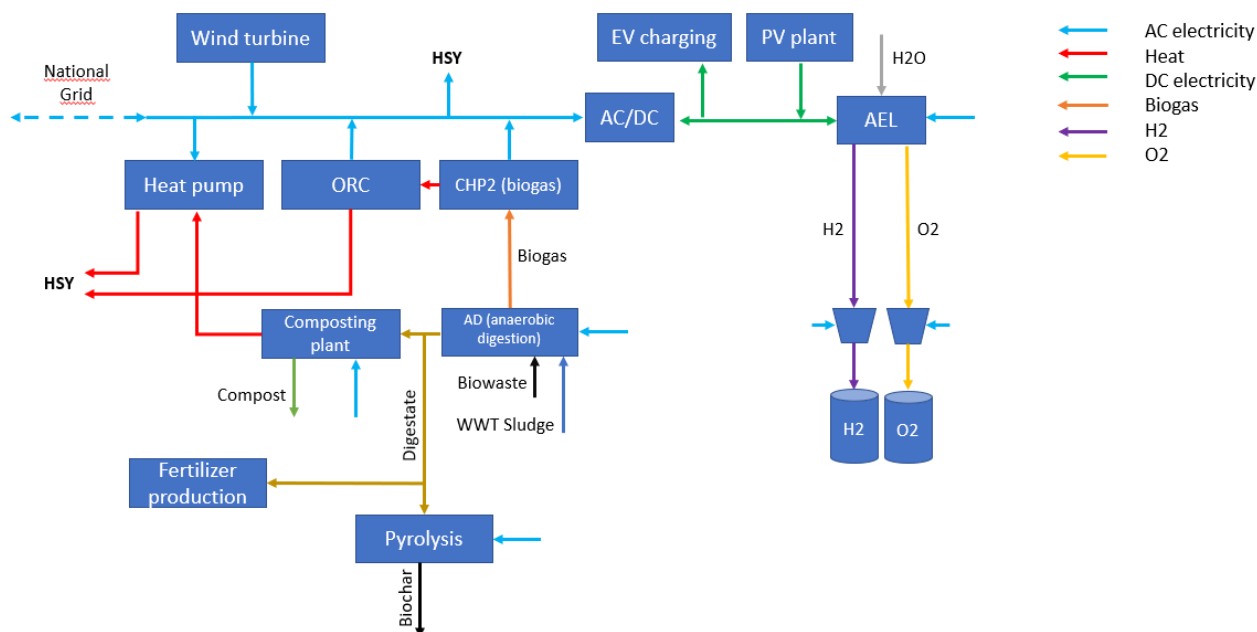


Figure 62: Scenario 3

Regarding heat energy the situation doesn't change, since the PV plant doesn't require nor produce heat, and the self-sufficiency has been achieved in Scenario 2 (Figure 59). Regarding electricity, similarly as the wind power analysis, it is possible to see how much energy can be obtained from the PV plant each month. The same assumptions made for Scenario 2 (Table 18) were made for the following table.

Table 23: Scenario 3, electricity

Heat [MWh]	Jan	Feb	Mar	Apr	May	Jun	Jul	Aug	Sep	Oct	Nov	Dec
CHP2*	2149	1798	2012	1766	1756	1234	1207	1395	1776	1861	1866	1991
Wind power	1541	1182	930	785	830	682	606	648	906	1142	1037	1275
Solar power	47	180	399	532	603	592	589	576	445	255	75	21
Heat pump	-100	-179	-134	-80	0	0	-5	-13	0	-22	-63	-116
Produced	3737	3160	3341	3083	3189	2508	2402	2619	3127	3258	2978	3287
Required*	2019	2005	1929	1751	1699	1793	1735	1719	1733	1779	1739	1811
Difference	1718	1155	1412	1332	1490	715	667	900	1394	1479	1239	1476

In Scenario 2, summer has been proven to be the period for which the surplus electricity was lowest throughout the year. Considering the nature of solar panels, which harvest more energy when the solar irradiation is stronger (ergo in the summer), they manage to noticeably balance out the situation. The surplus energy is however still lower in the warmer months, since more electricity tends to be utilised in the summer. A comparison between the two situations can be seen next page (Figure 63).

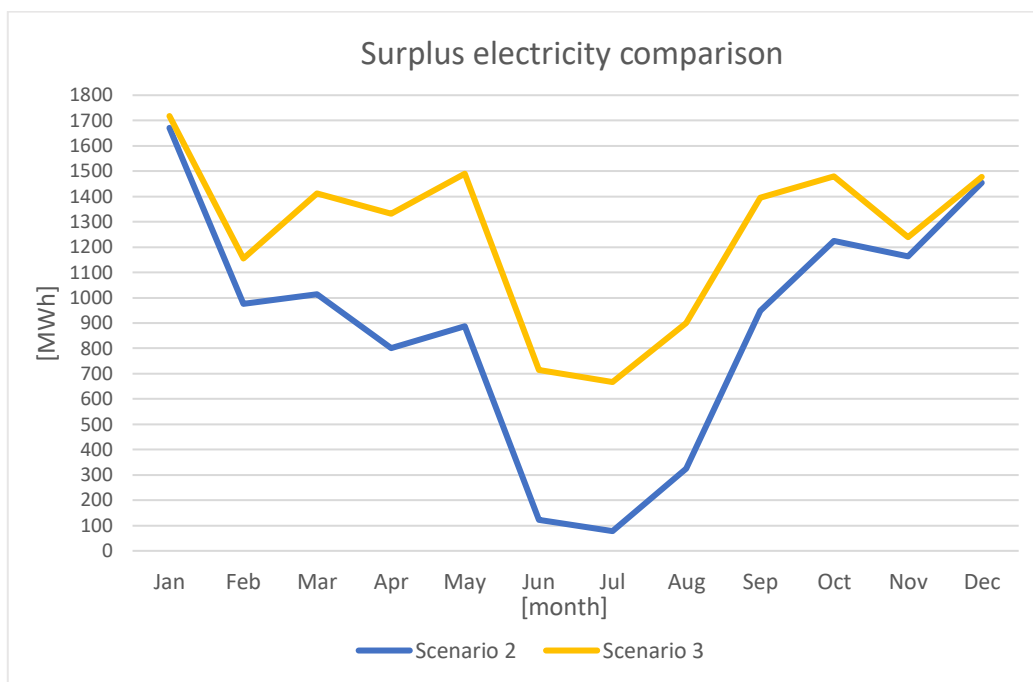


Figure 63: Comparison between surplus electricity of Scenario 2 and Scenario 3

The Scenario 3 surplus electricity, represented by the “Difference” row in Table 23 (previous page) and the yellow line in Figure 63 (above), can be sold and/or utilised to produce H₂ and O₂, using the electrolyser. The analysis is similar to the one conducted for Scenario 2, with the difference of having more energy at disposal. Knowing this, the monthly electrolyser load can be set at a higher value, for example 1200 MWh. Below, a graphical representation.

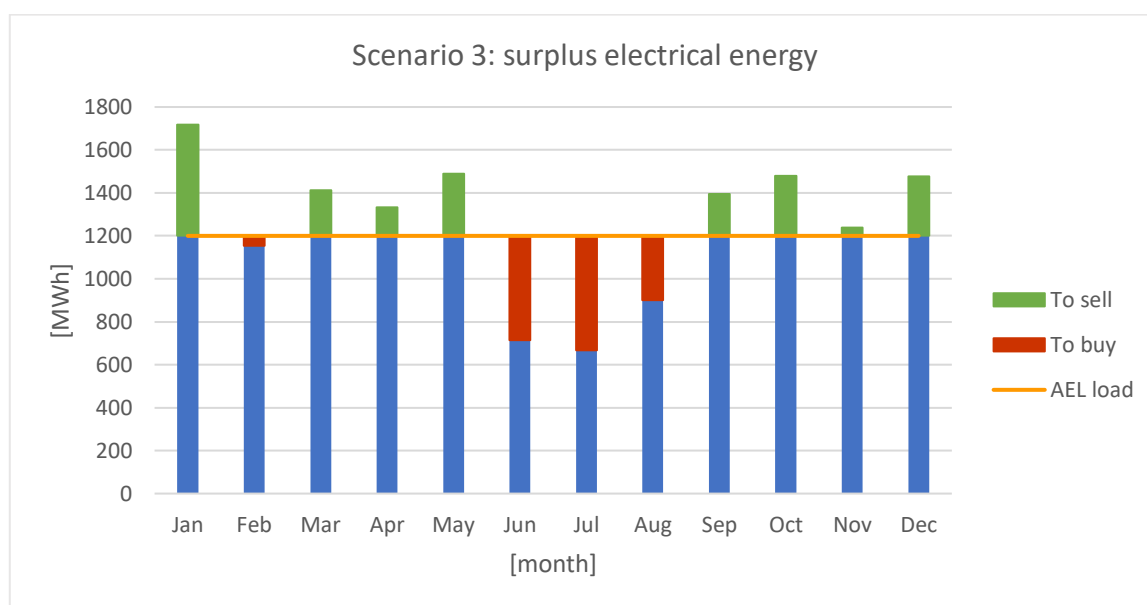


Figure 64: Scenario 3, surplus electrical energy, AEL = 1200 MWh

Considering the higher surplus energy that is present in the summer, it might not seem advantageous to stop the AEL in the months between June and August. However, by doing so, the electrolyser load can be brought to a higher value, for example 1400 MWh; also, more revenue can be obtained by selling the energy harvested during the summer. Below, a graphical representation.

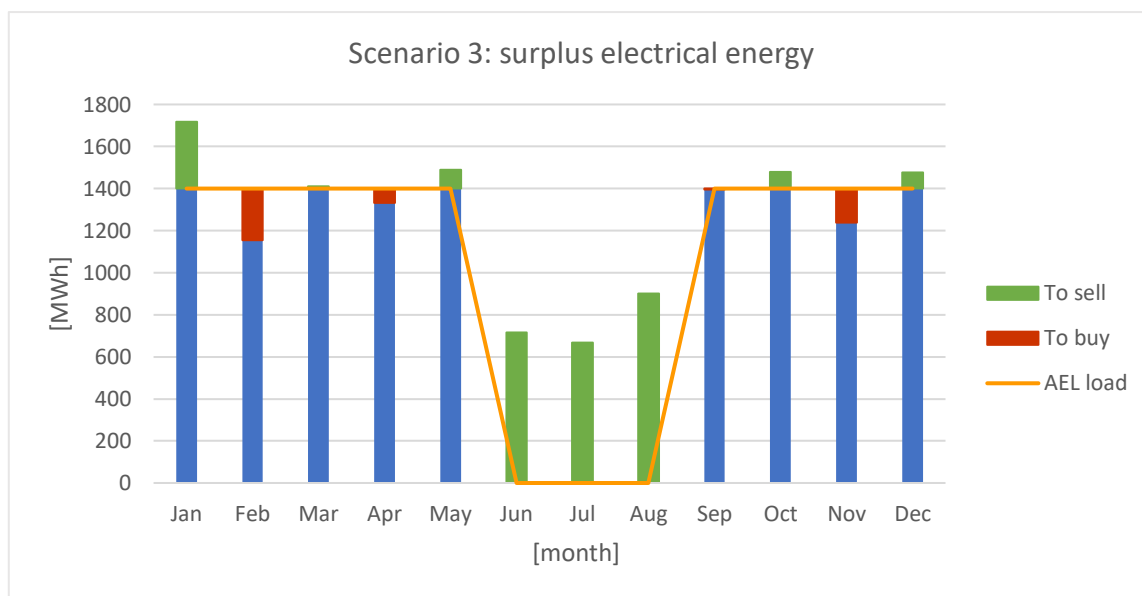


Figure 65: Scenario 3, surplus electrical energy, AEL = 1400 MWh, summer interruption

Similarly as it was done for Scenario 2, it's possible to use a table to summarise the results. In order to increase the operating hours of the electrolyser and thus reduce the relative costs, the AEL NEL A485 model was considered instead of the NEL A1000 model [69].

Table 24: Scenario 3, surplus electricity utilisation comparison

*the price to buy electricity and sell electricity from/to the grid is assumed to be the same, 0.1767 €/kWh [91]

**the power consumption is assumed to be 4.1 kWh/Nm³ (NEL AELs power consumption: 3.8-4.4 Nm³/h [69])

***the hydrogen density is assumed to be 0.08375 kg/m³ (normal conditions)

****the production rate is assumed to be 485 Nm³/h (NEL A485 AEL production rate: 300-485 Nm³/h [69])

	AEL load [MWh/ month]	Electricity sold [MWh]	Electricity bought [MWh]	Profit* (electricity) [€/year]	H2 produced [Nm ³]**	H2 produced [kg]***	O2 produced [kg]	Operating hours [h]****
No AEL	0	14,977	0	2,646,455	0	0	0	0
Continuous load	1,200	1,941	1,364	101,965	3,512,195.12	294,146.34	2,333,765.24	7,242 (82.67%)
Jun-Aug standby	1,400	2,780	480	406,511	3,073,170.73	257,378.05	2,042,044.59	6,336 (97.78%)

Scenario 3 effectively shows how much the solar panels can improve the revenue from selling the extra electricity and/or the quantity of useful end products generated. This will be compared with CAPEX and OPEX costs of the PV plant later in the chapter, in order to understand if the expense would be worthy for the Ämmässuo eco-centre.

4.6 Scenario 4: Addition of a methanation system

Scenario 4 proposes the addition of a methanation system, which creates the possibility to generate methane from the H₂ (produced by the AEL) and the biogas, which is mainly composed by CH₄ and CO₂. The graphical representation of the scenario is shown below.

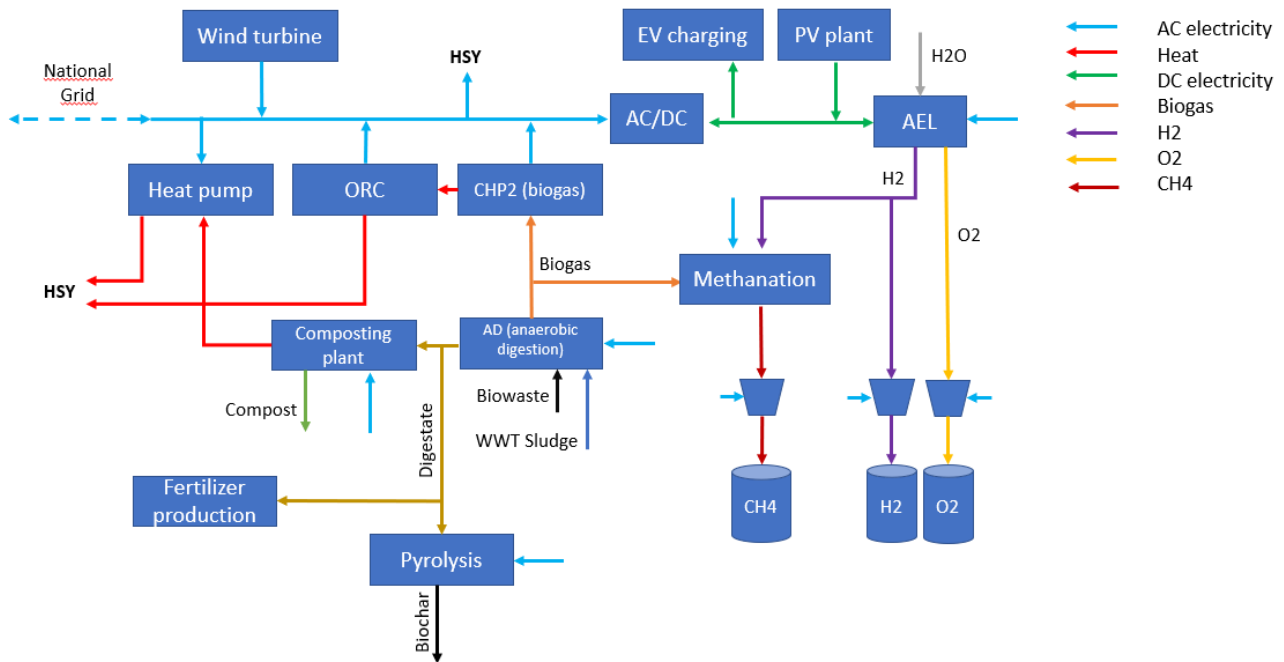


Figure 66: Scenario 4

To generate CH₄, the methanation system needs H₂, the biogas (due to its CO₂ content) and electricity. To produce H₂, electricity needs to be sent towards the electrolyser. Since part of the biogas will be sent to the methanation system, the electricity produced by CHP2 will be reduced. Finally, the methanation system needs electricity to function. To summarise, it is necessary to make sure that these three factors will not put in jeopardy the centre's electricity self-sufficiency, either by not using more than the surplus electricity at disposal or by buying electricity from the grid, if necessary.

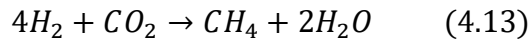
To consider the amount of biogas to be used for the methanation system, let's assume to use 20% of the biogas generated with the anaerobic digestion. According to Kantoluoto N.'s work [92], in 2019 the Ämmässuo eco-centre produced 7,124,000 kg of biogas. Since, for 2025, it is assumed to have the utilisation rate of the biogas reactors doubled, 20% of the produced biogas amount in 2025 would be $(7124000 \cdot 2) \cdot 0.20 = 2,849,600$ kg of biogas.

The biogas composition is, roughly, 65% CH₄ and 35% CO₂. To understand how much CO₂ can be utilised in the methanation system, it is necessary to use the following proportion:

$$x_{CH_4} \cdot MM_{CH_4} + x_{CO_2} \cdot MM_{CO_2} = MM_{biogas} = 0.65 \cdot 16.04 + 0.35 \cdot 44.01 = 25.83 \quad (4.11)$$

$$m_{CO_2} = m_{biogas} \cdot \left(x_{CO_2} \cdot \frac{MM_{CO_2}}{MM_{biogas}} \right) = 2849600 \cdot \left(0.35 \cdot \frac{44.01}{25.83} \right) = 1,699,274 \text{ kg} \quad (4.12)$$

Once the quantity of CO₂ is known, methane can be produced, according to the following reaction:



The amount of H₂ produced can be calculated like so:

$$m_{H_2} = \frac{mol_{H_2} \cdot MM_{H_2}}{mol_{CO_2} \cdot MM_{CO_2}} \cdot m_{CO_2} = \frac{4 \cdot 2.016}{1 \cdot 44.01} \cdot 1699274 = 311,363 \text{ kg} \quad (4.14)$$

Using the same logic, it's possible to understand how much CH₄ is produced with the process: 619,406 kg. The amount of electricity necessary to produce m_{H_2} can be calculated like so:

$$E_{AEL} [MWh] = 4.1 \left[\frac{kWh}{m^3} \right] \cdot \frac{1}{0.08375} \left[\frac{m^3}{kg} \right] \cdot 311363 [kg] \cdot \frac{1}{1000} \left[\frac{MWh}{kWh} \right] = 15,243 \text{ MWh} \quad (4.15)$$

Assuming to send towards the electrolyser a constant load throughout the year, 15243/12 = 1,270 MWh per month are needed. According to Moioli's work [93], the energy necessary to produce methane from CO₂ is 126,000 kJ/kg. Knowing this,

$$E_{CH_4} = \left(126000 \left[\frac{kJ}{kg} \right] \cdot 619406 [kg] \right) \cdot \frac{1}{3600 \cdot 10^3} \left[\frac{MWh}{kJ} \right] = 21,679 \text{ MWh} \quad (4.16)$$

If the methanation system is used in a continuous way throughout the year, 21679/12 = 1,807 MWh per month would be needed. If it is used with the summer interruption case (as shown for Scenario 2 and 3), 21679/9 = 2,409 MWh per month would be needed.

The three factors which, to produce CH₄ using 20% of the available biogas, would reduce the electricity at disposal of the eco-centre, are shown in the table next page (Table 25), which summarizes the situation regarding electrical energy (continuous AEL load case).

Table 25: Scenario 4, electricity, CH₄ production utilising 20% of the available biogas

[MWh]	Jan	Feb	Mar	Apr	May	Jun	Jul	Aug	Sep	Oct	Nov	Dec
CHP2	1719	1438	1610	1413	1405	987	966	1116	1421	1489	1493	1593
Wind power	1541	1182	930	785	830	682	606	648	906	1142	1037	1275
Solar power	47	180	399	532	603	592	589	576	445	255	75	21
Heat pump	-100	-179	-134	-80	0	0	-5	-13	0	-22	-63	-116
CH₄ production	-3507	-3436	-3479	-3430	-3428	-3324	-3318	-3356	-3432	-3449	-3450	-3475
Biogas (-20%)	-322	-270	-302	-265	-263	-185	-181	-209	-266	-279	-280	-299
AEL load	-1270	-1270	-1270	-1270	-1270	-1270	-1270	-1270	-1270	-1270	-1270	-1270
methanation	-1807	-1807	-1807	-1807	-1807	-1807	-1807	-1807	-1807	-1807	-1807	-1807
Produced	3307	2800	2938	2730	2838	2261	2160	2340	2772	2885	2605	2889
Required	5526	5441	5408	5181	5127	5117	5053	5075	5165	5228	5189	5286
Difference	-2219	-2641	-2470	-2451	-2289	-2855	-2893	-2735	-2393	-2343	-2584	-2397

Even without showing the summer standby case, it is evident from Table 25 above (especially from the last line) that the scenario is not feasible: not only all the surplus electricity would be consumed, but a large amount would have to be purchased from the grid each month to keep the eco-centre's electricity demand satisfied. Using 20% available biogas was found to be a quantity too large to be processed this way; a relatively acceptable percentage was found to be 6% of the biogas. The tables below and next page (Table 26 and 27) show the calculations.

Table 26: Scenario 4, electricity, CH₄ production utilising 6% of the available biogas, continuous load case

[MWh]	Jan	Feb	Mar	Apr	May	Jun	Jul	Aug	Sep	Oct	Nov	Dec
CHP2	2020	1690	1891	1660	1651	1160	1135	1311	1669	1749	1754	1872
Wind power	1541	1182	930	785	830	682	606	648	906	1142	1037	1275
Solar power	47	180	399	532	603	592	589	576	445	255	75	21
Heat pump	-100	-179	-134	-80	0	0	-5	-13	0	-22	-63	-116
CH₄ production	-1052	-1031	-1044	-1029	-1028	-997	-996	-1007	-1030	-1035	-1035	-1043
Biogas (-6%)	-129	-108	-121	-106	-105	-74	-72	-84	-107	-112	-112	-119
AEL load	-381	-381	-381	-381	-381	-381	-381	-381	-381	-381	-381	-381
methanation	-542	-542	-542	-542	-542	-542	-542	-542	-542	-542	-542	-542
Produced	3608	3052	3220	2977	3084	2434	2329	2535	3021	3146	2867	3168
Required	3071	3036	2973	2780	2727	2790	2731	2726	2763	2814	2774	2854
Difference	537	16	247	197	356	-356	-401	-191	258	332	92	314

Table 27: Scenario 4, electricity, CH₄ production utilising 6% of the available biogas, summer interruption case

[MWh]	Jan	Feb	Mar	Apr	May	Jun	Jul	Aug	Sep	Oct	Nov	Dec
CHP2	2020	1690	1891	1660	1651	1160	1135	1311	1669	1749	1754	1872
Wind power	1541	1182	930	785	830	682	606	648	906	1142	1037	1275
Solar power	47	180	399	532	603	592	589	576	445	255	75	21
Heat pump	-100	-179	-134	-80	0	0	-5	-13	0	-22	-63	-116
CH₄ production	-1360	-1339	-1351	-1337	-1336	-74	-72	-84	-1337	-1342	-1343	-1350
Biogas (-6%)	-129	-108	-121	-106	-105	-74	-72	-84	-107	-112	-112	-119
AEL load	-508	-508	-508	-508	-508	0	0	0	-508	-508	-508	-508
methanation	-723	-723	-723	-723	-723	0	0	0	-723	-723	-723	-723
Produced	3608	3052	3220	2977	3084	2434	2329	2535	3021	3146	2867	3168
Required	3379	3344	3280	3088	3035	1867	1807	1803	3070	3121	3082	3161
Difference	229	-292	-60	-111	49	567	522	732	-50	25	-215	7

Below and next page (Figure 67 and 68), visual representations of the two Scenario 4 cases (6% CHP2 biogas utilization) that include the different electricity requirement sources.

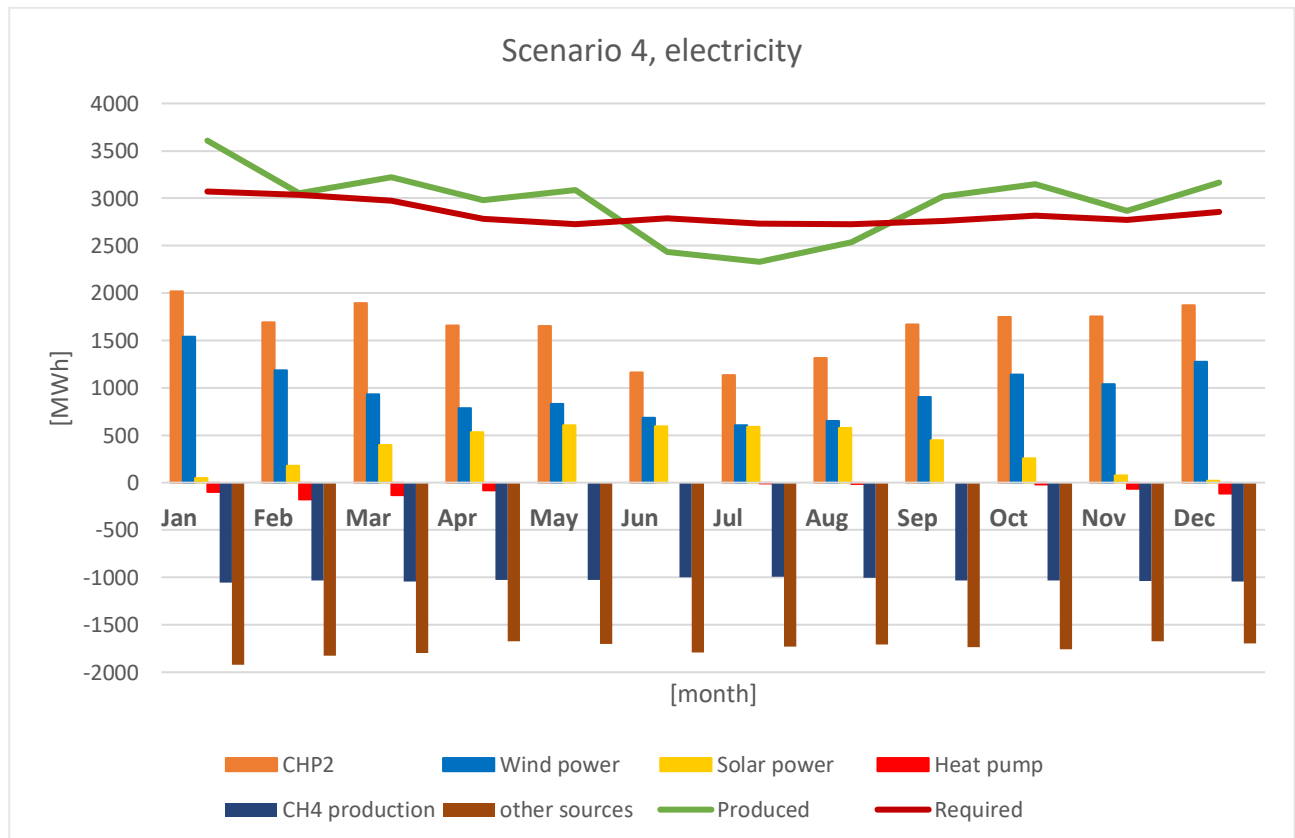


Figure 67: Scenario 4, electricity, continuous load case

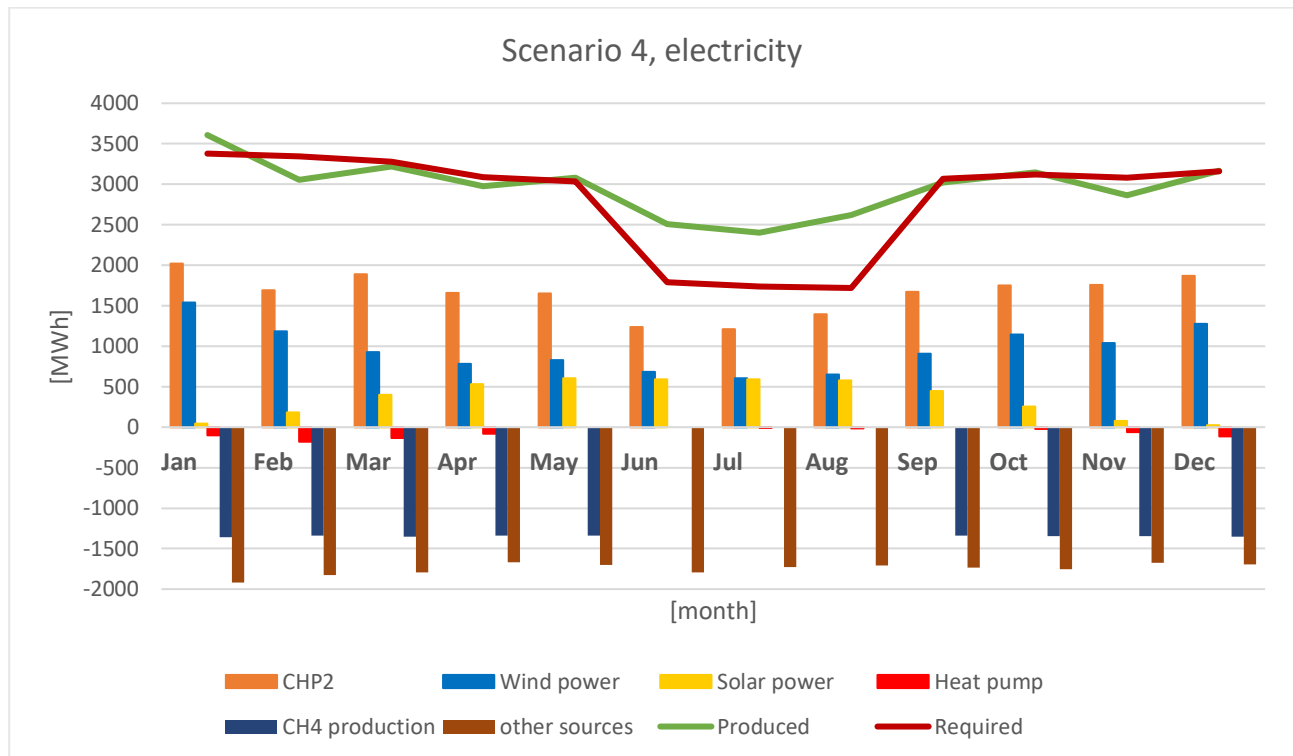


Figure 68: Scenario 4, electricity, summer interruption case

In order to produce CH₄ as previously described it is possible to use the AEL and the CO₂ methanation system continuously throughout the year, or with an interruption between June and August. Below and next page (Figure 69 and 70), two graphs showing the difference between the situations.

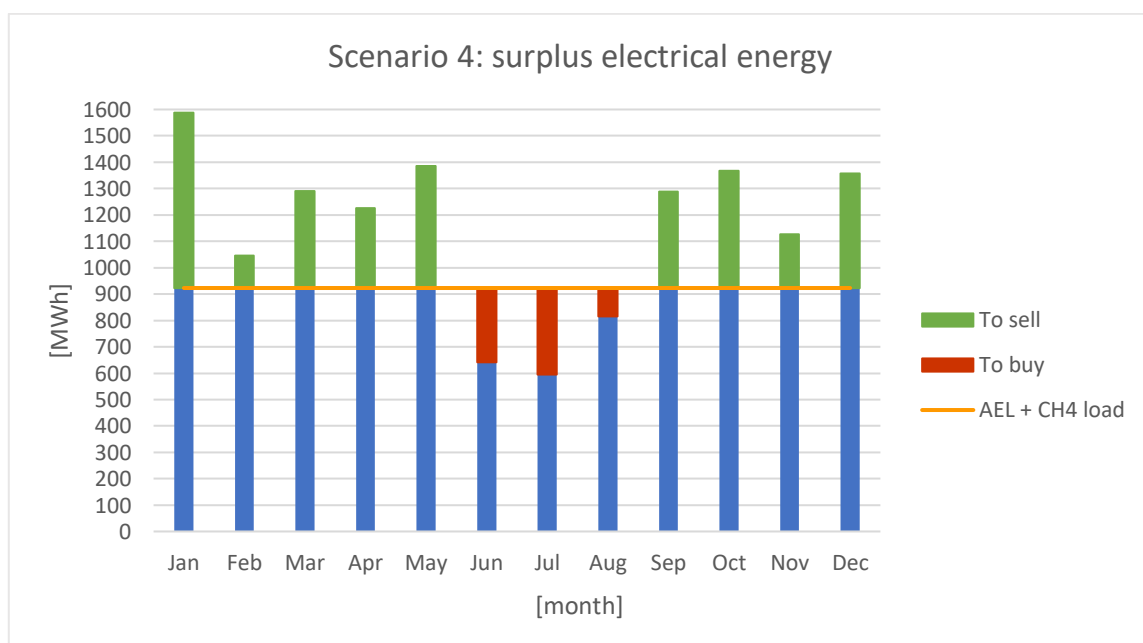


Figure 69: Scenario 4, surplus energy utilisation, continuous load

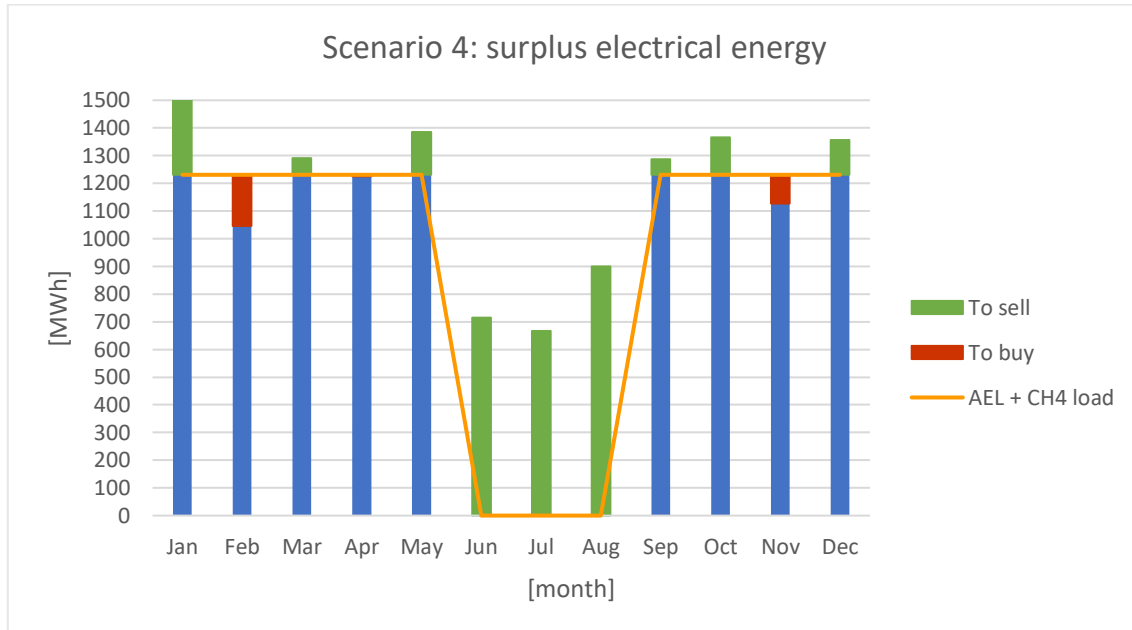


Figure 70: Scenario 4, surplus energy utilisation, summer interruption

An aspect that is necessary to consider is that the utilisation of a percentage of the biogas would affect the heat self-sufficiency of the eco-centre, since the partial removal of the resource would negatively impact the heat production of the centre as well.

Said leftover heat energy gap can however be compensated utilising the heat pump, according to the following formula:

$$E_{CH_4} = \frac{6\%}{COP_{HP}} \sum_{year} Q_{CHP_{monthly}} = \frac{0.06}{5} \cdot 20658 = 248 \text{ MWh} \quad (4.17)$$

The table below shows the resources that can be obtained using the Scenario 4 elements.

Table 28: Scenario 4, surplus electricity utilisation: CH₄ production using 6% of available biogas

*monthly load;

**electricity addition needed to compensate for the heat deficiency given by the partial biogas utilisation

*** the price to buy/sell electricity from/to the grid is assumed to be the same, 0.1767 €/kWh [91]

	AEL load* [MWh]	Methanation load* [MWh]	Electricity sold [MWh]	Electricity bought** [MWh]	Revenue*** (electricity) [€/y]	CH ₄ produced [kg]
Continuous load	381	542	3369	718 + 248	424,679.58	185,822
Summer interruption	508	723	3173	292 + 248	465,348.85	185,822

Even though methane is a useful end product, considering both the high capital costs that the regional authority would have to face for the wind turbine, solar panels, electrolyser and various auxiliary systems, adding the CAPEX (and OPEX) of a complex methanation system does not seem advantageous, especially considering that it's not possible to utilise even 10% of the available biogas without jeopardizing the self-sustainability of the Ämmässuo eco-centre.

4.7 End products, revenues and costs comparison

Considering the non-profitability of Scenario 4 described in the last paragraph, it is possible to compare the resources that can be obtained from the three remaining scenarios, in order to see which situation would be the most beneficial. The tables below summarize the CAPEX, OPEX and resources gathered in the three scenarios.

Table 29: Costs comparison, Scenarios 1,2,3

	Heat pump	Wind turbine	Solar panels	Electrolyser	Compressors	
POWER [kW]	400	4200	1350	1988.5	2	
	EUR/kW	EUR/kW	EUR/kWp	EUR/kW	EUR/unit	
CAPEX [€/x]	€ 736.00	€ 1,322.00	€ 771.00	€ 1,312.00	€ 123,490.00	TOT CAPEX
Scenario 1	€ 294,400.00	-	-	-	-	€ 294,400.00
Scenario 2A=2B	€ 294,400.00	€ 5,552,400.00	-	€ 2,608,912.00	€ 246,980.00	€ 8,702,692.00
Scenario 3A=3B	€ 294,400.00	€ 5,552,400.00	€ 1,040,850.00	€ 2,608,912.00	€ 246,980.00	€ 9,743,542.00
	EUR/kW	EUR/kW	EUR/kWp	EUR/kW	EUR/kgH2	
OPEX [€/x]	€ 11.70	€ 19.50	€ 8.80	€ 45.92	€ 0.71	TOT OPEX
Scenario 1	€ 4,680.00	-	-	-	-	€ 4,680.00
Scenario 2A	€ 4,680.00	€ 81,900.00	-	€ 91,311.92	€ 147,931.10	€ 325,823.02
Scenario 2B	€ 4,680.00	€ 81,900.00	-	€ 91,311.92	€ 143,580.18	€ 321,472.10
Scenario 3A	€ 4,680.00	€ 81,900.00	€ 11,880.00	€ 91,311.92	€ 208,843.90	€ 398,615.82
Scenario 3B	€ 4,680.00	€ 81,900.00	€ 11,880.00	€ 91,311.92	€ 182,738.41	€ 372,510.33

Table 30: Resources comparison, Scenarios 1,2,3

RESOURCES	Electricity	H2	O2		
	EUR/kWh	EUR/kg	EUR/kg		
Price [€/x]	€ 0.1767	€ 2.64	€ 0.06	TOT EARNINGS	(per year)
[MWh] or [kg]	MWh	kg	kg		
Scenario 1	600	-	-		€ 106,020.00
Scenario 2A	463	208,353.66	1,653,083.71		€ 731,050.78
Scenario 2B	763	202,225.61	1,604,463.61		€ 764,965.53
Scenario 3A	577	294,146.34	2,333,765.24		€ 1,018,528.16
Scenario 3B	2,301	257,378.05	2,042,044.59		€ 1,208,587.42

Looking at tables above (Table 29 and 30), various assumptions have been made:

- For the compressors, the capital costs have been calculated for two units (one for hydrogen, one for oxygen), but only the OPEX for increasing the H2 pressure has been considered
- The possibility of having either a continuous load or a summer interruption for the AEL subdivides the Scenarios 2 and 3 in two sub-scenarios each: 2A 2B and 3A 3B, respectively. From the CAPEX point of view, said sub-scenarios are equivalent, since the only variation regards the OPEX of compressors, which depends on the amount of H2 generated

- Auxiliary systems such as gas tanks, AC/DC converter and inverter, cables, water distillation system have not been considered for this economic analysis
- The hydrogen selling price has been assumed to be between the range of 2-4 USD/kg [94], hence 3 USD/kg, which corresponds to 2.64 €/kg
- The pure O₂ selling price has been assumed to be between the range of 40-70 €/tonne, hence 0.06 €/kg [95]
- The typical CAPEX for a 70 MPa (700 bar) H₂ compressor is 140,000 USD, while the typical operating costs are 0.80 USD/kg [96]. In euros, respectively, CAPEX = 123,490 €/unit, OPEX = 0.71 €/kg_{H₂}
- As mentioned before, the electricity price has been assumed to be the same for selling to the grid and for buying from the grid, and its value was set to 0.1767 €/kWh [91]

For each scenario, HSY has some fixed costs to cover, as well as some operating costs per year. Assuming that each leftover resource is going to be sold, the regional authority can rely on a yearly revenue to face the different expenses.

In order to understand the feasibility of the various investment planned for each scenario, the discounted payback period (DPBP) method will be utilised in the next sub-chapters. The discount rate used to calculate the present value (PV) of the cash inflows was set to 6%.

4.7.1 Scenario 1 cost analysis

The Scenario 1 economic point of view is fairly easy to analyse, since the only investment is the heat pump; the table below summarizes the situation.

Table 31: Scenario 1 cash flows and DPBP

Scenario 1	OPEX	Electricity	H ₂	O ₂	HSY
	- € 4,680.00	€ 106,020.00	-	-	€ 50,000.00
Year	Total cash inflow	PV (6%)	CAPEX	DPBP (partial)	
0			€ 290,400.00		
1	€ 151,340.00	€ 142,773.58	€ 147,626.42	1	
2	€ 151,340.00	€ 134,692.06	€ 12,934.35	1	
3	€ 151,340.00	€ 127,067.98	-	0.102	DPBP
4	€ 151,340.00	€ 119,875.45	-	0.000	2.102

The municipal federation has a total OPEX of 4,680 €/year (symbolised by the respective column on Table 31), while the revenue that can be obtained by selling the surplus electricity is 106,020 €/year. There is no revenue for hydrogen or oxygen since there aren't produced in this scenario. In order to face the CAPEX, HSY can contribute 50,000 € per year in order to reduce the DPBP to 2.102 years. For this scenario, however, the regional authority could avoid spending any money at all by simply utilising the surplus electricity revenue; the DPBP in that case would have been higher: 3.243 years. The potential HSY contribution will be a key parameter in this analysis, for every scenario.

Another option for Scenario 1 (and other scenarios) would be to utilise the surplus electricity to power E-buses, instead of selling it.

Even though the main objectives of HSY (waste treatment, air quality control, water treatment) would not justify their acquisition of any kind of transportation vehicle, it could be possible to strike a non-profit deal between the regional authority and their sister organization, Helsinki Region Transport, or HSL (Helsingin Seudun Liikenne in Finnish). This is mainly speculation, but an example would be the investment of HSL in the acquisition and maintenance of electrical buses, as well as all the necessary auxiliary elements, such as charging stations. HSY, in the meanwhile, would provide the energy necessary to power the E-buses, using the surplus energy from the Ämmässuo eco-centre when available.

According to Statistic Finland [97], in 2019 Finnish buses have driven a total of circa 353,500,000 km. Also, the number of registered Finnish buses is 19,282. Knowing this, it's possible to calculate the average yearly distance travelled by a bus in Finland: $353500000/19282 = 18,333.16$ km/year (the average daily distance would be 50.23 km/day, but that information is not relevant to this analysis).

Since the average fuel consumption can be estimated to be 1.50 kWh/km [84], the average electricity required per year, per E-bus in Finland is $1.50 \cdot 18,333.16 = 27,499.741$ kWh/bus. Knowing this, it's possible to understand how many electrical buses could be powered with the leftover electricity of Scenario 1. Since the surplus is 600 MWh = 600,000 kWh,

$$\frac{600000 \text{ [kWh]}}{27499.741 \text{ [kWh/bus]}} = 21 \text{ buses} + 22,505.445 \text{ kWh} \quad (4.18)$$

The remainder of the division from Equation 4.18 can be sold to the grid for a profit of $22,505.445 \cdot 0.1767 = 3,976.71$ €.

As it was shown in the previous analysis, using a potential money contribution from HSY would affect the final use of the resources that can be harvested from the scenario. In this case, starting from the number of E-buses that are planned to be utilised, it's possible to calculate how much electricity should be bought/sold, thus how much money should HSY invest.

An example of this would be planning to have 22 E-buses instead of 21: in this case, the remainder of 22,505.455 kWh from Equation 4.18 is utilised to partly power the 22nd E-bus, together with $(27,499.741 - 22,505.455)$ kWh of electricity, bought from the grid. HSY at this point would not have a profit, but a yearly expense, which can be computed like so:

$$\epsilon_{buses(22)_1} = 0.1767 \cdot [600000 - (27499.741 \cdot 22)] = -4,994.30 \text{ €/year} \quad (4.19)$$

Equation 4.19 (previous page) can be expressed in a general form:

$$\epsilon_{buses(x)_y} = 0.1767 \left[\frac{\text{€}}{\text{kWh}} \right] \cdot \left\{ \text{Surplus}_y [\text{kWh}] - \left(27,499.741 \left[\frac{\text{kWh}}{\text{bus}} \right] \cdot x [\text{bus}] \right) \right\} \quad (4.20)$$

The “x” in Equation 4.20 represents the targeted number of buses, while Surplus_y represents the extra electrical energy available for Scenario y (thus y can be 1,2 or 3). $\epsilon_{buses(x)_y}$ represents the cash flow in respect to the E-bus investment; it can be either positive or negative. This indicator does not give any information about other possible investments about the buses, such as vehicle costs, charging stations costs, maintenance costs, etc.

It’s important to understand that, regardless of the target number of the E-buses, if part or all of the surplus electricity is utilised for the electrical vehicles, it won’t be available to be sold to the grid. This in turn means that, in order to not affect (increase) the DPBP value for the other investments, the corresponding cash inflow contribution will have to be matched by HSY.

The table below shows how a target of 30 E-buses affects the Scenario 1 DPBP.

Table 32: Scenario 1 cash flows and DPBP with a target of 30 E-buses

Scenario 1					30	
	OPEX	Electricity	H2	O2	E-buses	HSY
	- € 4,680.00	€ 106,020.00	-	-	- € 145,776.13	€ 195,750.00
Year	Total cash inflow	PV (6%)	CAPEX	DPBP (partial)		cost increase:
0			€ 290,400.00			291.50%
1	€ 151,313.87	€ 142,748.94	€ 147,651.06	1		
2	€ 151,313.87	€ 134,668.81	€ 12,982.25	1	DPBP	
3	€ 151,313.87	€ 127,046.05	-	0.102	2.102	

It’s possible to see that, since the target number of buses is higher than 21, there is no more surplus electricity, thus the cash inflow from the grid becomes a cash outflow (to the grid). To keep the DPBP at the same value as it would have been without the E-bus investment (2.102 years), the regional authority has to contribute a higher cost each year: 195750 € instead of 50000 €, for a cost increase of 291.50%, as indicated by the table above.

4.7.2 Scenario 2 cost analysis

The logic followed for the analysis of this scenario will be the same as the one applied for Scenario 1. The costs to cover, however, are noticeably higher: the wind turbine CAPEX by itself was estimated to be 5.6 million of euros, and the costs for the other investments must be added as well.

Knowing this, even though the cash inflow produced by selling the surplus electricity and generated resources (H₂, O₂) is an important asset, the HSY yearly contribution will be crucial for the scenarios analysis.

By looking at Table 29 and 30, the most advantageous case between Scenario 2A and 2B would be the latter, that is the one relative to the summer interruption situation. This is due to the total OPEX being lower and the total earnings being higher. Because of this, Scenario 2 will refer to the 2B case from this point onward (unless otherwise specified).

Table 33 next page summarizes the DPBP analysis for this scenario.

Table 33: Scenario 2 cash flows and DPBP

Scenario 2					
OPEX	Electricity	H ₂	O ₂	CAPEX	HSY
- € 321,472.10	€ 134,822.10	€ 533,875.61	€ 96,267.82	€ 8,702,692.00	€ 1,700,000.00
Year	Total cash inflow	PV (6%)		DPBP (partial)	
1	€ 2,143,493.42	€ 2,022,163.61	€ 6,680,528.39	1	
2	€ 2,143,493.42	€ 1,907,701.52	€ 4,772,826.88	1	
3	€ 2,143,493.42	€ 1,799,718.41	€ 2,973,108.47	1	
4	€ 2,143,493.42	€ 1,697,847.56	€ 1,275,260.91	1	DPBP
5	€ 2,143,493.42	€ 1,601,742.98	-	0.796	4.796

Considering the very high CAPEX to cover, even with the additional resources to be sold (O₂, H₂) and the HSY yearly contribution of 1.7 million euros, the regional authority would be able to break even only after 4.8 years. The graph below underlines how the HSY yearly contribution can affect the DPBP.

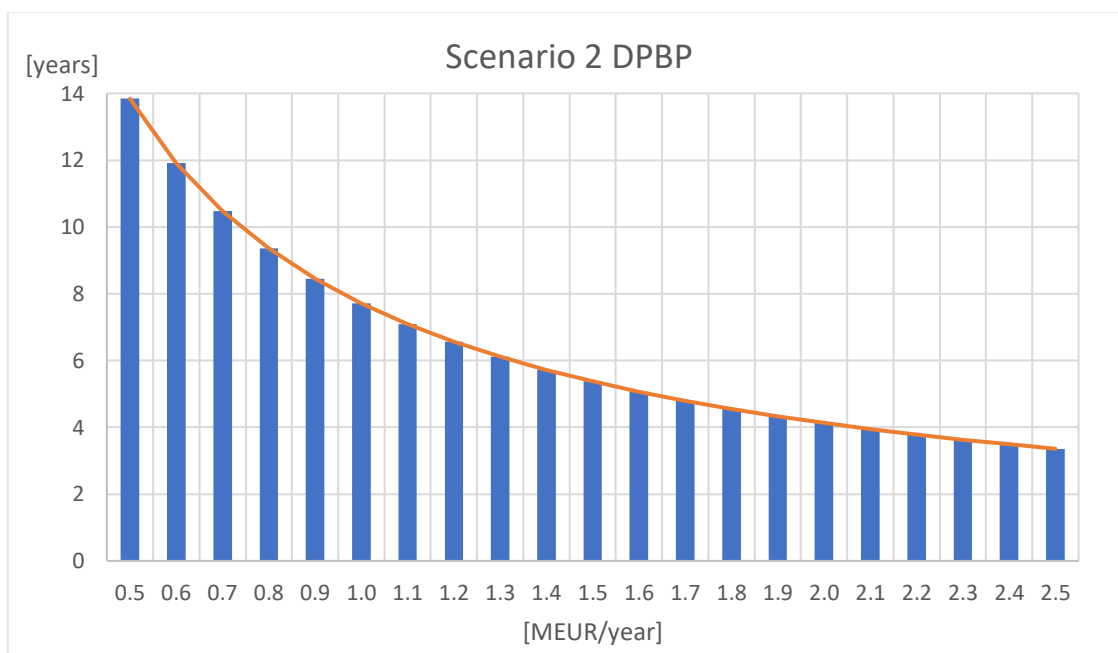


Figure 71: Scenario 2, correlation between HSY's yearly contribution and the DPBP

Assuming to have a range between 0.5 and 2.5 million of euros (MEUR) per year, Figure 71 shows how much each 0.1 MEUR increment affects the DPBP; said increments effect gets progressively lower due to the present value of money, as shown by the orange curve. In fact, increasing the HSY yearly contribution from 0.5 to 1.0 MEUR reduces the DPBP by 6.128 (-44.28%); increasing said contribution from 1.0 to 1.5 MEUR reduces it by 2.335 (-30.28%); increasing said contribution from 1.5 to 2.0 MEUR only reduces it by 1.248 (-23.20%).

Scenario 2's resources include not only surplus electricity, but also H₂ and O₂. Leaving the oxygen aside, there is a possibility to utilise said resources to operate E-buses and/or hydrogen powered buses (H-buses). However, if planning to invest in alternative public transportation, it's better to consider E-buses than H-buses.

First of all, since electricity is used to generate hydrogen, a certain amount of energy is lost in the transformations, due to the overall efficiency of the processes, which is naturally lower than 100% (65-70% for alkaline water electrolysis itself). Considering that electrification of buses is possible, is more efficient to use directly electricity to power the vehicles.

Secondly, the specific amount of electricity is lower than the specific amount of hydrogen needed to power the vehicles. Respectively, the ranges found for this work are 1.2 – 1.6 kWh/km for E-buses and 8.6 – 16.5 kgH₂/km for H₂ powered buses.

Finally, for this case study, the amount of hydrogen produced is too low to consider the implementation of H-buses, as shown by the table below: all the available H₂ from every possible scenario would be consumed every year just to power a single H-bus.

Table 34: Unfeasibility of H₂ power buses implementation.
2A and 3A refer to the AEL continuous mode cases, 2B and 3B refer to the summer interruption cases

Finland statistics			Scenario	H2 available [kg]	H-buses
<i>Km driven by buses</i>	353,500,000		1	0.00	0
<i>Number of buses in Finland</i>	19,282		2A	208,353.66	1
<i>Average distance per bus (yearly)</i>	18,333.16		2B	202,225.61	1
<i>Fuel consumption [kgH₂/km]</i>	9.0		3A	294,146.34	1
<i>H2 required per year, per bus</i>	164,988.44		3B	257,378.05	1

Shifting the focus back on electrical buses, the problem with investing in them would be the further reduction of the total cash inflow in situations for which there are considerable CAPEX to cover already. If this is not viewed as an obstacle, it's possible to keep considering instances for which said vehicles are implemented.

Following the method shown for Scenario 1 and described by Equation 4.20, it's possible to power 27 E-buses with the 763,000 MWh electricity surplus of Scenario 2. Assuming to have a target of 50 electric powered buses, the situation would be the following:

Table 35: Scenario 2 cash flows and DPBP, with a target of 50 E-buses

Scenario 2				50	
OPEX	Electricity	H2	O2	E-buses	HSY
- € 321,472.10	€ 134,822.10	€ 533,875.61	€ 96,267.82	- € 242,960.21	€ 1,943,100.00
					cost increase:
Year	Total cash inflow	PV (6%)	CAPEX	DPBP (partial)	14.30%
0			€ 8,702,692.00		
1	€ 2,143,633.21	€ 2,022,295.48	€ 6,680,396.52	1	
2	€ 2,143,633.21	€ 1,907,825.93	€ 4,772,570.59	1	
3	€ 2,143,633.21	€ 1,799,835.78	€ 2,972,734.81	1	
4	€ 2,143,633.21	€ 1,697,958.28	€ 1,274,776.53	1	DPBP
5	€ 2,143,633.21	€ 1,601,847.44	-	0.796	4.796

Table 35 shows that, in order to power 50 E-buses and keep the DPBP at the same value as it was before, it is necessary for HSY to increase the yearly contribution of 14.30%.

4.7.3 Scenario 3 cost analysis

The situation for this scenario is similar to the one for Scenario 2, which is to be expected, since the two cases were found to be similar in the technical analysis as well. The first main divergence is given by the solar panels CAPEX, which increases the total capital cost of 1.04 million of euros; both the operating costs and the resources generated vary as well, but not as noticeably as the CAPEX.

Another noticeable difference is given by the available resources of this case, namely the surplus electrical energy, whose value is remarkably higher in respect to the other scenarios: 2,301 MWh. This is caused by the combination between the summer interruption of the AEL load and the implementation of the solar panels, which harvest more energy in the summer due to their nature.

The table below summarizes the DPBP analysis for this scenario.

Table 36: Scenario 3 cash flows and DPBP

Scenario 3					
OPEX	Electricity	H2	O2	CAPEX	HSY
- € 372,510.33	€ 406,586.70	€ 679,478.05	€ 122,522.68	€ 9,743,542.00	€ 1,600,000.00
Year	Total cash inflow	PV (6%)		DPBP (partial)	
1	€ 2,436,077.09	€ 2,298,185.93	€ 7,445,356.07	1	
2	€ 2,436,077.09	€ 2,168,099.94	€ 5,277,256.13	1	
3	€ 2,436,077.09	€ 2,045,377.30	€ 3,231,878.83	1	
4	€ 2,436,077.09	€ 1,929,601.23	€ 1,302,277.60	1	DPBP
5	€ 2,436,077.09	€ 1,820,378.51	-	0.715	4.715

It's possible to notice that, even with a CAPEX close to 10 million euros, the DPBP to break even is lower than the one of Scenario 2 (4.715 against 4.796), even with a HSY's yearly contribution that is slightly lower than the one of the previous scenario (1.6 MEUR against 1.7 MEUR). Most of the credit can be given to the surplus electricity, which can provide circa 400,000 € per year (as showed in Table 36) when sold to the grid.

The graph below, similarly to Figure 71, shows the relationship between the yearly HSY cash flow and the DPBP for Scenario 3.

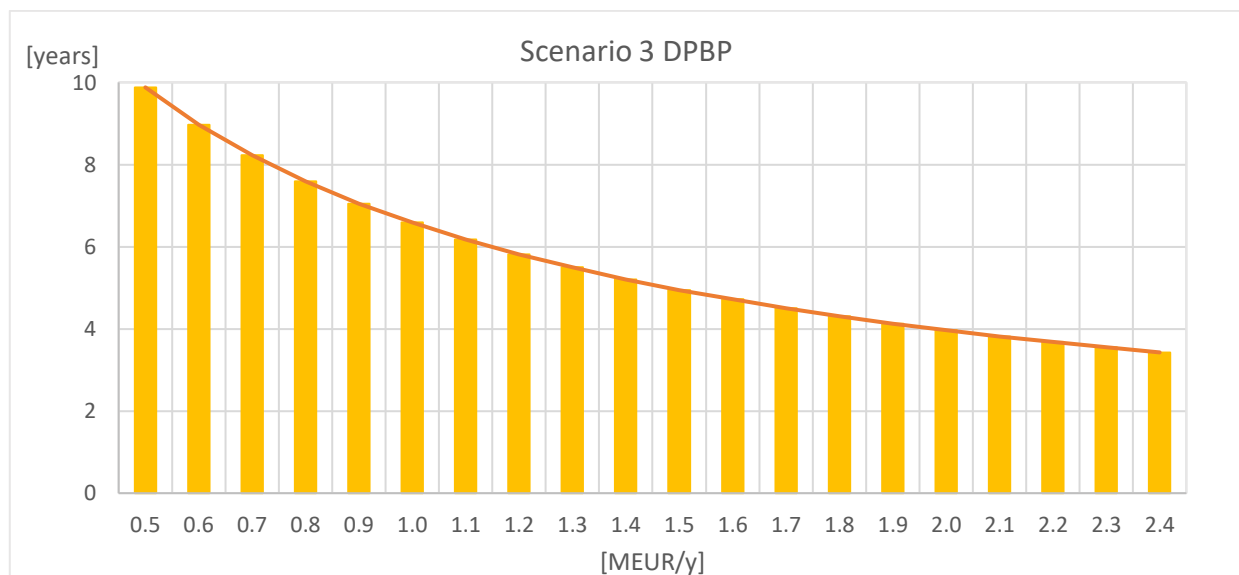


Figure 72: Scenario 3, correlation between HSY's yearly contribution and the DPBP

The picture below shows a comparison between the Scenario 2 and Scenario 3 DPBP:

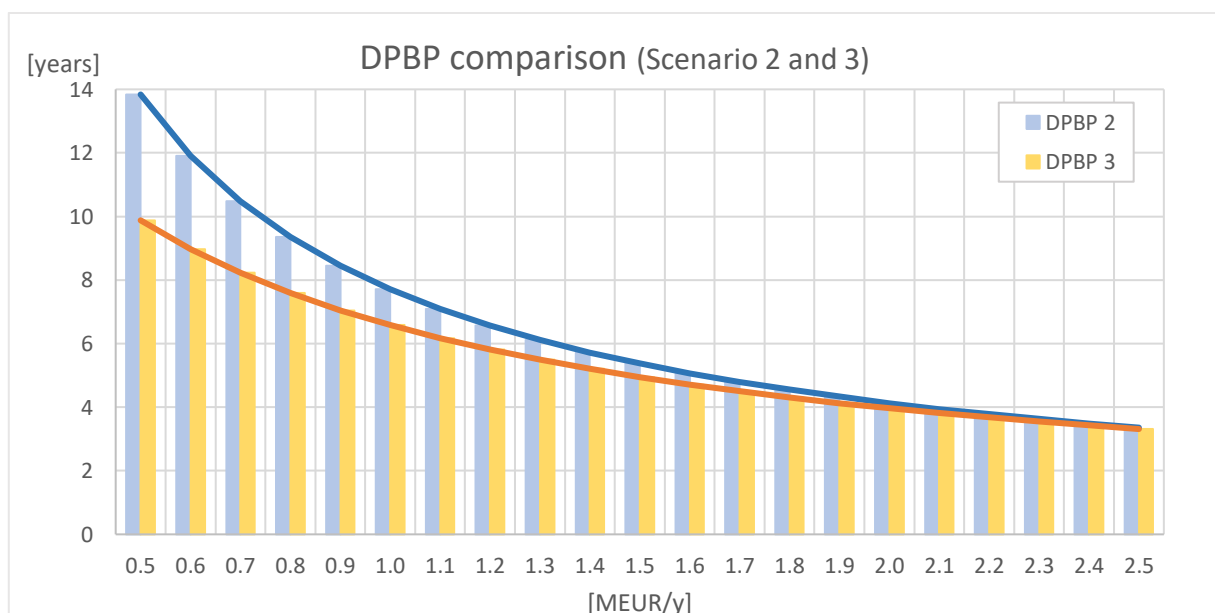


Figure 73: Scenario 2 and 3 DPBP comparison

Due to the higher cash inflows the Scenario 3 DPBP (Figure 73, previous page) is noticeably lower, especially in the lower range of the potential HSY contribution; the difference between the two DPBPs decreases as the value on the x-axis increases, due to the present value of money's influence.

Similarly as it was done for the previous scenarios, it's possible to consider the implementation of E-buses using the available energy surplus. What is interesting to note is that, given the wide availability of extra resources (especially electricity) up to 83 electrical vehicles could be implemented without having to buy any energy from the grid. Knowing this, it's possible to set the target number of E-buses to a relatively high value, e.g. 100; with said implementation the situation would be the following:

Table 37: Scenario 3 cash flows and DPBP, with a target of 100 E-buses

Scenario 2				100	
OPEX	Electricity	H2	O2	E-buses	HSY
- € 372,510.33	€ 406,586.70	€ 679,478.05	€ 122,522.68	- € 485,920.42	€ 2,085,900.00
					cost increase:
Year	Total cash inflow	PV (6%)	CAPEX	DPBP (partial)	30.37%
0			€ 9,743,542.00		
1	€ 2,436,056.67	€ 2,298,166.67	€ 7,445,375.33	1	
2	€ 2,436,056.67	€ 2,168,081.76	€ 5,277,293.57	1	
3	€ 2,436,056.67	€ 2,045,360.15	€ 3,231,933.42	1	
4	€ 2,436,056.67	€ 1,929,585.05	€ 1,302,348.37	1	DPBP
5	€ 2,436,056.67	€ 1,820,363.25	-	0.715	4.715

The cost increase necessary to invest to obtain 100 E-buses for this scenario is 30.37%, which is not relatively high per se, especially considering that the target number of vehicles is remarkable. However the regional authority would have to spend more than 2 MEUR per year to obtain the necessary energy, a cost which not only is high, but also it does not include all the necessary costs for the acquisition and maintenance of the buses themselves (even though it wouldn't be the regional authority to pay for said costs).

The table next page (Table 38) shows the cash flows for each scenario to utilise the surplus energy to power the electrical vehicles; the highlighted values represent the target number of E-buses, previously set.

Table 38: Surplus energy for E-buses utilisation and relative cash flows

	Scenario 1	Scenario 2	Scenario 3
		Surplus electricity [kWh]	
	600,000	763,000	2,301,000
E-buses		Cash flows	
10	€ 57,427.96	€ 86,230.06	€ 359,584.96
20	€ 8,835.92	€ 37,638.02	€ 310,992.92
30	- € 39,756.13	- € 10,954.03	€ 262,400.87
40	- € 88,348.17	- € 59,546.07	€ 213,808.83
50	- € 136,940.21	- € 108,138.11	€ 165,216.79
60	- € 185,532.25	- € 156,730.15	€ 116,624.75
70	- € 234,124.29	- € 205,322.19	€ 68,032.71
80	- € 282,716.33	- € 253,914.23	€ 19,440.67
90	- € 331,308.38	- € 302,506.28	- € 29,151.38
100	- € 379,900.42	- € 351,098.32	- € 77,743.42

A visual representation of the information of Table 38 can be seen below:

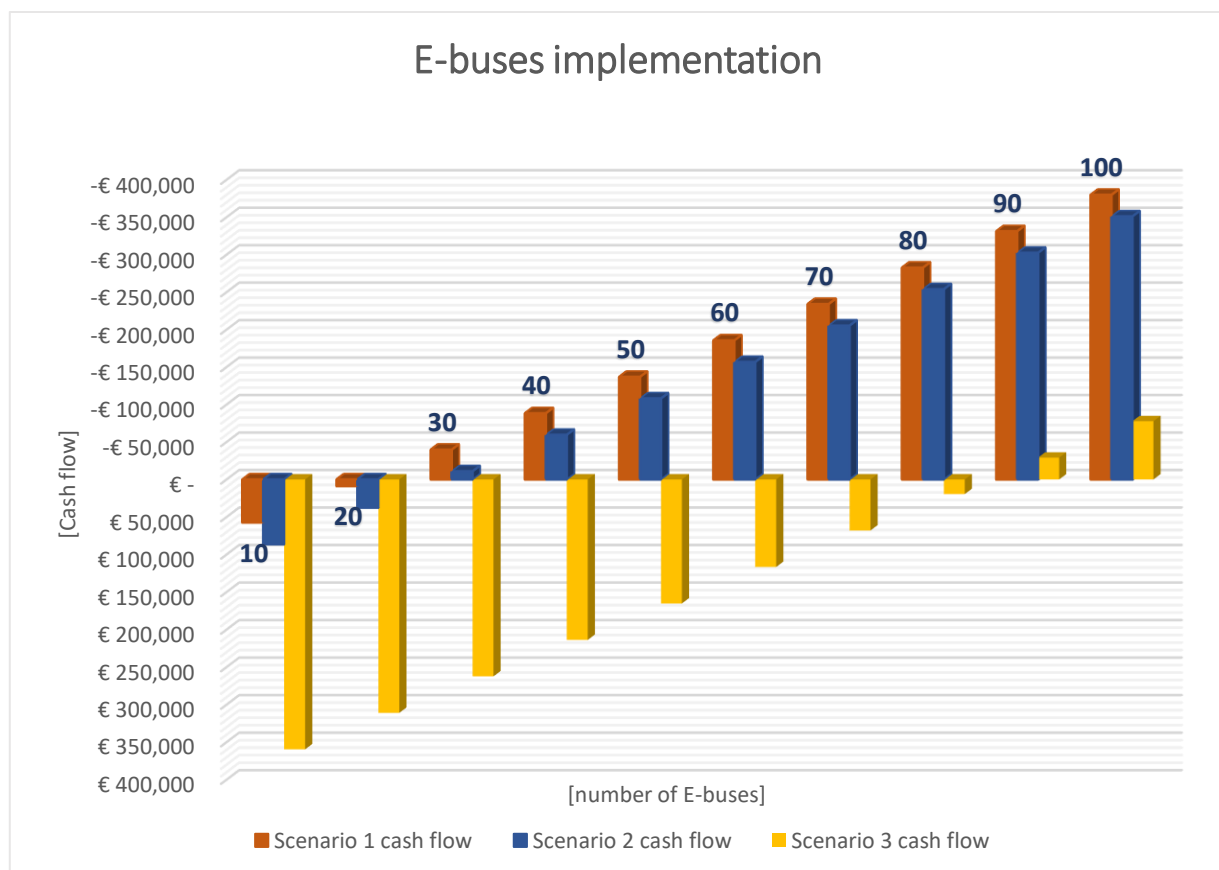


Figure 74: E-buses implementation and relative cash flows

CHALMERS UNIVERSITY OF TECHNOLOGY
Gothenburg, Sweden, December 2021
www.chalmers.se

Figure 74 (previous page) shows the y-axis in reverse order, so the higher the number of buses (shown in dark blue, from 10 to 100), the higher the columns' height, the higher the investment cost.

The data from Scenario 1 and Scenario 2 show a similar behaviour, for which the total cash flow is positive while the number of buses is lower than 30 (21 for the former, 27 for the latter), then it steadily grows. Due to the higher electricity surplus of Scenario 2 (763 MWh against 600 MWh) its relative cash flow is always lower than Scenario 1's.

Scenario 3 data series' behaviour is not different than the other series, but considering the remarkable electrical surplus (2301 MWh), the relative cash flow on the graph does not become negative before reaching the value of 90 E-buses (83 buses, as previously mentioned).

5. Summary

The techno-economic analysis showed that there are different possibilities to not only ensure the energy self-sustainability of the Ämmässuo eco-centre, but also to utilise the surplus energy to generate useful end products. The higher the complexity of the system (scenarios), the greater the number of possibilities.

Scenario 1 showed that the acquisition of a heat pump and the doubling of the composting facilities' capacity would ensure the eco-centre self-sufficiency and also generate some profit, thanks to the surplus electricity which can be sold to the national grid.

The heat pump investment can be considered a pillar for any energy scenario. In fact, since every possible situation can be characterized by a certain amount of heat and electricity demand, the utilisation of a heat pump makes it so that the only requirement for the eco-centre would be electricity, since any potential thermal energy gap could be covered by the heat pump.

Scenario 2 showed that the installation of a wind turbine would generate an amount of electricity so high that, after covering the energy demand of the eco-centre, there would still be surplus electricity each month. Said amount of energy could be sold to generate profit, or it could be used to generate hydrogen via electrolysis.

Due to the renewable energy sources' nature, the amount of surplus electricity harvested is not constant; for this work, a monthly analysis was constructed, but the intermittency of the source makes it so that an hourly analysis would have been the most accurate.

Knowing this, the pairing between the wind turbine and the AEL could be possible but tricky, since the electrolyser operates better with a constant load; to achieve this, after choosing a constant amount of electrical energy to send towards the AEL, the corresponding gap/surplus electricity can be bought from/sold to the grid each moment (each month for this master thesis' analysis), in order to keep the amount of energy sent to the electrolyser consistent.

A similar option explored in this work would be to operate the AEL in the same way but to interrupt its operation in the summer, due to the lower amount of surplus electricity at disposal of the eco-centre in the months between June and August.

For both of the beforementioned options, the AEL pairing with the wind turbine and the grid would simplify the operation of the electrolyser, due to the resulting constant load. This however would also question the possibility of green hydrogen production: using electricity purchased from the grid eliminates the assurance of using only renewable electricity for the production of H₂, since there is no guarantee that grid electricity is being produced using only renewable sources.

Scenario 3 is very similar to Scenario 2, since the only difference between the two is the introduction of solar panels, which would increase the amount of surplus electricity, thus the amount of energy to be sold to generate profit or to be used to produce H₂.

By looking at the economic analysis of the previous chapter, comparing the increased capital cost against the similarity between Scenario 2 and Scenario 3, it might seem like there is no

real benefit to installing solar panels, especially considering that Finland does not receive a great amount of solar irradiation throughout the year. However the PV plant would bring two benefits to the system.

First of all, the increased amount of energy expands the possibilities of the Ämmässuo eco-centre, both for applications that require electricity directly (i.e. E-buses), and also for any coupling that requires electrical energy, such as the use of an alkaline electrolyser, analysed in this work.

Secondly, as it can be seen from Figure 37 of Chapter 3.1.3 of this thesis (presented again below, Figure 75), the wind turbine and the solar panels by themselves generate energy in a way that is not constant throughout the months, as it can be seen from their profiles (blue curve and green curve, respectively). Together, however, their energy generation could be considered approximately constant, as it can be seen from the green curve: at least 1200 MWh can be harvested each month, which can be useful for applications that require a constant load, as well as to assure the reliability of the energy system.

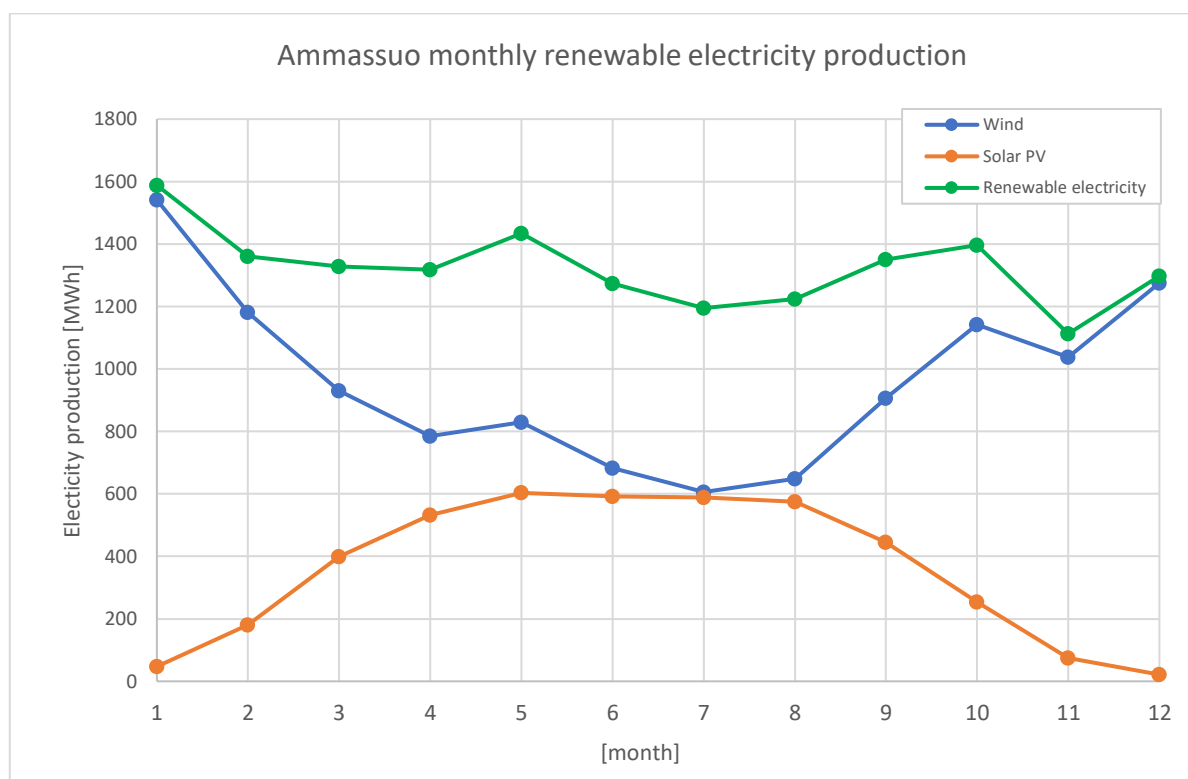


Figure 75: Ämmässuo monthly renewable electricity production [54][59]

Scenario 4 does not add any energy generation elements to the structure, but assumes that a methanation system could be included, in order to generate CH₄ via hydrogenation, utilising the H₂ from the AEL and the CO₂ from the biogas.

The idea behind this scenario would be to subtract part of the biogas from the CHP2 to obtain the CO₂ needed for the hydrogenation. This, however, was deemed unfeasible: since CHP2 is the main source of energy production, removing biogas from that part of the system would reduce the amount of electricity and heat produced by the eco-centre, to the point that only a percentage of 6% of biogas was deemed acceptable to be taken away from the combined heat and power engines.

The issue could theoretically be solved by taking directly the CO₂ produced by the biogas combustion, hence installing a carbon capture utilization and storage (CCUS) system, in order to utilize the carbon dioxide without having to subtract the biogas from the CHP2.

This solution, however, poses some problems. Firstly, CCUS can be an expensive technology: according to Kearney's report [98], CCUS CAPEX can reach even a value of 1.42 billion \$ (Saskpower Boundary Dam Project), while according to IEA [99] CCUS OPEX can vary between 13 and 107 €/t_{CO₂}. Secondly, it makes sense to deploy a CCUS system for much larger scales than the Ämmässuo eco-centre, considering not only the costs and the CO₂ that would be processed, but even the physical dimensions of a CCUS plant.

From an environmental standpoint, even if the CCUS option was doable, the production of CH₄ might generate controversy. In fact, all the effort necessary to remove CO₂ from the system would essentially generate a product that, when burned, would still release carbon dioxide, rendering the whole process pointless. This is why, originally, the hydrogenation process was intended to generate methanol: even if CH₃OH contains carbon, it wouldn't be utilised for combustion, but for wastewater treatment.

However, as mentioned in Chapter 3.1.6 of this work, internal methanol production is not feasible with the potential amount of surplus electricity at disposal of the eco-centre. The energy requirement of 90,229 MWh (shown in Table 13) corresponds to about 20% of all the surplus electrical energy that can be obtained in Scenario 3, and this without considering the energy necessary for the methanation process nor the investment costs for the methanation system.

A situation for which internal methanol production can be possible could be theoretically achieved. First of all, the internal energy production should be noticeably increased, for example with the installation of multiple wind turbines. Secondly, the CO₂ should be obtained from an external source (e.g. capturing it from another HSY process or buying it), in order to avoid the ordeal of generating it internally. Once this is achieved, a methanation system could easily generate the methanol required by HSY (or at least a considerable percentage) via CO₂ hydrogenation. This whole process however would require a remarkable capital investment, which means that, currently, buying methanol is still more profitable than producing it for the eco-centre.

Another possibility that was considered for each scenario (excluding Scenario 4) was the implementation of E-buses, for which Scenario 3 seems to be the optimal one considering its high yearly electricity surplus (2301 MWh). It should be mentioned again, however, that the economic analysis was limited to the electricity necessary to power the buses, and elements such as the capital costs of the vehicles and the operating costs for their maintenance were not considered.

Having excluded Scenario 4 from the future possibilities, the tables below and next page (Table 39, 40, 41, 42, 43) compare the various resources, costs and DPBs for the Ämmässuo eco-centre's future energy scenarios. For Scenarios 2 and Scenario 3, their respective summer interruption cases were considered, since they have resulted to be more profitable.

Table 39: Scenarios' surplus electricity profit, H₂ generation, O₂ generation

	Scenario 1	Scenario 2	Scenario 3
AEL monthly load [MWh]	-	1,100	1,400
Electricity bought [MWh]	-	876	480
Electricity sold [MWh]	600	1,639	2,780
Profit [€/year]	106,020.00	134,822.10	406,511.03
H ₂ produced [tonne/year]	-	202.23	257.38
O ₂ produced [tonne/year]	-	1,604.46	2,042.84

Table 40: Scenarios' total CAPEX, OPEX and profit

	Scenario 1	Scenario 2	Scenario 3
Total CAPEX [€]	294,400.00	8,702,692.00	9,743,542.00
Total OPEX [€/year]	4,680.00	321,472.00	372,510.33
Profit:			
Electricity [MWh]	600	763	2,301
Electricity (0.1767 €/kWh)	106,020.00	134,822.10	406,511.03
H ₂ [kg/year]	-	202,225.61	257,378.05
H ₂ (2.64 €/kg)	-	533,875.61	679,478.05
O ₂ [kg/year]	-	1,604,463.61	2,042,044.59
O ₂ (0.06 €/kg)	-	96,267.82	122,522.68
Total Profit [€/year]	106,020.00	764,965.53	1,208,587.42

Table 41: Scenarios' DPBP against HSY yearly investment

	DPBP [year]	(no E-buses)	
	Scenario 1	Scenario 2*	Scenario 3*
HSY yearly investment [€/year]			
500,000	0.512	13.893	9.897
1,000,000	0.279	7.712	6.586
1,500,000	0.192	5.377	4.945
2,000,000	0.146	4.129	3.963
2,500,000	0.118	3.358	3.313

Table 42: Scenarios' electricity surplus/requirement against number of E-buses to be powered

		Scenario 1, surplus = 600 MWh	Scenario 2, surplus = 763 MWh	Scenario 3, surplus = 2301 MWh
E-buses	Required electricity [kWh]	Grid electricity to sell/buy [kWh]	Grid electricity to sell/buy [kWh]	Grid electricity to sell/buy [kWh]
10	274,997.407	325,002.593	488,002.593	2,026,002.593
20	549,994.814	50,005.186	213,005.186	1,751,005.186
30	824,992.221	-224,992.221	-61,992.221	1,476,007.779
40	1,099,989.628	-499,989.628	-336,989.628	1,201,010.372
50	1,374,987.035	-774,987.035	-611,987.035	926,012.965
60	1,649,984.441	-1,049,984.441	-886,984.441	651,015.559
70	1,924,981.848	-1,324,981.848	-1,161,981.848	376,018.152
80	2,199,979.255	-1,599,979.255	-1,436,979.255	101,020.745
90	2,474,976.662	-1,874,976.662	-1,711,976.662	-173,976.662
100	2,749,974.069	-2,149,974.069	-1,986,974.069	-448,974.069

Table 43: Scenarios' cash flow against number of E-buses (relative to the electricity necessary to power them)

		Scenario 1, DPBP = 2.102	Scenario 2, DPBP = 4.796	Scenario 3, DPBP = 4.715
E-buses	Required electricity [kWh]	Grid cash flow [€/year] (E-buses electricity)	Grid cash flow [€/year] (E-buses electricity)	Grid cash flow [€/year] (E-buses electricity)
10	274,997.407	57,427.96	86,230.06	357,994.66
20	549,994.814	8,835.92	37,638.02	309,402.62
30	824,992.221	-39,756.13	-10,954.03	260,810.57
40	1,099,989.628	-88,348.17	-59,546.07	212,218.53
50	1,374,987.035	-136,940.21	-108,138.11	163,626.49
60	1,649,984.441	-185,532.25	-156,730.15	115,034.45
70	1,924,981.848	-234,124.29	-205,322.19	66,442.41
80	2,199,979.255	-282,716.33	-253,914.23	17,850.37
90	2,474,976.662	-331,308.38	-302,506.28	-30,741.68
100	2,749,974.069	-379,900.42	-351,098.32	-79,333.72

6. References

- [1] European Commission. EU climate action and the European Green Deal continent. EU official site. https://ec.europa.eu/clima/policies/eu-climate-action_en. Consulted on 10 July 2021.
- [2] System of environmental economic accounting. The European Green Deal and What it Means for Natural Capital Accounting. <https://seea.un.org/news/european-green-deal-and-what-it-means-natural-capital-accounting> Consulted on 12 July 2021.
- [3] United Nations. Department of Economic and Social Affairs. Sustainable Development. The 17 goals. <https://sdgs.un.org/goals> Consulted on 13 July 2021.
- [4] SDG tracker: Measuring progress towards the Sustainable Development Goals. <https://sdg-tracker.org> Consulted on 16 July 2021.
- [5] Cell, F. and Undertaking, H.J., 2019. Hydrogen Roadmap Europe: A Sustainable Pathway for the European Energy Transition; Executive Summary.
- [6] Kothari R., Buddhi D., Sawhney RL. Comparison of environmental and economic aspects of various hydrogen production methods. Renewable Sustainable Energy Review 2008; 12(2):553–63.
- [7] POSCO Newsroom. POSCO to Establish Hydrogen Production Capacity of 5 Million Tons. <https://newsroom.posco.com/en/posco-to-establish-hydrogen-production-capacity-of-5-million-tons/> Consulted on 19 July 2021.
- [8] Castro DFJ, Barth F, Vanhoudt W, Altmann M, Weindorf W. CertifHy green hydrogen. CertifHy; EU22 Aug 2016.
- [9] Dawood, F., Anda, M. and Shafiullah, G.M., 2020. Hydrogen production for energy: An overview. International Journal of Hydrogen Energy, 45(7), pp.3847-3869.
- [10] Divisek, J., Murgan, J., 1983. Diaphragms for alkaline water electrolysis and method for production of the same as well as utilization thereof. US Patent 4, pp 394-244.
- [11] Bard, A., Faulkner (2001). Electrochemical methods: fundamentals and applications, John Wiley & Sons, New York.
- [12] Viswanath RP (2004). A patent for generation of electrolytic hydrogen by a cost effective and cheaper route. Int J Hydrogen Energy, 29, 1191–4.
- [13] Colli, A.N. et al (2019). Non-Precious Electrodes for Practical Alkaline Water Electrolysis. Materials (Basel) 2019 Apr; 12(8): 1336. Published online 2019 Apr 24.
- [14] Taibi, E., Miranda, R., Vanhoudt, W., Winkel, T., Lanoix, J.C. and Barth, F., 2018. Hydrogen from renewable power: Technology outlook for the energy transition.
- [15] Funk JE. Thermochemical hydrogen production: past and present. Int J Hydrogen Energy 2001; 26(3): 185–90.
- [16] Kothari R, Buddhi D, Sawhney RL. Comparison of environmental and economic aspect of various hydrogen production methods. Renewable Sustainable Energy Review. 2008; 12(2): 553–63.

CHALMERS UNIVERSITY OF TECHNOLOGY
Gothenburg, Sweden, December 2021
www.chalmers.se

- [17] Aroutiounian VM, Arakelyan VM, Shahnazaryan GE. Metal oxide photo electrodes for hydrogen generation using solar radiation-driven water splitting. *Solar Energy* 2005; 78(5): 581–90.
- [18] Kapdan IK, Kargi F. Bio-hydrogen production from waste materials. *Enzym Microb Technol* 2006; 38(5): 569–82.
- [19] Demirbaş A. Biomass resource facilities and biomass conversion processing for fuels and chemicals. *Energy Conversion Management* 2001; 42(11): 1357–78.
- [20] Iribarren D, Susmozas A, Petrakopoulou F, Dufour J. Environmental and exergetic evaluation of hydrogen production via ligno-cellulosic biomass gasification. *J Clean Prod* 2014; 69:165–75.
- [21] Ni M, Leung DY, Leung MKH, Sumathy K. An overview of hydrogen production from biomass. *Fuel Processing Technologies* 2006; 87(5):461–72.
- [22] Nikolaidis, P. and Poullikkas, A., 2017. A comparative overview of hydrogen production processes. *Renewable and sustainable energy reviews*, 67, pp.597-611.
- [23] Zheng J, Liu X, Xu P, Liu P, Zhao Y, Yang J. Development of high pressure gaseous hydrogen storage technologies. *Int J Hydrog Energy* 2011;37(1):1048–57.
- [24] Léon, A. ed., 2008. *Hydrogen technology: mobile and portable applications*. Springer Science & Business Media.
- [25] Nandi, T.K. and Sarangi, S., 1993. Performance and optimization of hydrogen liquefaction cycles. *International journal of hydrogen energy*, 18(2), pp.131-139.
- [26] Martin, E. and Papageorgopoulos, D., 2015. DOE hydrogen and fuel cells program record.
- [27] Sternberg A, Bardow A. Power-to-What? - environmental assessment of energy storage systems. *Energy Environ Sci* 2015; 8:389–400.
- [28] Mehmeti A, Angelis-Dimakis A, Arampatzis G, McPhail SJ, Ulgiati S. Life cycle assessment and water footprint of hydrogen production methods: From conventional to emerging technologies. *Environments* 2018; 5:24.
- [29] North M, Styring P. Perspectives and visions on CO₂ capture and utilisation. *Faraday Discuss* 2015; 183: 489–502.
- [30] DW. Power-to-X: The secret to a 100% renewable energy system? <https://www.dw.com/en/power-to-x-the-secret-to-a-100-renewable-energy-system/a-51662014>. Consulted on 20 July 2021.
- [31] Koj, J.C., Wulf, C. and Zapp, P., 2019. Environmental impacts of Power-to-X systems-A review of technological and methodological choices in Life Cycle Assessments. *Renewable and Sustainable Energy Reviews*, 112, pp.865-879.
- [32] Li, W., Wang, H., Jiang, X., Zhu, J., Liu, Z., Guo, X. and Song, C., 2018. A short review of recent advances in CO₂ hydrogenation to hydrocarbons over heterogeneous catalysts. *RSC advances*, 8(14), pp.7651-7669.

CHALMERS UNIVERSITY OF TECHNOLOGY
Gothenburg, Sweden, December 2021
www.chalmers.se

- [33] Lai, C.S. and McCulloch, M.D., 2017. Levelized cost of electricity for solar photovoltaic and electrical energy storage. *Applied energy*, 190, pp.191-203.
- [34] Gielen, D., Taibi, E. and Miranda, R., 2019. Hydrogen: A renewable energy perspective. Abu Dhabi: International Renewable Energy Agency (IRENA).
- [35] Tapang, B. and Mendoza, L., *Introductory Economics*.
- [36] Goyal, B., 2014. *Decision Making in Finance: Time Value of Money, Cost of Capital and Dividend Policy*.
- [37] Jain, P.K., 1999. *Theory and problems in financial management*. Tata McGraw-Hill Education.
- [38] Fernandes, N., 2014. *Finance for Executives: A practical guide for managers*. NPVPublishing.
- [39] Helsingin seudun ympäristöpalvelut HSY. Visits to HSY's locations: Ämmässuo eco-industrial centre. <https://www.hsy.fi/en/hsy/visits-to-hsys-locations/#Ämmässuon%20ekoteollisuuskeskus>. Consulted on 14 September 2021.
- [40] Ämmässuon jätteenkäsittelykeskus ottaa käyttöön Vaisalan huoltovapaan biokaasumittarin. <https://www.vaisala.com/sites/default/files/documents/VIM-G-BG-SuccessStory-B211824FI.pdf>. Consulted on 15 September 2021.
- [41] Government Decree on Landfills (331/2013; amendments up to 960/2016 included). Translation from Finnish; Legally binding only in Finnish and Swedish. Ministry of the Environment, Finland. https://www.finlex.fi/fi/laki/kaannokset/2013/en20130331_20160960.pdf. Consulted on 16th September 2021
- [42] HSY kaasumoottoriselvitys raportti. Final draft: 2021-06-24. Kappale 2: Kaatopaikkakaasun määrän kehitys. Yrityksen sisäinen dokumentti. HSY/Sweco.
- [43] The difference between biogas and landfill gas. IPPTS Anaerobic Digestion Community. <https://anaerobic-digestion.com/biogas-and-anaerobic-digestion/difference-biogas-landfill-gas/>. Consulted on 19 September 2021.
- [44] HSY kaasumoottoriselvitys raportti. Final draft: 2021-06-24. Kappale 3: Kaasuvoimalat. Yrityksen sisäinen dokumentti. HSY/Sweco.
- [45] Ämmässuon kaatopaikkakaasut tuottavat nyt sähköä. 21-5-2010. Yleisradio Oy (YLE). <https://yle.fi/uutiset/3-5566383>. Consulted on 19 September 2021
- [46] Gas Engine TCG 2032. MWM: Energy, Efficiency, Environment. <https://www.mwm.net/en/gas-engines-gensets/gas-engine-tcg-2032/>. Consulted on 20 September 2021
- [47] ORC operating principle. Rank® Technology. <https://www.rank-orc.com/2019/06/21/rank-technology-orc-operating-principle/>. Consulted on 20 September 2021

CHALMERS UNIVERSITY OF TECHNOLOGY
Gothenburg, Sweden, December 2021
www.chalmers.se

- [48] Annual statistics for the waste management in the Helsinki metropolitan area. HSY. <https://www.hsy.fi/en/environmental-information/open-data/avoin-data---sivut/annual-statistics-for-the-waste-management-in-the-helsinki-metropolitan-area/>. Consulted on 20th September 2021
- [49] Lehteva V., 2021. Ämmässuo eco-industrial centre energy flows. Metropolia University of Applied Sciences, Bachelor of Engineering, Energy and environmental technology. Ämmässuon energiavirrat: HSY Yrityksen sisäinen dokumentti.
- [50] HSY kaasumootoriselvitys raportti. Final draft: 2021-06-24. Kappale 4: Sähkön ja lämmön kulutus. Yrityksen sisäinen dokumentti. HSY/Sweco.
- [51] Ji Bin et al, 2015. Aerobic denitrification: A review of important advances of the last 30 years. Biotechnology and Bioprocess Engineering, vol 20
- [52] HSY raportti. Jätevedenpuhdistus pääkaupunkiseudulla 2020, Viikinmäen ja Suomenojan jätevedenpuhdistamot. Yrityksen sisäinen dokumentti, HSY.
- [53] Renewable ninja. Ämmässuo 2019 weather data. <https://www.renewables.ninja/about>. Consulted on 10th November 2021.
- [54] Vestas 4MW Platform. https://www.vestas.com/en/products/4-mw-platform/v150-4_2_mw#!aep. Consulted of 6th October 2021.
- [55] The Wind Power: Wind Energy Market Intelligence. Vestas turbines: V150/4000-4200. https://www.thewindpower.net/turbine_en_1490_vestas_v150-4000-4200.php. Consulted of 8th October 2021.
- [56] Aalto University. 2021. AAE-E3090, Renewable Energy Engineering course.
- [57] Zhang, M.H., 2015. Wind resource assessment and micro-siting: science and engineering. John Wiley & Sons. Appendix II.
- [58] Ma, Ke & Yang, Yongheng & Wang, Huai & Blaabjerg, F. 2014. Design for Reliability of Power Electronics in Renewable Energy Systems. 10.1007/978-3-319-03224-5_9.
- [59] Aurinkoenergian kannattavuus ja toteutus teollisuussähkö verkossa. 2016. Kappale 4: Aurinkoenergian edellytykset Ämmässuolla. Yrityksen sisäinen dokumentti. HSY/Elomatic.
- [60] Die Verwirrung um das Watt-Peak, The confusion around watt-peak. 2009. <https://photovoltaikbuero.de/pv-know-how-blog/die-verwirrung-um-das-watt-peak/>. Consulted on 9th October 2021.
- [61] ASTM International. ASTM G173 - 03(2020). <https://www.astm.org/Standards/G173.htm>. Consulted on 9th October 2021.
- [62] Alternative Energy Tutorials. Solar Cell IV Characteristics. <https://www.alternative-energy-tutorials.com/photovoltaics/solar-cell-i-v-characteristic.html>. Consulted on 12th October 2021.
- [63] WAAREE. 250 Wp SPV module characteristics. https://www.waaree.com/documents/WS-250_4BB_60%20Cells_40mm_datasheet.pdf. Consulted on 12th October 2021.

CHALMERS UNIVERSITY OF TECHNOLOGY
Gothenburg, Sweden, December 2021
www.chalmers.se

- [64] Aurinkoenergian kannattavuus ja toteutus teollisuussähkö verkossa. 2016. Kappale 3.1: Aurinkosähkön tuottaminen Suomessa. Yrityksen sisäinen dokumentti. HSY/Elomatic.
- [65] Saeed Maddah, Marjan Goodarzi, Mohammad Reza Safaei. 2020. Comparative study of the performance of air and geothermal sources of heat pumps cycle operating with various refrigerants and vapor injection. Alexandria Engineering Journal, Volume 59, Issue 6, Pages 4037-4047.
- [66] Specific heat of some common substances. The Engineering Toolbox.
https://www.engineeringtoolbox.com/specific-heat-capacity-d_391.html. Consulted on 15th October 2021
- [67] Air source vs ground source heat pumps. Kensa Heat Pumps: a Kensa group company.
<https://www.kensaheatpumps.com/air-source-vs-ground-source-heat-pumps/>. Consulted on 16th October 2021
- [68] Tom Smolinka, Emile Tabu Ojong, Jürgen Garche. 2015. Hydrogen Production from Renewable Energies. Electrolyzer Technologies: Chapter 8. Electrochemical Energy Storage for Renewable Sources and Grid Balancing. Elsevier. pp 103-128.
- [69] Atmospheric Alkaline Electrolyser: A-series. NEL hydrogen electrolyzers.
<https://nelhydrogen.com/wp-content/uploads/2020/03/Electrolysers-Brochure-Rev-C.pdf>. Consulted on 19th October 2021
- [70] Alfredo Ursúa et al. 2013. Stand-alone operation of an alkaline water electrolyser fed by wind and photovoltaic systems. International Journal of Hydrogen Energy. Volume 38, Issue 35, Pages 14952-14967.
- [71] Ervsolar. Bornay 6000W 48V Wind Turbine. Bornay Small Wind Turbines.
<https://www.ervsolar.com/Bornay-6000W-48V-Wind-Turbine>. Consulted on 20th October 2021.
- [72] Second Sol, the photovoltaic marketplace. Bp solar. BP585 U/S/H.
<https://www.secondsol.com/en/anzeige/21516/modules/crystalline/mono/bp-solar/bp-585-ush>. Consulted on 22th October 2021
- [73] Troncoso E, Newborough M. 2007. Implementation and control of electrolyzers to achieve high penetrations of renewable power. International Journal of Hydrogen Energy. Volume 32, Pages 2253-2268.
- [74] Frilund, C. 2016. CO₂ Hydrogenation to Methanol. M.Sc. Thesis, Aalto University, School of Chemical Technology.
- [75] Vesterinen, E., 2018. Methanol production via CO₂ hydrogenation. M.Sc. Thesis, Aalto University, School of Engineering.
- [76] Kiss, A. et al. 2016. Novel efficient process for methanol synthesis by CO₂ hydrogenation. Chemical Engineering Journal, 284/2016, pp. 260-269.
- [77] Bertau, M. 2014. Methanol: The Basic Chemical and Energy Feedstock of the Future Asinger Vision Today. Berlin, Heidelberg, Imprint: Springer.

CHALMERS UNIVERSITY OF TECHNOLOGY
Gothenburg, Sweden, December 2021
www.chalmers.se

- [78] Lurgi. 2017. Methanol And Derivatives. Proven Technologies For Optimal Production. Air Liquid Engineering Construction, Editor.
- [79] Frontera, P., Macario, A., Ferraro, M. and Antonucci, P., 2017. Supported catalysts for CO₂ methanation: a review. *Catalysts*, 7(2), p.59.
- [80] Götz, M., Koch, A.M. and Graf, F., 2014, September. State of the art and perspectives of CO₂ methanation process concepts for power-to-gas applications. In International Gas Union Research Conference (Vol. 13). Fornebu, Norway: International Gas Union.
- [81] Environmental and Energy Study Institute (EESI). Fact Sheet. Biogas: Converting Waste to Energy. <https://www.eesi.org/papers/view/fact-sheet-biogasconverting-waste-to-energy>. Consulted on 10th November 2021.
- [82] Moioli, E., Mutschler, R. and Züttel, A., 2019. Renewable energy storage via CO₂ and H₂ conversion to methane and methanol: Assessment for small scale applications. *Renewable and Sustainable Energy Reviews*, 107, pp.497-506.
- [83] ViriCiti Report: E-bus performance. 2020. Netherlands. <https://viriciti.com/wp-content/uploads/2020/07/ViriCiti-E-bus-Performance-Report-July2020.pdf>. Consulted on 6th November 2021.
- [84] Xylia, M. et al. 2017. Locating charging infrastructure for electric buses in Stockholm. *Transportation Research Part C: Emerging Technologies*, 78, pp.183-200.
- [85] Lozanovski, A. et al. 2018. Sustainability assessment of fuel cell buses in public transport. *Sustainability*, 10(5), p.1480.
- [86] IRENA. 2021. Renewable Power Generation Costs in 2020. International Renewable Energy Agency, Abu Dhabi.
- [87] NERA, A., 2009. The UK Supply Curve for Renewable Heat. Study for the Department of Energy and Climate Change.
- [88] GREBE: Generating Renewable Energy Business Enterprise. 2017. Advice Notes on GHSP and ASHP. Finland. Northern Periphery and Artic Programme.
- [89] ASSET project. 2021. Hydrogen generation in Europe: Overview of costs and key benefits. Publications Office of the European Union.
- [90] Nyári, J., 2018. Techno-economic feasibility study of a methanol plant using carbon dioxide and hydrogen.
- [91] Costat. Electricity Price Statistics. https://ec.europa.eu/costat/statistics-explained/index.php?title=Electricity_price_statistics. Consulted on 20th November 2021.
- [92] Kantoluoto, N., 2020. Ämmäsuon ekoteollisuuskeskuksen biojätteen käsittelyn massatase ja energiatase.
- [93] Moioli, E., Mutschler, R. and Züttel, A., 2019. Renewable energy storage via CO₂ and H₂ conversion to methane and methanol: Assessment for small scale applications. *Renewable and Sustainable Energy Reviews*, 107, pp.497-506.

CHALMERS UNIVERSITY OF TECHNOLOGY
Gothenburg, Sweden, December 2021
www.chalmers.se

- [94] Laurikko, J., Ihonen, J., Kiviaho, J., Himanen, O., Weiss, R., Saarinen, V., Kärki, J. and Hurskainen, M., 2020. National Hydrogen Roadmap for Finland. Business Finland.
- [95] Kärki, J., Tsupari, E.V. and Vakkilainen, E., 2016, March. The most promising business cases for P2X deployment in renewable energy systems. In Proceedings of the 10th International Renewable Energy Storage Conference (IRES 2016), Düsseldorf, Germany (pp. 15-17).
- [96] Richardson, I.A., Fisher, J.T., Frome, P.E., Smith, B.O., Guo, S., Chanda, S., McFeely, M.S., Miller, A.M. and Leachman, J.W., 2015. Low-cost, transportable hydrogen fueling station for early market adoption of fuel cell electric vehicles. international journal of hydrogen energy, 40(25), pp.8122-8127.
- [97] Statistics Finland. Transport and Tourism. Transport network and passenger transport; Registered vehicles on 31 December.
https://www.stat.fi/tup/suoluk/suoluk_liikenne_en.html. Consulted on 31st November 2021.
- [98] Romain Debarre, Prashant Gahlot, Céleste Grillet, Mathieu Plaisant. 2021. Carbon Capture Utilization and Storage: Towards Net-Zero. Kearney Energy Transition Institute.
- [99] IEA. 2021. Is carbon capture too expensive?, International Energy Agency, Paris
<https://www.iea.org/commentaries/is-carbon-capture-too-expensive>. Consulted on 5th December 2021
- [100] IRENA. 2020. Green Hydrogen: A guide to policy making, International Renewable Energy Agency, Abu Dhabi
- [101] Daiyan, R. et al. 2020. Opportunities and challenges for renewable power-to-X.



CHALMERS
UNIVERSITY OF TECHNOLOGY